Design of a Grasping Mechanism for a Friction-Based Transport Mechanism

H.J. Kooiman

Design of a Grasping Mechanism for a Friction-Based Transport Mechanism

Design of a Grasping Mechanism for a Friction-Based Transport Mechanism.

By

H.J. Kooiman

In partial fulfilment of the requirements for the degree of

Master of Science
in Mechanical Engineering

at the Delft University of Technology,
to be defended on Friday May 21st, 2021 at 14:00 PM.

Supervisors:	Dr. Ir. A. Sakes	
	Ir. E. P. de Kater	
Thesis committee:	Prof. Dr. P. Breedveld,	TU Delft
	Dr. Ir. A. Sakes,	TU Delft
	Ir. K. Lussenburg,	TU Delft

TU Delft

Contents

Abstract

This report describes the design of a wire rope based grasper for a tissue transport mechanism based on friction including means for operation. The previous transport mechanism design had no mechanism to transfer tissue into the lumen to be transported. To create the grasper, the wire ropes were plastically deformed to bend outward, creating the open shape of the grasper. A sheath consisting of magnets, springs, and a shrink tube can be slid over the plastically deformed section, straightening the wire ropes. This closed the grasp to constrain tissue. Operation was done by four finger handles, two on the main device and two clamped on the slidable sheath with magnets. Springs were used to make the passively hold the grasper in closed position, making it voluntary opening. To maintain the shape of the grasper, wire ropes were soldered together at the grasper tip, constrained in the sliders of the transport mechanism and wire rope guides were placed to the side of the magnets. After constraining the tissue, transfer into the lumen was done by actuating the transport mechanism. Gelatin phantom tissue samples were used to test the functionality the of the grasper. Results show successful constraining of 3mm, 4mm, 5mm spheres as well as a cylinder of 4mm with a length of 6.5mm. The spherical samples were all successfully transferred into the transport mechanism. The cylindrical sample was successfully transferred when inserted in axial orientation, but three out of six samples failed when insertion was perpendicular to the transport mechanism. Tissue samples were successfully grasped from a surface in three different orientations and the grasper was tested with the transport mechanism in a bend to test if no original functionality was lost. This grasper allows for a step towards a new surgical instrument.

Keywords: Grasper, Compliant, Mechanism, Transport, Friction

1 Introduction

1.1 Tissue Transport in Surgery

During surgery, tissue is sometimes taken out of the body. For instance, when a biopsy is needed for analysis, tumour removal, unclogging of an artery or removing parts of an organ. Especially during minimally invasive surgery removing tissue is hard as it needs exit the human body through small. These incisions are small to limit the impact of the surgery on the patient. Currently the following methods of tissue transport for minimally invasive surgery are being used.

1. Transport tissue out of the body by aspiration. A pressure difference between the input and output of a tube that is inserted in the body sucks tissue out. For instance fine needle aspiration for taking a biopsy [1], aspiration of organ tissue out of a morcellator [2], or aspiration of a blood clot in a thrombectomy. A problem with tissue aspiration is the risk of clogging, making the device lose function. Another risk is damaging healthy tissue that is sucked into the catheter opening by the pressure difference.

2. Extract the surgical instrument holding the tissue out of the body. After this the instrument needs to be reinserted. This is very time-consuming.

3. Using a tissue pouch. The pouch is inserted in the body through a small incision. Inside the body the pouch is opened and holds tissue that is to be extracted at the end of the surgery [3]. This method can only be used if there is sufficient space for the pouch, which is often limited during minimally invasive surgeries.

A new transport mechanism is being developed based on the ovipositor of the parasitic wasp. The parasitic wasp can transport its eggs through its ovipositor. A relatively long and thin tubular organ. These properties are also wanted in minimally invasive surgery. Research in mimicking the parasitic wasp ovipositor has resulted in transport mechanisms using friction, adding a new category.

1.2 Bio-inspiration: Parasitic Wasp

Previously a friction based transport mechanism has been developed by Esther de Kater [4] and van de Steeg [5]. Inspiration for this mechanism was the ovipositor of the parasitoid wasp. The ovipositor consists of 3 sliding parts that are used to penetrate the skin of host animals and transport eggs into the body, as shown in Figure 1. In Figure 1B, the ovipositors ventral and dorsal side of the tip is illustrated. Figure 1C shows a cross-section of the ovipositor with the rail like sliding joint between, called the olistheter, the two ventral valves at the bottom and the dorsal valve at the top. This rail-like sliding joint makes longitudinal movement between the valves possible while staying connected. Most parasitoid wasp species have scales inside their ovipositor. It is hypothesised that the scales allow transportation of eggs when two ovipositor elements slide relative to each other. Resistance of the scales is low when the egg in contact with the ovipositor element moves towards the tip of the ovipositor. However, an egg encounters a high resistance of the scales when moved towards the body of the wasp. The hypothesized working principle shown in Figure 2, makes transport of the egg towards the tip of the ovipositor possible. Figure 2A shows the initial situation. One of the two ovipositor elements slide to the right. Because of the scale direction the friction force of the moving element is lower than the friction force of the element that remains in place, resulting in an egg (red) that also stays in place. Figure 2C shows the ovipositor element is slid back into its original position. Now the friction force of the moving element on the egg (red) is higher than the friction force of the stationary element on the egg resulting in the egg moving towards the ovipositor output. The same hypothesis for transport can be used with three independent sliding elements without scales as shown

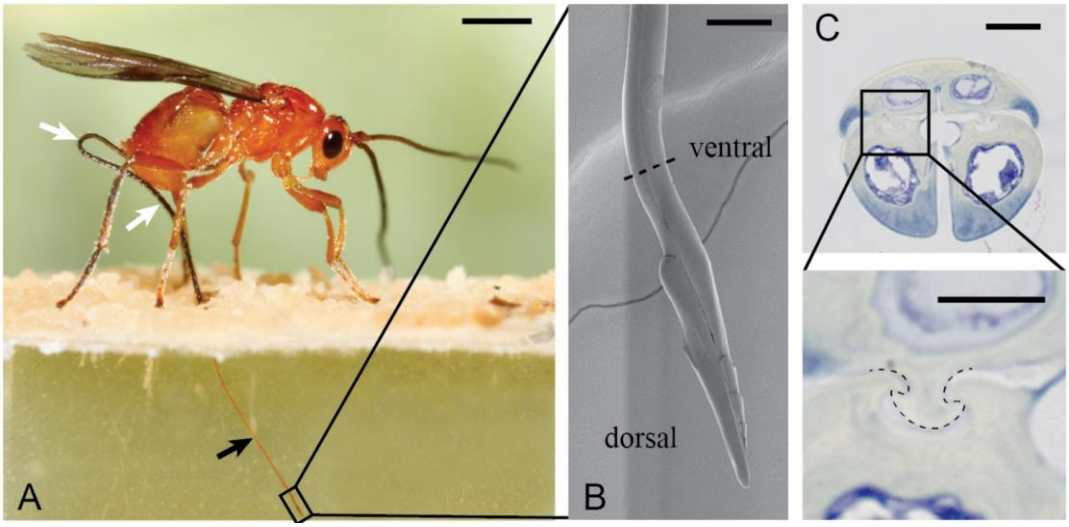

Figure 1: The ovipositor. A, The Parasitoid wasp with ovipositor indicated by arrows. B: Tip of the ovipositor with indication of the dorsal and ventral side. C: Cross-section of an ovipositor. As shown, it consists of three parts. A top, bottom left and bottom right part connected by a sliding joint [21].

in Figure 3. Figure 3A is the initial position of the three sliding elements of the ovipositor and the egg (red). The contact interface between the egg and each element is the same (Equation 1). First, element one is moved upward, as shown in Figure 3B. Because the friction force of element one on the egg ($F_{w1}[N]$) is smaller than the friction on the egg of elements two and three ($F_{w2}[N] + F_{w3}[N]$) the egg stays in position (Equation 2). The same happens in Figure 3C when element two is moved upwards and element one and three remain stationary. The friction of the stationary elements on the egg is higher than the friction of the moving element resulting in a stationary egg (Equation 3). Now two elements have been slid upwards they can be used to transport the egg towards the output of the ovipositor. By sliding element one and two towards the output at the same time, as shown in Figure 3D, the egg also slides towards the distal output as the combined friction forces of the moving elements on the egg are bigger than the friction force of the stationary element (Equation 4).

$$F_{w1} = F_{w2} = F_{w3} \quad (1)$$

$$F_{w1} < F_{w2} + F_{w3} \quad (2)$$

$$F_{w2} < F_{w1} + F_{w3} \quad (3)$$

$$F_{w1} + F_{w2} > F_{w3} \quad (4)$$

1.3 Prior Work: Wasp-inspired Tissue Transport Mechanism

Based on the explained principle of egg transport in parasitoid wasps, a flexible transport mechanism has been developed. Figure 4 shows the transport mechanism in its current form consisting of wire ropes, magnets, springs, a heat shrinking tube and a handle to operate it. Six independently moving groups of three wire ropes provide the necessary sliding motion and contact with tissue. The total of 18 wire ropes are held together by magnets with an inner diameter of 5mm, an outer diameter of 10mm and a thickness of 2mm as shown in Figure 5. The wire rope total diameter is 0.6mm and is made of 7 thinner wires of 0.2mm. Figure 5 shows a cross section of the transportation device with the wire ropes shown in red. The magnets that guide the wires ropes are indicated in yellow. Springs, shown in orange, keep the magnets at the right distance from each other while maintaining flexibility. They also keep the lumen from collapsing by the heat shrink. Finally, the heat shrink tube, shown in green, keeps the magnets and springs in place. Because the wire ropes are pulled towards the magnets, a circular lumen is created that allows for

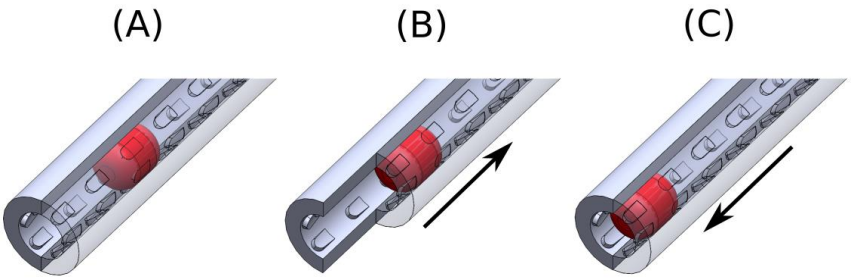

Figure 2: Two ovipositor elements with scales transporting an egg (red) to the output. From initial position A, one element slides to the right. Because of the scale orientation the friction on the egg of the moving ovipositor element is lower than the friction on the egg from the stationary element resulting in a stationary egg shown in B. In part C the ovipositor element is slid back towards the output. Because of the scale orientation the friction force between the moving element and the egg is higher than the friction force between the stationary element and the egg resulting in the egg moving towards the output along with the moving element.

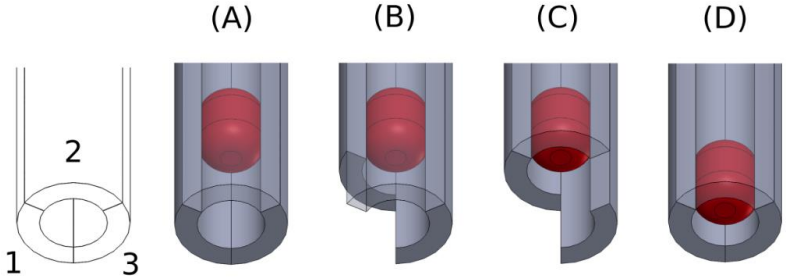

Figure 3: Three schematic sliding ovipositor elements shown transporting an egg (red). The egg has an equal friction force with each element (Equation 1). When one element slides upward (B and C) the friction force of the stationary elements on the egg is bigger than the friction force of the moving element on the egg resulting in a stationary egg (Equation 2 and 3). When elements one and two move down together the friction force of the moving elements on the egg is higher than the friction force of the single stationary element on the egg (Equation 4). This results in transportation of the egg towards the ovipositor output.

transportation of tissue. Transportation is achieved by moving more wire ropes at the same time towards the output side. This means the combined friction force of the wire ropes moving towards the output on the tissue is higher than the friction force of the wire rope moving towards the input, assuming each wire rope has an identical contact with the tissue, resulting in an identical friction force. The transport of tissue can be continuous due to an internal cam mechanism that shifts the wire ropes back towards the input quicker than towards the output. This way there are always more wire ropes sliding towards the output to transport the tissue. Figure 6 shows the cam profile of de Kater, where $Rc[m]$ is the radius of the cam, $S_b[m]$ is the stroke of the shifting wire ropes, and n is the number of wire rope groups.

Figure 7 displays the resulting motion pattern of the six different sections of the transport system. This was also used in the design of a rigid friction based transport system by van der Steeg [6].

1.4 Problem Statement

Currently the flexible transport mechanism has been proven to be able to transport tissue phantoms of different elasticity, though so far there is no system to smoothly grasp tissue and transfer it into the lumen to be transported [4]. The wire ropes of the transport mechanism are not perfectly straight. Therefore, they point in random directions at the input of the transport mechanism, where they are not supported by magnets.

Figure 4: Friction based transport mechanism by de Kater [4].

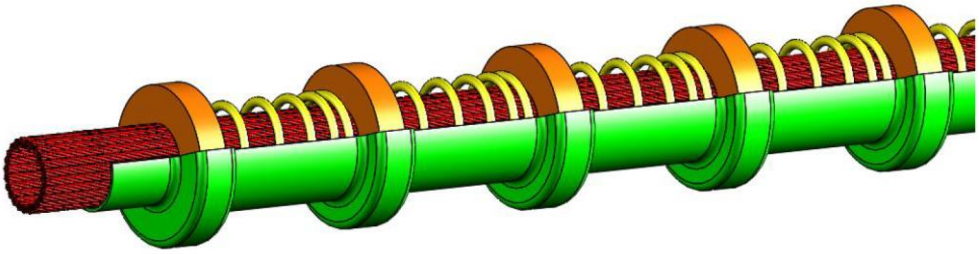

Figure 5: 3D view of the transport mechanism by de Kater [4]. The wire ropes (red) held together by magnets (orange) which are separated by springs (yellow). Everything is encapsulated by a heat shrink (green).

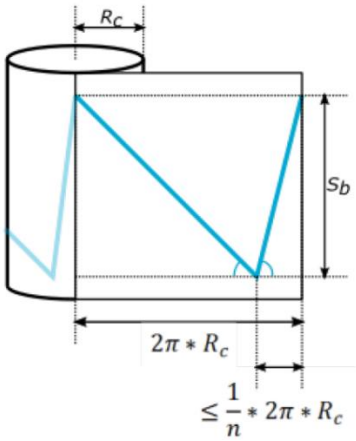

Figure 6: Cam design. The cam design used by de Kater [4]. Rc[m] is the cam radius. Sb[m] is the stroke of the shifting wire rope groups and n is the number of wire rope groups.

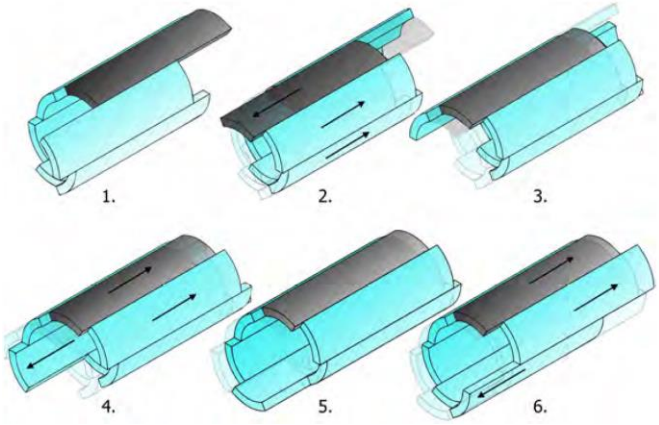

Figure 7: Motion steps of solid friction-based transport mechanism by van der Steeg [6]. In each step one blade is being slid towards the transport mechanism input while the other five are slid in opposite direction. The friction difference makes tissue move in the same direction as the five blades, away from the input.

The current wire rope end shape makes it impossible to get tissue into the transport mechanism during a surgery.

To be able to use the transport mechanism to transport tissue out of a patient during a surgery, a grasper needs to be developed that picks up and transfers tissue into the transport mechanism while being operated from outside the patient's body.

As the wire ropes of the transport mechanism are moving during actuation of the transport mechanism, it will be hard to create a transition between a separate grasping mechanism and the wire ropes. To circumvent this problem the wire ropes can be given a compliant hinge and turned into a grasper themselves. Using a compliant hinge to open and close the grasper also eliminates the need for small components that traditional hinges need. The grasper needs to be able to be operated independently of the transportation to have the choice between continuing transport while grasping or grasp without transporting for higher grasping accuracy.

1.5 Goal of the Study

The goal of this study is to design a wire rope based grasping mechanism that grasps and transfers tissue into the lumen of the transport mechanism. This also includes means to operate the grasper. The original transport mechanism should remain functional, also in bent configuration. The grasper does not have to cut tissue and does not have to be steerable. It is assumed the tissue is already cut to the right size by another instrument and is ready to be grasped.

1.6 Thesis Outline

In Chapter two the design process is explained. Existing compliant grasper designs are discussed, and a possible solution direction is explained. After this in Chapter three, various opening and closing methods for the grasper are listed, and a way to fabricate the chosen shape is found by empirical tests. Chapter four shows how a way to operate the grasper is determined for the final design. Chapter five shows the final design resulting from the choices made in chapters three and four. The 3D model made in Solidworks is displayed, followed by the assembly steps. Finally, the design is evaluated in Chapter six by testing if the grasper success fully constrains tissue and transfers it into the lumen. Results of the tests are also displayed in Chapter six. A discussion of the main findings, limitations of the study and suggestions for further research are done in Chapter seven. The report is closed with a conclusion in Chapter eight.

2 Design Process

2.1 Proposed Solution Direction

A suggested solution to grasp with the wire ropes is to give them an initial bent outward shape and straighten the wire ropes to close the grasper around tissue. Opening and closing is achieved by compliance of the wire rope, which depends on the right material stiffness, strength, and shape. The challenge is to make the grasping motion without permanently deforming the wire ropes and to keep the lumen open for transport. Figure 8 shows the proposed solution with the wire ropes in yellow, and the sheath with springs and magnets in blue.

Currently there are already surgical tools available that use compliant grasping methods. These are shown in Figure 9 to Figure 12. Figure 9 depicts the I-flex, a steerable 2 DOF grasper for eye surgery. The grasper is closed by pulling a cable running through the lumen. When the cable pulls the grasper into the sheath, the grasper deforms elastically and closes. Figure 10 shows an endoscopic suturing instrument where the sheath also closes the pinching motion. Four cross-sections are shown with the compliant elements when the blue sheath is slid over them. Figure 11 shows a two DOF laparoscopic grasper. One DOF to control the grasp angle and one DOF to actuate the grasp itself. It must be noted that the compliant grasping elements and the solid sheath do not move relatively to each other as with the other designs. Figure 12 shows a narrow-gauge surgical forceps with a contact Point A that lowers the highest material bending stress in the design [7]. All solutions have a collapsing lumen or no lumen available for a transportation mechanism. While all mentioned

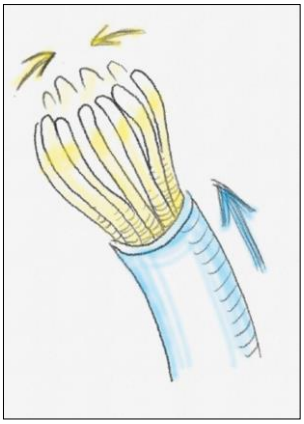

Figure 8: Proposed concept by Paul Breedveld. Displacement between the wire ropes and the sheath straightens the wire ropes and closes the grasp.

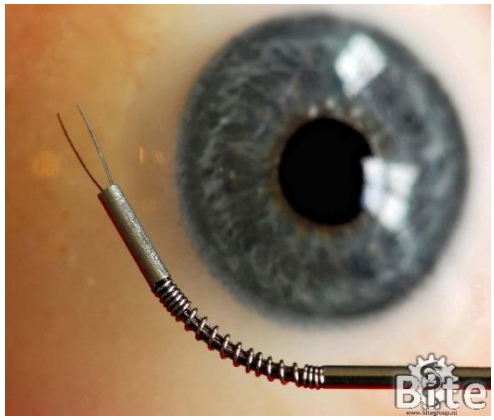

Figure 9: I-Flex developed by the bio-inspired technology group at the TU Delft.

designs have interesting elements a new solution with an open lumen needs to be created.

2.2 Intended Use

The transport mechanism and grasper will be used during minimally invasive surgery. It will be inserted in a natural orifice or through a small incision in the human body. In case of an endoscopy procedure, the device is inserted in a natural opening of the body. The flexible transport mechanism allows the device to move through bends in natural orifices to get to places in the body that are not reachable by stiff instruments. Once the place in the body is reached, tissue can be cut by another instrument and the grasper will pick it up to transport it out of the body.

The main goal of the grasper is to get tissue in the existing flexible transport mechanism. Currently phantom tissue samples have been manually inserted to the transport mechanism with a special tool to test its functionality. This procedure is not possible during surgery. It is desired that a grasper can pick up cut pieces of tissue to not be dependent on other instruments during surgery.

The grasper needs to perform the following steps, also displayed in Figure 13. First the grasper needs to be inserted in the human body. This can be through a natural orifice or incision. Just like the flexible transport mechanism, the grasper should be able to follow any natural orifice curves. In the second step the grasper has arrived at the location of the tissue sample that needs to be transported and the grasper is opened. The grasper must be able to open far enough to let the tissue sample in. After opening, the grasper is positioned around the tissue in step three. In step four the grasper is closed to constrain the tissue. At this point the tissue should not be able to leave the grasper. The tissue is transferred into the lumen of the transport mechanism in step five. When tissue transfer into the lumen has been accomplished the grasper can be reopened to grasp another tissue sample, repeating steps two to five. The alternative is extraction of the grasper as shown in step six when the surgery has been completed. Besides the grasper itself, a system must be developed to operate the grasper. Currently the transport mechanism has a handle to manually actuate the transport motion of the wire ropes. To add operation of the grasper, the handle will need to be redesigned.

The goal is to keep the device operable by one person. The proposed concept uses the wire ropes both for grasping and for tissue transportation. As the wire ropes shift back and forth, they can influence the grasping precision.

2.3 Requirements

Grasper

For the grasper to get tissue into the transport mechanism lumen three requirements need to be

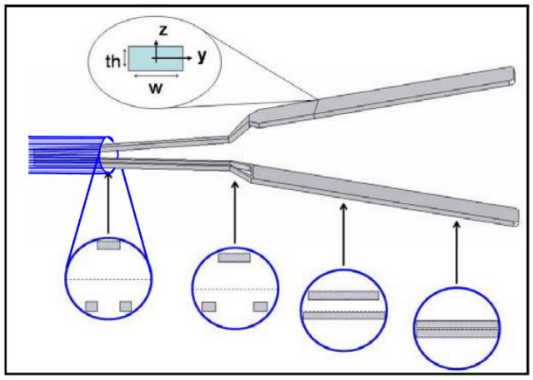

Figure 10: Compliant instrument for endoscopic suturing by Cronin et al. [22]*. The blue sheath slides over the compliant elements. Four cross-sections are shown with the situation of the sheath slid over the elements.*

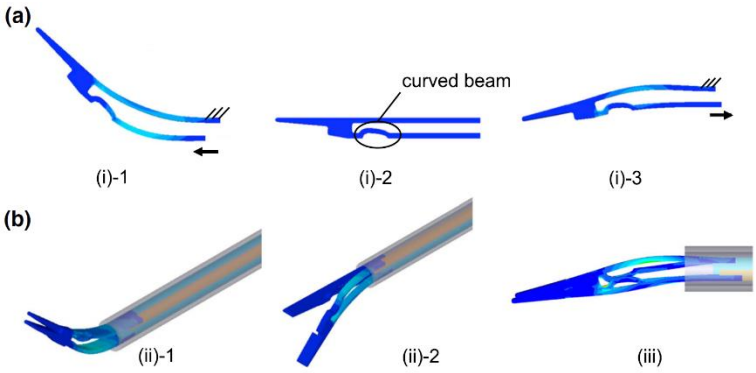

Figure 11: Compliant laparoscopic grasper by Arata et al. [23].

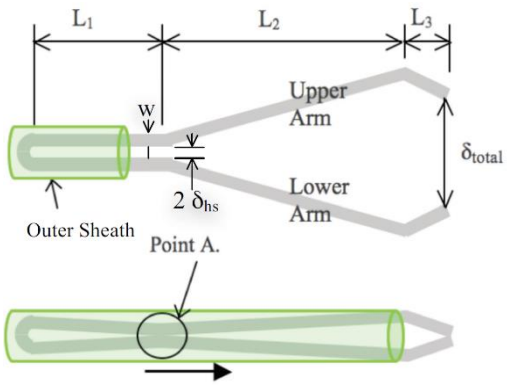

Figure 12: Compliant narrow-gauge surgical forceps design by Aguirre and Frecker [7].

fulfilled.

- The grasper needs to open far enough. The lumen diameter of the transport mechanism is 3.8mm [4]. To be transported, tissue needs to contact multiple moving wire ropes. To ensure good wire rope contact it is preferred that tissue is slightly larger than the lumen diameter. Therefore, 4mm is the required circular opening size of the grasper. If the grasper cannot open far enough to grasp this tissue size, it is not a good match for the transport mechanism as transport cannot be guaranteed.

- When the grasper is closed the tissue needs to be constrained in the grasper. This means that it is unable to leave the grasper once the grasper has closed.

- After closing the grasper, tissue needs to be transferred into the lumen of the transport mechanism.

Operation Handle

Besides the design of the grasper itself, it also needs to be operated. Means to actuate and operate the opening and closing of the grasper need to be designed.

- The device needs to be operable by one person. The operation force should be low enough so the average female can operate it, depending on the operation type chosen. For instance, the available force for a pulp pinch between the thumb and the index finger, is 3.6kg for the major hand. A chuck pinch with the index and middle finger opposing the thumb has an average available force of 5.2kg [8]. These are maximum strength values and should not be necessary to use. When the force that needs to be applied is exerted 30% of the time, while having a 70% rest period, 60% of the maximum force can be used long term, without fatigue [9]. For instance laparoscopic graspers need 15N of input force [10].

- Actuation of the grasper needs to be independent from actuation of the transport mechanism. This is required to assure transporting can be turned off, so it does not influence grasping performance.

Transport Mechanism

Adding the grasper should not limit the existing transport mechanism. To compare the device with the grasper to the original transport mechanism, comparable requirements are used.

- The grasper should be able to transfer tissue into the transport mechanism lumen with the transport mechanism in bent configuration. This is a corner with an angle of 60 degrees and a radius of 59mm. The transport mechanism was previously tested in this configuration. This bending radius is smaller than tested colonoscopes ranging from 60-90mm [11].

- The diameter of the transport mechanism can be maximum 12mm, the same as currently used colonoscopes [12].

- The grasper should not block or collapse the lumen of the existing transport mechanism.

- The transport section has to be at least the same length as the original device, which is 101mm[4].

3 Grasper Tip Design

3.1 Challenges

When designing the grasper challenges can arise. Beforehand the following problems shown in Figure 14 are considered. During **opening and closing of the grasp**, the wire ropes should diverge enough to create an opening for tissue to be grasped. To create the grasper the current wire ropes of the transport mechanism need to be given a diverging shape.

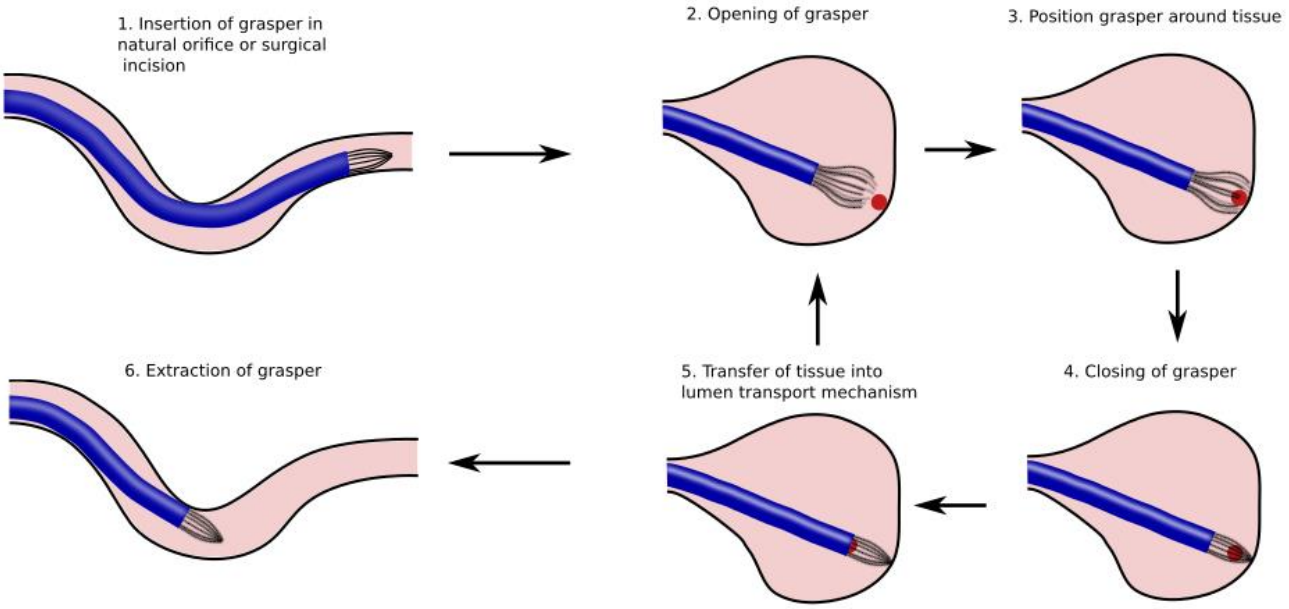

Figure 13: Operational steps in usage of the grasper. 1. The grasper is inserted through a natural orifice or incision. 2. The grasper is opened. 3. The grasper is positioned around the piece of tissue (indicated as a red dot) that must be transported. 4. The grasper is closed. 5. The piece of tissue is transferred into the transport mechanism lumen. Steps 2, 3, 4 and 5 can be repeated. Finally step 6 is extraction of the grasper out of the body.

Currently it is not known what a practical and consistent method is to do the **grasper wire rope shaping**. Tests need to be done with various options to determine what is best.

When closing the grasper, the shape of the wire ropes may pose a problem when pulling all the wire ropes into the sheath. When the radius of the wire ropes to open the grasp is too small, plastic deformation or **collapsing of the lumen** may occur when the wire ropes are retracted and straightened by the magnets in the sheath. A severely collapsed lumen may stop the transport mechanism and grasping from working.

Besides opening and closing the grasper. A **grasper tip configuration** needs to be developed that can pick up and constrain tissue samples. It is important that after closing the grasper, the sample cannot fall out during transfer into the lumen. When designing the tip of the grasper it is also important that the wire ropes remain unentangled. Entangled wire ropes can cause plastic deformation or lumen collapse and make the grasper inoperable. Because of these threats, the shape of the wire ropes for the grasper should be verified to work before making a prototype of the device.

When the device is inserted and extracted it is important that the wire ropes of the grasper are not extended too far out of the lumen and are able to be pushed through a bent section. During insertion and extraction of the instrument the wire ropes of the grasper need to be compact or flexible enough to be able to manoeuvre it through a bent section. During designing of solutions, the flexibility of the transport mechanism needs to be maintained.

Finally, a way of actuating the grasper needs to be developed in Chapter four. Actuating the grasper should not impact the actuation of the transport mechanism. A consideration needs to be made how to combine the grasper with the existing transport mechanism. This also includes operation of the new device. A user-friendly way of operating the device needs to be developed considering the operational steps of the grasper.

3.2 Challenge 1: Opening and Closing of the Grasper

Challenge

To open and close the grasper, wire ropes need to be deformed. A diverging shape of the wire ropes is needed to get the grasper in an open position and be able to position the grasper around the tissue. Putting the wire ropes in a straight shape closes the grasp. This needs to be done in a way that there is no risk of lumen collapse and no entangling wire ropes.

There are two ways to create a grasper with the diverging and straight shape. Deform the wire ropes so their rest position is bent outward in a diverging shape. To close the grasper, they need to be actively straightened. The alternative is having straight wire ropes in a closed rest position that are being actively bent outward to open the grasper. The following solutions create the diverging and straight wire rope shapes.

Solutions

Figure 15A shows the option of using a wire rope that has been given a shape before inserting them into the sheath. In this case the shape is a bend with radius R, indicated by the blue section. When the wire ropes are out of the sheath the grasp is open. The size of the opening depends on the angle of the radius and shape of the tip. To close the grasp, the sheath can be slid over the wire ropes. When the magnets in the sheath are strong enough the wire ropes will be pulled against the wall and straightened like in Figure 15B. This keeps the lumen open for transport. When the magnets are too weak, the lumen will collapse making transport impossible shown in Figure 15C. This needs to be

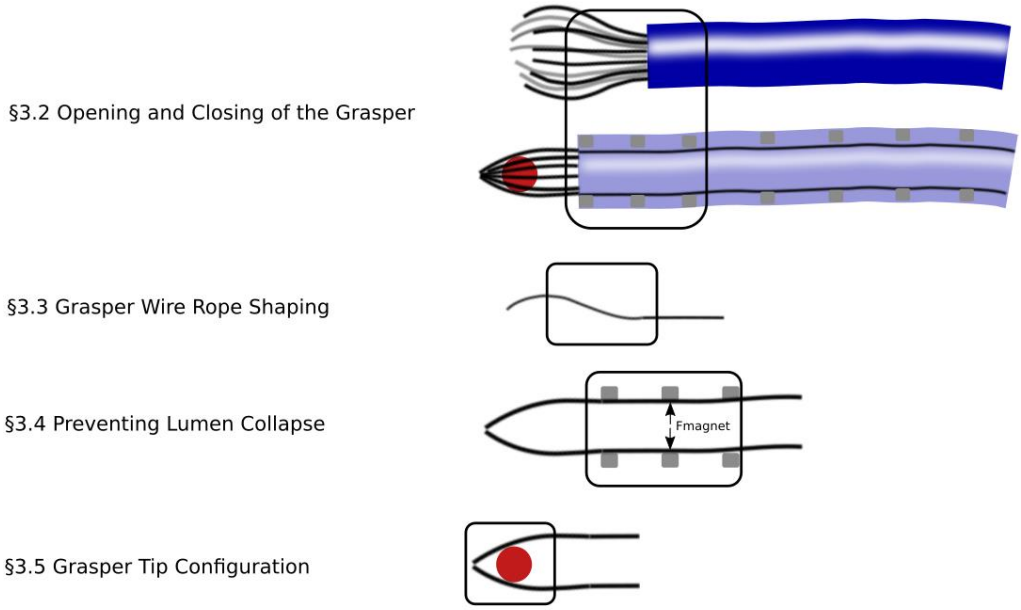

Figure 14: Challenges that need to be solved with the paragraph where the solutions are discussed. Square selection highlights the grasper section discussed in the paragraph.

avoided.

Another option is to use one of the seven wire rope strands to bend the remaining six wire rope strands, see Figure 16. The figure depicts the routing of a single strand of the wire rope through a drilled hole in the magnet. The strand is then reconnected to the wire rope. Figure 16A shows the closed position of the grasp. To open the grasper the sheath is moved relatively to the wire ropes to pull the tip of the wire ropes outward with the separated wire rope strand like in Figure 16B.

It is also possible to actuate a magnet that has a larger diameter than the magnets placed in the sheath. Figure 17 displays the effect on the wire rope angle when the magnet is displaced. The design shown has no need for pre shaped wire ropes as the oversized magnet pulls the straight wire ropes outwards.

Choice

The concept with the preshaped wire rope sections is relatively simple. The same wire ropes, springs and magnets can be used that are in the current transport mechanism. A downside of the opening and closing solution is the needed change of shape of the wire ropes. An investigation will need to be performed on how to achieve this deformation in a consistent way, with a bending radius and angle that still allow the magnets to straighten the wire rope.

The concept with the separated wire rope strand is very complex to manufacture. Separating and reconnecting the strands at the same positions of the wire ropes will be very hard. Also, when opening the grasp the grasper needs to be decoupled from the transport mechanism. It is not possible to move the wire ropes while grasping as the wire rope position determines the opening of the grasper. The wire ropes will need to be temporarily detached from the cam profile for a grasping action, adding another layer of complexity. An advantage of this method is the low risk of lumen collapse as there is no premade radius in the wire rope and the strand separated from the wire rope can act as a support connection to the magnet.

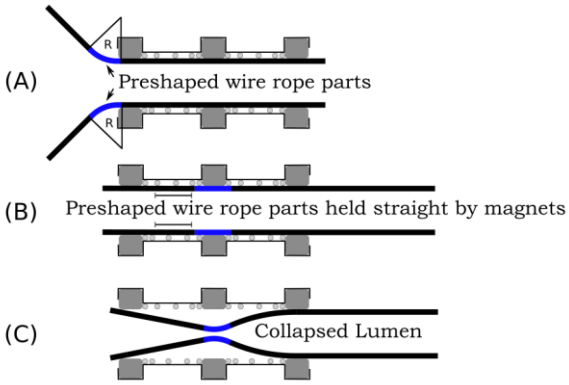

Figure 15: Preshaped wire rope. (A) When the wire ropes are outside of the sheath, they are in open position with a given radius R. (B) When the sheath surrounds the wire ropes the attraction of the magnets pulls the curved wires to the wall straightening them. (C) If the magnets are not strong enough or the radius is too small the lumen collapses.

The concept with the increased diameter magnet also has a low risk of lumen collapse as the wire ropes are kept straight and are bent outward by the magnet with the increased diameter. However, it is possible that the wire ropes detach from the magnet, closing the grasp involuntarily. Another problem is the remaining V-shape when the grasp is closed as was shown in Figure 17B. This shape pushes tissue out and makes it harder for tissue to enter the transport mechanism lumen. The need for a magnet with a bigger diameter increases the tip size, requiring more space during surgery.

While all three designs remain flexible and could work, the concepts with the separated wire rope strand and increased magnet size pose more problems than that of the concept with the bent compliant section in the wire rope. Therefore, the concept with the bent compliant section is chosen to open and close the grasper.

3.3 Challenge 2: Grasper Wire Rope Shaping

Challenge

The compliant section that is bent outward when the grasper is opened needs to diverge far enough to grasp the tissue. To allow for a broad range of tissue sizes a goal of a 10mm opening diameter is chosen. A sketch in Solidworks was made to determine a range of bending radii and angles for achieving a 10mm opening. A range of outward bending radii of 15mm, 25mm and 35mm combined with bending angles of 15, 25, 35 degrees was investigated for use. The outward bending of a 15mm radius combined with a 15° angle, and a 35mm radius with a 35° angle is displayed in Figure 18. A small angle and radius combined needs a straight section added for a sufficiently far opened grasp, as the bent compliant section will not open far enough by itself. A way to create the wire rope shape needs to be found.

Solutions

To determine the best way to obtain the bent compliant

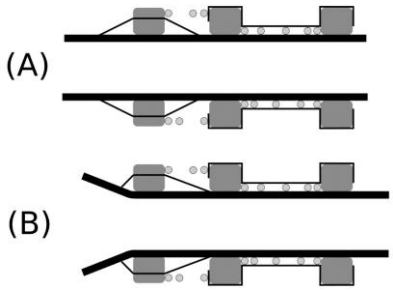

Figure 16: (A) A single strand of the wire rope is routed through a hole in the magnet and used to bend the wire rope open as shown in part (B).

section multiple methods were investigated. Four solutions are considered. Two types of glue. A thin capillary one that can flow between the wire rope strands and keep the wire rope in the desired shape. Also, a thicker metal glue that is applied to the outside of the wire rope is tried to see if there is any change in performance between the place where the glue is applied. Another option is using solder, which is expected to have higher strength compared to the glue but may not be as flexible. Plastically deforming the original wire rope is also considered. This does not increase stiffness of the wire rope while the stiffness is expected to increase with additional materials. When all options fail a combination of solutions can also be tried. For instance, plastically deforming the wire rope, combined with a glue or solder.

Experiment Goal

Determine the best method to shape the wire ropes in a 35mm radius and 35-degree angle.

Variables

The independent variables are the deformation methods used. Thin Cyanolit capillary glue, Bison two component metal glue, soldering the wire rope and plastic deformation. The dependent variable is the resulting shape of the wire rope.

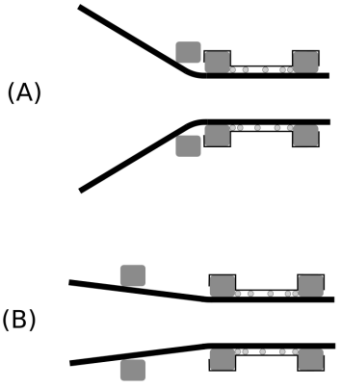

Figure 17: Actuated magnet with a different diameter changes the outward angle of the wire ropes between situation A and B. This can be used to open and close the grasper.

Method

To get the wire rope in the desired shape and modify bending stiffness two strategies were used.

- Plastic deformation
- Adding material on the wire rope to maintain a given shape, like glue and solder.

A mould was developed with the ability to constrain the wire rope in the desired bending radius and angles (35mm, 35°). Two glues were used. A thin capillary one, Cyanolit [13] and thick two component Bison metal epoxy glue [14]. The solder used was a general tin/lead alloy. Welding was not used as it was advised by DEMO that this would cause brittleness in the wire ropes. Before treating the wire ropes possible contaminations were removed using refined petrol. After constraining the wire rope, the treatment material is added. The 35-degree bending angle and 35mm radius were drawn on a piece of paper. After treatment the wire ropes were placed on the paper to see whether the desired curve was obtained.

Setup

Figure 19 displays the mould used to clamp the wire ropes in a fixed position to obtain the desired radius and angle. Straight grooves were put in the 3D-printed parts to constrain the wire rope and to ensure bending only occurs in the open area that is treated with glue or solder. For plastically deforming the wire ropes a 3D-printed tool with multiple cylindrical diameters was made. Multiple diameters were printed to find the right shape to constrain the wire rope in a bend with a radius of 35mm.

Results

Figure 70 displays the shape of two wire ropes that have been clamped in the mould at an angle of 35° with a radius of 35mm and treated with Cyanolit glue. The curved line dawn with pencil is the shape of the

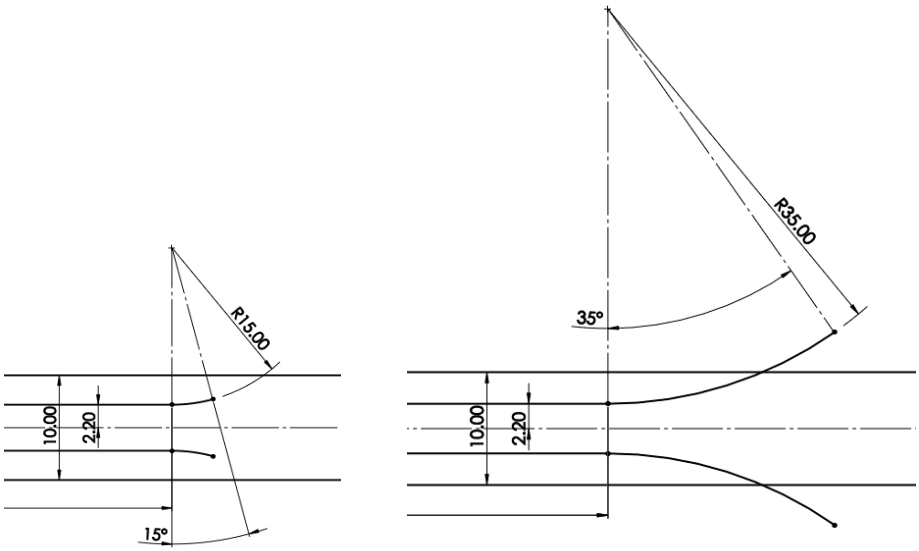

Figure 18: Picture of minimum outward shape of a radius of 15mm combined with an angle of 15 degrees and the maximum outward shape of a radius of 35mm combined with a 35 degree angle. The dotted line is the center of the lumen.

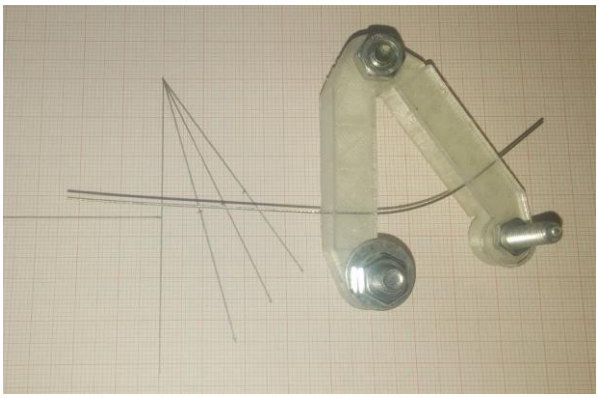

Figure 19: Mould to constrain the wire rope in desired 35mm bending radius and 35-degree angle while leaving space to apply glue and solder.

wire rope in the mould. After releasing the wire rope, the wires do not remain in shape. The same happens with the wire rope treated with Bison two component epoxy metal glue. In both cases changing the mould to 'overbend' the wire rope during applying the glue, it results in a shape closer to the desired one shown in Figure 71. Though to get the exact desired shape multiple tries with different moulds are needed.

Soldering and plastic deformation are shown in Figure 20. The soldered wire rope remains in the shape of the bend put in the wire by the mould with only a slight error. Also, the surface finish of the soldered wire rope was very rough. Plastically deforming over a 10mm radius for 180° also results in a curve with the right shape. Using a 3D-printed tool with various steps in diameter to wrap the wire rope around it was relatively easy to get a consistent deformation.

Choice

Only plastic deformation and soldering succeeded in matching the desired bent shape. The glues needed a different mould to induce extra bending as the glues were not able to hold the shape after releasing. Even then the desired shape was not achieved. The surface finish of the soldered wire rope was very rough, not allowing good contact with the magnets. This will lower the magnetic force available to straighten the wire rope. Therefore, it was decided to create the compliant bent wire rope section by plastic deformation.

3.4 Challenge 3: Preventing Lumen Collapse

Challenge

Now a convenient method of creating the diverging wire rope shape has been found, the bending angle and radius of the deformation need to be determined. Important is that the deformation remains after straightening the wire rope to close, otherwise the grasper will not open far enough after one use cycle. Also, the force of the magnets needs to be strong enough to straighten the wire ropes for closing. If the magnet force is too low the wire ropes can detach from the magnets causing lumen collapse. The correct combination of wire rope bending radius and angle needs to be found.

Solutions

To evaluate the effect of different outward angles and tip shapes on lumen collapse, multiple tests were performed. First, the magnetic force needed to keep the straightened wire rope connected to the magnet to prevent lumen collapse was investigated by a bending simulation using Ansys APDL. Figure 21 a simulation example. For each bending radius combined with the bending angle a model is made. By applying forced displacements on the simulated wire rope Key Points 2, 4 and 6, straightening is achieved. The wire rope reaction force in Key Point 4 is calculated. This is the force the magnet needs to provide to straighten the wire rope and prevent detaching from the magnet. The process and results are displayed in Appendix II and Table 1. The smallest force needed to straighten the wire rope occurred with a 35mm radius combined with a 35-degree angle. As expected, a smaller radius, thus a sharper corner needs a stronger force.

After determining the needed magnet force on the wire rope, another simulation in Appendix II investigates the actual available force of the magnet on the piece of wire rope. Because exact magnetic material properties of the wire rope are not available according to the

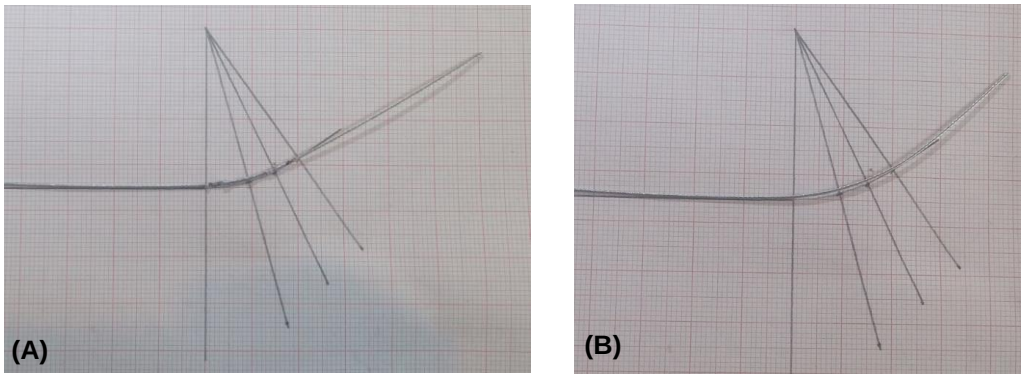

Figure 20: (A) Soldered wire rope remaining in a 35° angle and 35mm radius shape after being released from the mold. (B) Plastically deformed wire rope after bending 180°over a 10mm radius. Both follow the expected curve close.

manufacturer, it was decided to perform a test to empirically investigate lumen collapse.

Experiment Goal
Determine at what bending radius and angle from Table 1, the magnet can straighten the wire rope without lumen collapse.

Variables
Independent variables: Bending radii 15mm, 25mm and 35mm. Bending angles of 15, 25 and 35 degrees.
Dependent variable: State of the lumen after pulling in the wire rope to straighten it. Open or collapsed.

Method
Three wire ropes are soldered together at the tip and are plastically deformed in a bend according to the variation to be tested. First the 35mm radius combined with the 35° angle is made. In the Ansys APDL simulation this configuration needs the lowest magnetic force to straighten the wire rope. When unsuccessful there is no need to test the other configurations as they require a higher magnet force. If this configuration is successful a 25mm or even 15mm bending radius will be tested to see if a more compact version of the grasper is possible. A smaller radius results in a shorter grasper. When a lumen collapse appears a second attempt will be done with more distance between the magnets. This creates a larger bending moment in the middle of the compliant wire rope section and may allow straightening with the same magnet force. If this does not help, the configuration will be dropped and means that configurations in Table 1 with a higher needed force are not feasible. If straightening is successful there will be a check to see whether the wire rope has been plastically deformed.

Setup
A modular version of the transport mechanism is developed to test different bending radii and angles and is displayed in Figure 22. It can be opened from the side to see any wire ropes detaching from the magnets. The number of magnets can be varied as well as the distances between them. A sheet of paper was used to check for plastic deformation of the wire ropes.

Results
Pictures of all results are shown in Appendix III. Figure 22A displays the group of bent wire ropes with a 35-degree angle and a 35mm radius. In Figure 22B the wire ropes are successfully straightened by the force of the magnets without collapsing into the lumen. Comparing the shape of the wire rope group before and after straightening shows that the previously applied plastic deformation remains after straightening. The wire ropes with a bending radius of 25mm over an angle of 35-degrees collapse. This also happens with magnets placed further apart. The extra distance between the outer magnets increases the bending

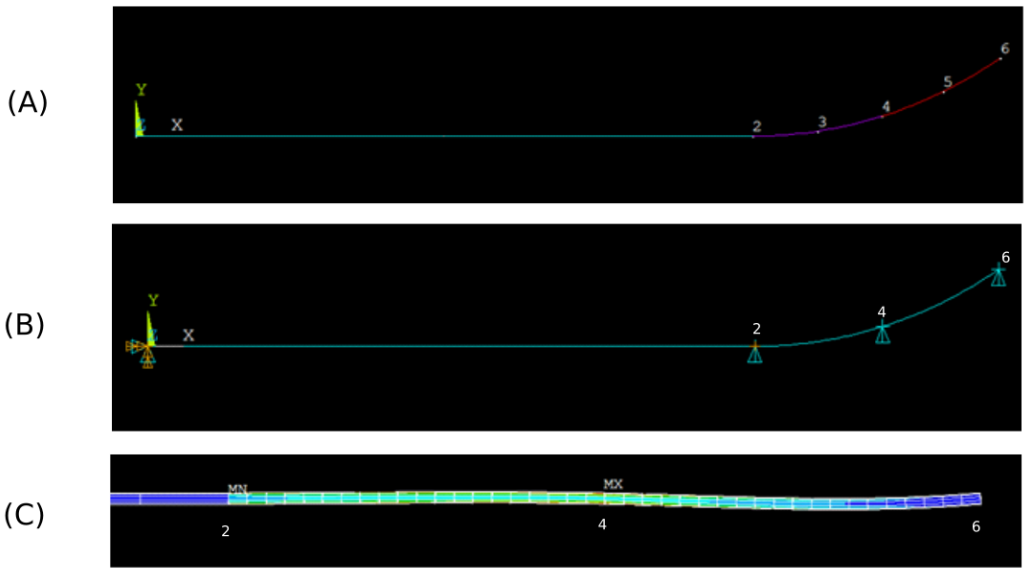

Figure 21: Ansys APDL screenshots of a plastically deformed wire rope that is straightened. (A) Shows the Key Points 2-6, used to create the curve. (B) Displays the points where constraints and forced deflections are applied to straighten the wire rope. (C) Displays the final deformed result with Key Point 4 being the point where the magnet force applies.

Table 1: Reaction forces in Key Point 4 needed to prevent the collapse of the lumen.

Radius \ Angle	15 degrees	25 degrees	35 degrees
15mm	6.2161 N	3.7985 N	2.7274 N
25mm	2.2780 N	1.3765 N	0.98528 N
35mm	1.1679 N	0.70358 N	0.50316 N

moment in the middle with the same magnet force but it is not enough to prevent lumen collapse.

Choice
The bent wire rope with a radius of 35mm over an angle of 35-degrees is successfully straightened by the magnets. A bending radius of 25mm over an angle of 25-degrees collapsed in both the standard configuration and a configuration with extra magnet distance. Because of this, bending radii of 15mm and 25mm will not be considered for making the grasper. As the 35mm radius bent over 35 degrees compliant section opens the grasper far enough for an opening of 10mm, this will be used in further development. Now the compliant section is determined, a closer look will be taken at possible grasper tip configurations.

3.5 Challenge 4: Grasper Tip Configuration

Challenge
Now a way of opening and closing the grasper has been developed. A tip on the wire ropes is needed to constrain tissue in the closed grasp. This is done by exerting a force on the tissue with contact points. Depending on whether the tissue is constrained by friction or by shape a minimum number of contact points is needed to fully constrain an object. A 2D spherical object needs two contact points opposite to each other when friction forces on the object are high enough. This situation is displayed in Figure 23A. The object cannot translate in x direction due to the contact oints normal forces Fn and not in y direction due to the friction force Fmu. Without friction an extra contact point is needed as shown in part B of the figure. Here, translation in x and y direction is blocked but a rotation is still possible. Part C and D show the amount of contact points needed to constrain a sphere and a cube. The grasper that needs to be designed does not have to constrain all translations. Entrance into the lumen should remain open for tissue to be transferred into the transport mechanism. To create contact points on the tissue, the right tip shape and tip arrangement needs to be chosen.

Tip Shape Solutions
Options to open the grasper wire ropes have been explained. Though these options need a tip shape to enclose tissue. Figure 24 shows three possibilities in open and closed positions. Figure 24A displays a grasper with a bent tip. The tips bending angle is lower than 90-degrees. An alternative is having a tip with a bending angle of over 90-degrees.

Tip Arrangement Solutions
The bending radius and angle of the compliant section is determined but there is no shape at the tip yet to

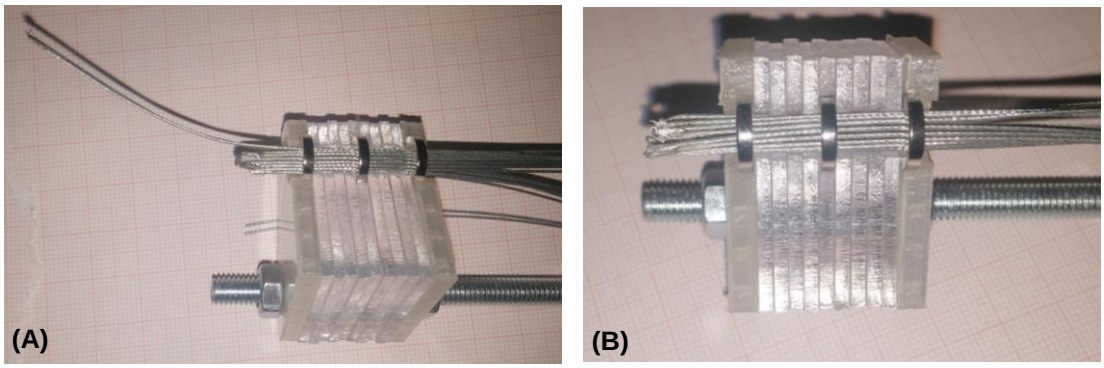

Figure 22: (A) Bent group of three wire ropes, connected with solder at the tip. (B) Group of wire ropes is pulled into the magnets without collapsing the lumen.

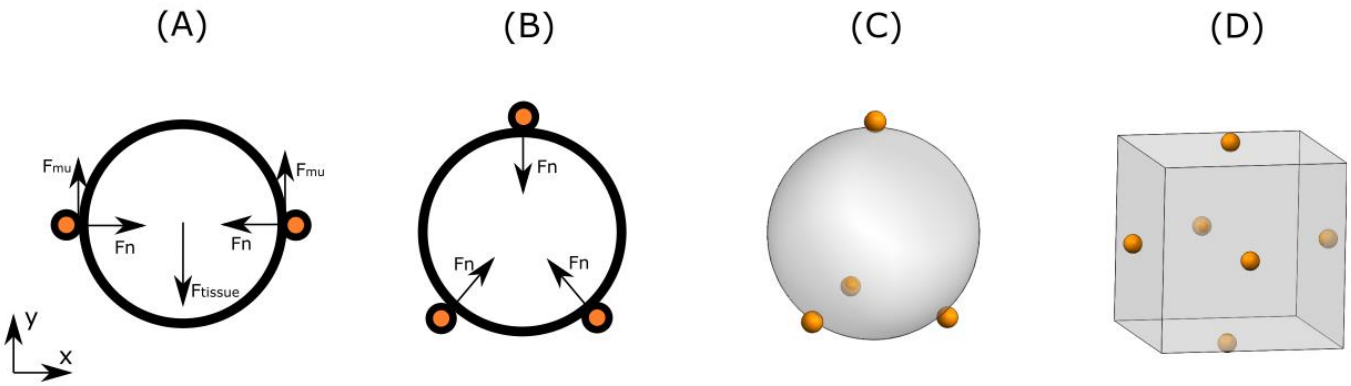

Figure 23: Spherical object constrained in by contact points in 2D with friction A and without friction B. Part C and D show the amount of contact points needed to constrain a 3D sphere and cube.

constrain tissue. The current transport mechanism design has six groups of three wire ropes. Each group is actuated by one slider on the cam. This is done to not need a slider in the cam for each individual wire rope. The individual wires in the tip are very sensitive to twisting when moving. They are never fully straight which makes them behave in an unpredictable way. Because of these imperfections the wires make a small rotation in different directions when moved back and forth by the cam. this will lead to an inconsistent grasp shape and makes it impossible to pick up a piece of tissue in a controlled manner. Therefore, to add stability multiple wire ropes are connected in groups at the tip.

Figure 25A shows the arrangement of straight wire ropes inside the magnetic ring and is the current input of the transport system. It is not possible for all wires to converge to the centre. They will touch and leave a hole making it possible for tissue to escape as in Figure 25B. Because of this problem other arrangements are considered. Figure 25C has four of the eight groups converging to the centre and the rest of the wire rope groups are straight to leave room for the converging pairs. Significant changes need to be made to the existing mechanism to increase from six independently actuated pairs to eight actuated pairs. The configuration in Figure 25D is similar but does not need these modifications as it complies with the original six groups of three wire ropes. Option E is rotation symmetric. Each group of three wire ropes has the middle rope converge towards the centre when closing the grasp. The three tip configurations are made to see what their up and down sides are.

Tip Shape Choice

Shape A has no risk of entangling and is easy to manufacture as the bend in the tip has a relatively big radius and can be plastically deformed. Shape B can be more reliable in keeping tissue constrained in the grasp as the hook shape prevents tissue from falling out. On the other hand, the sharp wire rope ends can also puncture tissue and make it get stuck and impossible for tissue to transfer into the transport mechanism lumen. For B there is also a risk of wire ropes hooking into each other when they are bent and being actuated for transport. The shape in Figure 24C is more complex to make by having a diverging and converging radius at the tip. However, the shape makes it easy to insert tissue in the grasp due to the outward pointing round edges but also makes entangling wire ropes a risk.

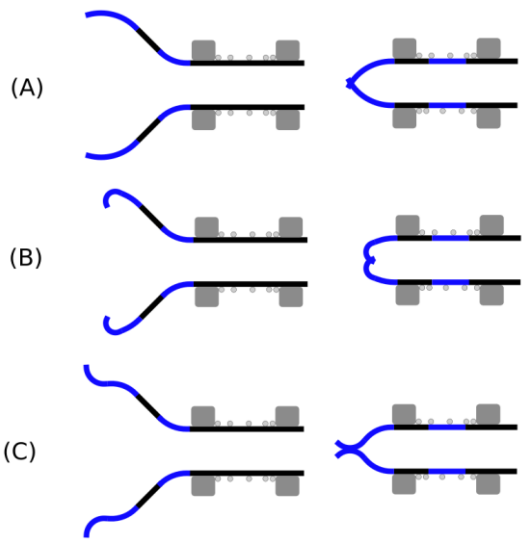

Figure 24: Pre shapes wire ropes with the pre shaped parts highlighted in blue. A shows a tip with a big radius. B shows a tip with a low radius. C displays a tip with a converging and a diverging part.

While all pictured tip shapes can constrain tissue, the design in Figure 24A does not have the risk of entangling tip wire ropes and is the easiest to fabricate. The pointy tip of A is also suitable to grasp tissue from a surface when the transport mechanism is in orthogonal orientation to it. Design B and C cannot fully reach around tissue when the tip is pressed against a surface. For these reasons, the shape in Figure 24A was chosen to be used.

Tip Arrangement Choice

To see practical limitations of the tip arrangements, prototypes were made. First configuration C was made by plastically deforming the wire ropes and soldering them together. Figure 26A shows the result. A problem when trying to shift the bent wire rope groups back and forth is that they get stuck on the pair next to them due to the bent tip as displayed in Figure 26B.

Configuration D and E did not have this problem. A problem that both C and D do have is the possibility of tissue being pushed to the side or even out of the grasp when the transport system is being actuated. When a pair of wire straight wire ropes is slid back a gap is created. This gap can be closed by making the straight wire rope groups longer than the converging wire rope pairs but that makes it impossible to grasp tissue from a flat surface in a perpendicular orientation. Type E configuration does not have this problem unless the piece of tissue is smaller than half the lumen diameter which is 1.9mm. Each tip of the wire rope groups converges to the centre of the grasper and contributes to pushing tissue towards the centre of the transport mechanism lumen. The smaller gap of arrangement E combined with the fact that each wire rope contributes to pushing tissue to the lumen centre is the reason that configuration E was chosen to create a prototype.

Design Integration

Two versions of the type E configuration were made. The first suffered lumen collapse. After changes to the fabrication method and design, the second version was able to grasp and constrain a piece of sponge successfully. After multiple times of opening and closing the grasp, torsion of the wire ropes occurred, deforming the grasper.

As shown in Figure 29 two problems can cause deformation of the grasper. Torsion of individual wire ropes and movement of the wire ropes over the magnet surface. To stop torsion of individual wire ropes, the wire ropes are connected in the tip. Besides this they should also be constrained on the other end of the wire ropes in the sliders. A 3D printed ring to clamp the wire ropes was made to simulate this situation, shown in Figure 30. This figure also shows that the wire ropes are still moving over the magnet surface. To stop movement of the wire ropes over the magnet surface, wire rope guides were made to constrain the wire ropes. Two small pins divide the wire ropes in two groups of nine and prevent any unwanted movement of the wire ropes over the magnet surface. The guides are placed on the side of the magnet as shown in Figure 31.

The wire rope guides will be placed on the magnets of the grasper tip as well as on the magnets in the shaft of the transport system. Figure 32 shows a schematic overview of the grasper magnets and transport mechanism magnets combined with the wire rope guides. The wire rope guides on magnets 1 and 3 divide the same wire rope groups to not add any bending in the grasper section. This can cause collapse of the lumen. In the section of the transport mechanism the wire rope guides are rotated as shown on Magnet 5, 7 and 9. This is done to divide the force of the wire rope guides over different wire rope groups. When the wire rope groups are always split in the same place, the force of multiple wire rope groups pressing on the guide risk wire ropes skipping over the guide. At the grasper tip and slider connection of the wire ropes the precautions against individual wire rope

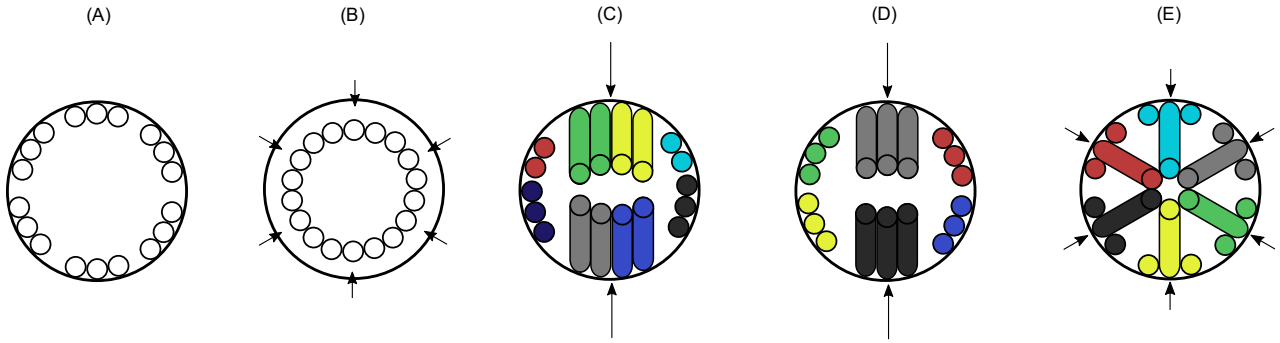

Figure 25: Tip configurations. Each coloured wire rope group is separately actuated by the cam. (A) Straight tip arrangement. (B) All tips converging to centre. As there is no space a big hole remains. (C) Four pairs of two wire ropes converging to the middle. (D) Two pairs of 3 wire ropes converging to the centre. (E) Six pairs of three wire ropes with the middle wire rope of each pair converging to the centre.

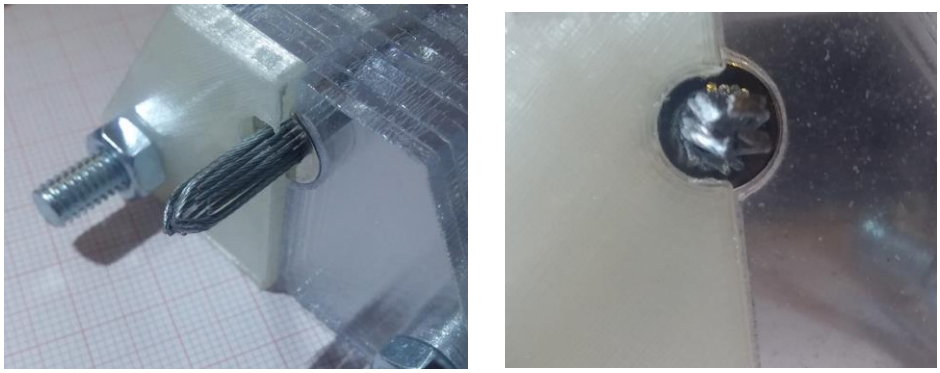

Figure 26: Two pairs of two soldered wire ropes with bent tips opposing each other. On both sides to prevent tissue from falling out four straight wire ropes are placed.

Figure 27: Two pairs of two soldered wire ropes with bent tips opposing each other. On both sides to prevent tissue from falling out two pairs of three soldered straight wire ropes are placed.

torsion are shown as previously discussed. This design was successful. Due to the straight section the grasper is longer than the first version but still opens far enough to grasp tissue the size of the lumen. The grasper was successfully able to pick up a piece of sponge in perpendicular orientation to the paper displayed in Figure 28. Due to the sponge being smaller than the opening distance between two wire rope groups of three, it is also possible to grasp from the side. Shifting the wire rope groups one by one manually successfully transported the sponge.

4 Actuation Design

4.1 Components to Actuate

To create the grasping motion and make the preformed compliant section straight, the wire ropes need to move relatively to the sheath. This motion can be achieved in multiple ways, by moving different components. A consideration needs to be made what the impact of each option is and what is the most effective solution. Besides choosing what components to move for actuation of the grasper, placement of the sliders and the cam that actuates the transport mechanism is also important.

Figure 33 schematically displays the transportation system with the grasper. Part A is the sheath, B the wire ropes, C the cam and component D the motor that actuates the cam. Part E is the housing that is fixed to the ground and F the tissue that needs to be grasped. To achieve the relative motion either the sheath or wire ropes have a connection to the ground while the other is displaced.

An option to do this in section one of Figure 33 is using a pulley system. The length needed to extend the wires for grasping is ‘stored’ in adjustable pulleys. When a pulley is shifted the ‘stored’ wire rope is used to push the grasp open. This can be done while cam actuation of the transport mechanism is maintained.

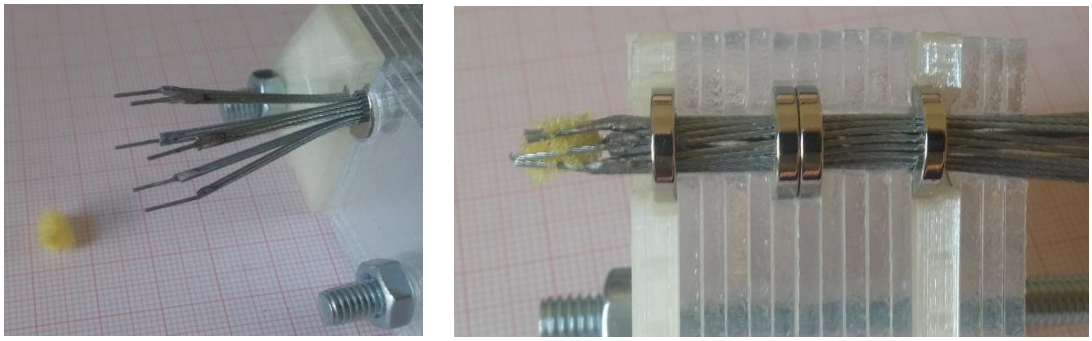

Figure 28: Multiple pictures of grasping a piece of a sponge. Picture A shows the open grasper. As can be seen in B, torsion of the wire ropes occurs after closing and opening a few times.

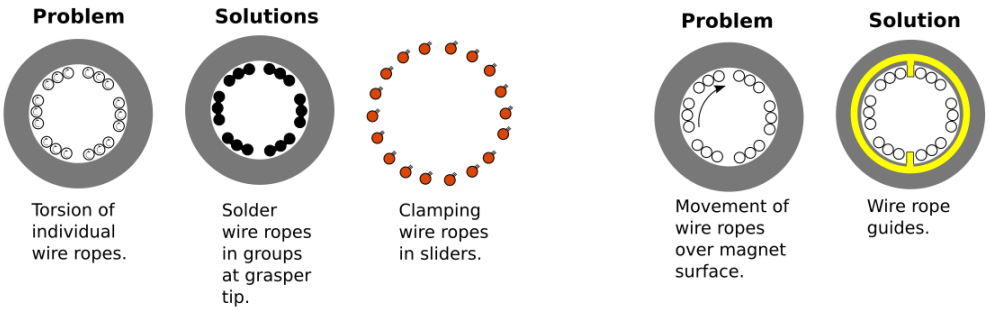

Figure 29: Solutions against deformation of the grasper. Grey being the magnets, yellow the wire rope guide, black the wire rope groups soldered together in the grasper tip and red the wire ropes clamped in sliders.

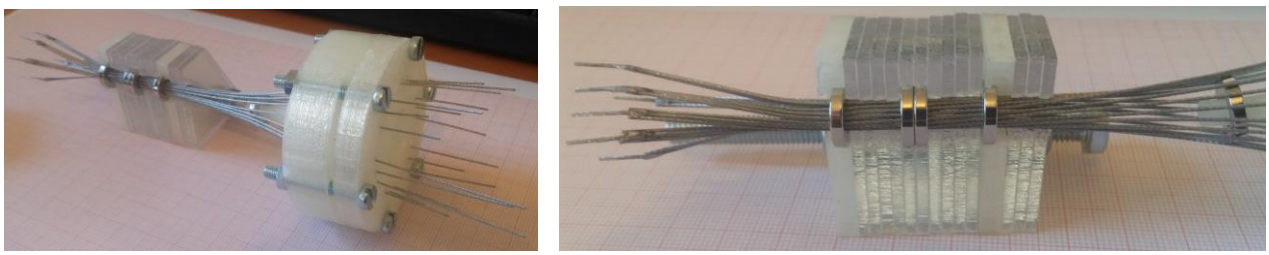

Figure 30: Wire ropes constrained with ring. Not solving the torsion problem that occurs after opening and closing multiple times. Wire rope guides are needed as a combined solution.

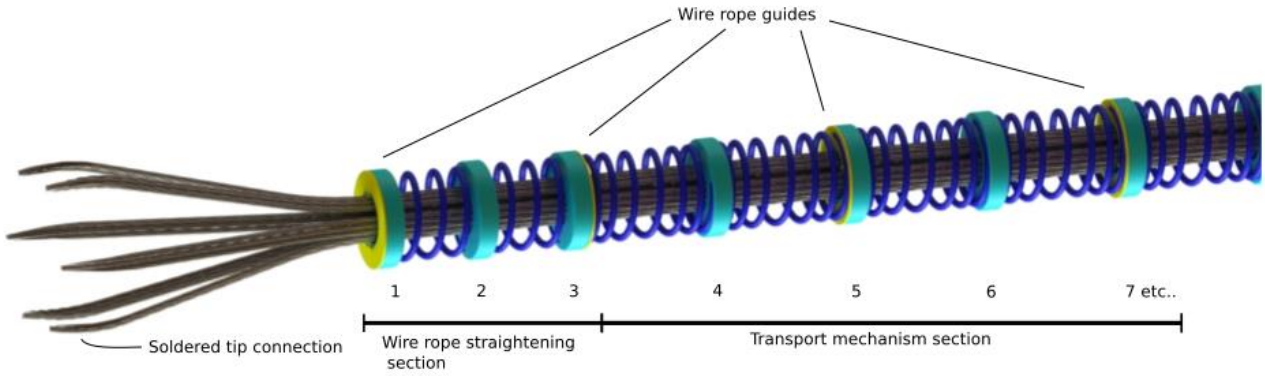

Figure 31: Final grasper design. With the wire ropes in grey, the magnets light green, the wire rope guides in yellow and springs in blue. Magnets 1,2 and 3 form the section where the wire ropes are straightened to close the grasper. Magnet number 4 and higher are part of the transport mechanism and have more space between them. The yellow wire rope guides keep the wire ropes in place.

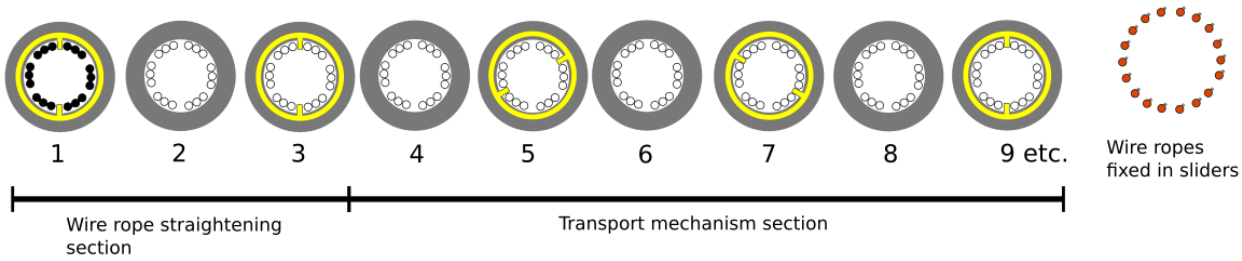

Figure 32: Grasper and transport mechanism magnets with wire rope guides. The first three magnets are used to straighten the wire ropes and close the grasper. Grey being the magnets, yellow the wire rope guides, black the wire rope groups soldered together in the grasper tip and red the wire ropes clamped in sliders. Wire rope guides on keep the grasper in shape. To not add any additional unintended bending the wire rope guides on Magnet 1 and 2 split the same wire rope groups. In the transport mechanism section the wire rope guides are rotated as can be seen on Magnet 5, 7 and 9. This is done to divide the sideways

An option in section two of Figure 33 to perform the grasp is displacing the cam that drives the wire ropes. Doing this will also retract or extend the wire ropes. It must be considered that the cam is fixed to a motor and needs to have a bearing to facilitate the rotating motion.

The last option to grasp by displacing the wire ropes B is to take all components B, C and D in section three and make them slidable in the housing. This can be done by placing the parts on a linear guide mounted on housing E. Another solution is to make the sheath A slidable. This is relatively simple if it is guided properly in linear direction just as the previously mentioned solutions.

Displacing the sheath instead of the wire ropes is another way to open and close the grasper. This is favourable as the sheath only needs a connection to the housing. The wire ropes also interact with guidance by the housing and the cam. A sliding mechanism can be made to connect the sheath and the housing while leaving a translational degree of freedom unconstrained for movement relative to the wire ropes.

It is also possible to actuate the grasper in the tip. The relative displacement of the tip magnets compared to the wire ropes opens and closes the grasp. This does require wire ropes that do not contribute to transporting tissue. The wire ropes can pull back the magnets in the tip to open the grasper and a spring between sheath magnets and tip magnets can close the grasper by sliding the tip magnets back.

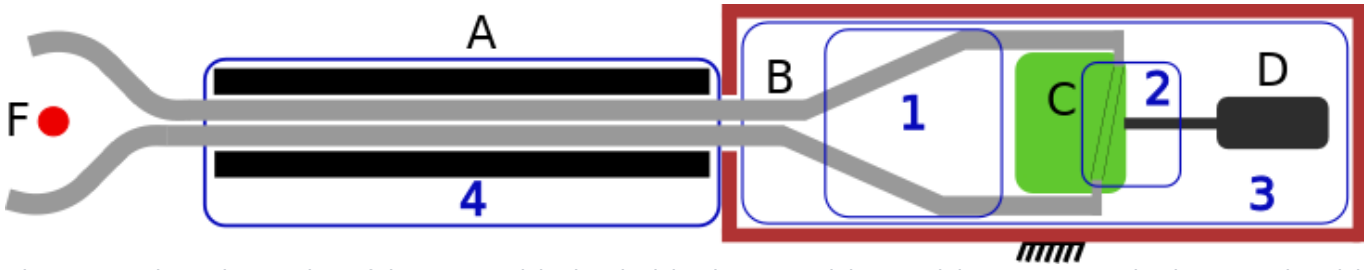

Figure 33: Schematic overview of the system. (A) Sheath, (B) Wire ropes, (C) Cam, (D) Transport mechanism actuation, (E) Housing connected to the ground. Options to move different components or component groups for grasper actuation are numbered from one to four.

An alternative to mechanical actuation in the tip is using an electromagnet. The magnet can be actuated by current that runs through the wire ropes of the transport mechanism. Though the magnet coil would need to fit in the tip and exert enough force.

Mentioned options to create the relative motion between the sheath and the wire ropes have up and downsides. A downside from using a pulley system to retract and extend the wire ropes is the complexity of the moving pulleys and a bent wire rope that needs to be thoroughly supported to prevent buckling. Support will need to be provided by multiple rollers to not increase friction. Moving the cam C is more realistic but also has problems. As the cam is constantly actuated by for instance a motor or manual transport mechanism actuator D, the drive shaft or transmission needs to be able to adjust to the movement as the motor is fixed to the housing E. This can be hard to do as the constant force on the transmission makes sliding solutions have extra friction. Displacing components B, C and D in section three to move the wire ropes can be done by placing the parts on a linear guide mounted on the housing. This option is realistic but will lead to a big device as it comes down to making a smaller housing inside the external housing to mount for the cam, motor and guiding of the wire ropes.

Instead of moving the wire ropes it is also possible to move the sheath. This is very favourable as the sheath only needs a connection to the housing. The wire ropes B, cam C, and transport mechanism actuator D have the other components interacting with them. Moving the sheath only requires a slider between the housing and the sheath.

Actuation in the tip of the sheath is also possible. A downside of this is that it needs wire ropes for actuation of the opening action and a spring for the closing action. The transport wire ropes cannot be used as every wire rope that is not moving with the other transporting wire ropes is working against it. Putting wire rope on the outside magnets is possible but creates unwanted steering when the transport mechanism is put in a bend. When the sheath is bending, a length difference occurs between the actuation wire ropes causing unwanted steering of the tip. This needs to be compensated, causing a complex device. Also introducing a spring that needs to compress a significant amount can introduce buckling in the sheath. Instead of mechanically actuating the tip, it can also be done with an electromagnet. An upside of electric actuation in the tip is that the friction force of multiple sheath magnets does not need to be overcome as the energy is transferred to the tip by electricity. A downside is that a coil needs to fit in the tip with a good sliding electrical connection to the wire ropes. Also, the stroke needed to displace the sheath and close the grasp is about 20mm. Relatively this is a very long stroke for a magnet with a maximum diameter of 10mm with a hole of 5mm and the force will be too low for actuation over the full stroke.

Because the sheath only needs a sliding connection to the housing it was chosen as solution to actuate the grasper. Other options had more complex problems to be solved without having a significant advantage.

4.2 Opening and Closing Configurations

A way to perform the manual actuation must be determined. Manually opening and closing can be done in various ways, each with their own advantages and disadvantages. As explained before the sheath will be moved to open and close the grasper. Operation needs to be user friendly and the circumstances where the grasper will be used in need to be considered.

The first possibility is creating a voluntary closing grasp. Figure 34A displays movement of the sheath (black) connected to a slider that guides the movement (yellow). While closing the grasp, actuation energy from the operator is stored in a spring, also shown in the figure. When the operator releases this force, the energy stored in the spring actuates the return motion to the open state.

A second possibility is a voluntary opening configuration in Figure 34B. When the slider is actuated to the right and the spring in the system is compressed the grasp opens. To close the system the actuation force is removed, and the force of the tensioned spring closes the system.

There is also a bi-directional configuration option without energy storage in a spring as displayed in Figure 34C. The operator will need to actuate the slider in both directions. Though the sheath is being ‘transported’ to the right by the moving wire ropes, putting the system in an open position. This can be solved by introducing a lock.

A hybrid of the voluntary opening configuration and the bi-directional configuration is also possible. This has the same design as the voluntary opening configuration, but no manual force needs to be applied to keep the grasper open. The pretension of the voluntary opening grasper is set lower to a force so it can stay in open and closed position, but it still counteracts the friction force on the sheath when the transport mechanism is actuated. This can be done because the static friction of the wire ropes on the magnets in the sheath is higher than the dynamic friction.

Mechanisms to actuate the opening and closing configuration are shown in Figure 35. Figure 35A displays a trigger mechanism. The trigger is connected by a flexure to the slider. The flexure is wrapped around the cylinder section of the trigger. The axis of the trigger is constrained in moving left or right but not up or down. With this design it is possible to try different diameters of the cylinder section of the trigger. A different radius of the trigger for a different transmission can be tested while only needing to change the connection of the flexure.

Figure 35B shows another possible type of actuation. By putting the index and middle finger on the sheath the slider can be actuated. Another grip for the thumb on a fixed part is needed to provide an opposing force within the hand and give comfortable actuation. Because there are two fingers on each side of the sheath contracting towards each other, no bending

moment is created. This way no unnecessary friction force is added in the sliding of the sheath.

An overview of the upsides and downsides of each configuration is given in Table 2. A downside of a voluntary closing grasper is that to keep the grasp closed a constant force needs to be applied which can be very exhausting. During insertion and extraction, the grasper also needs to stay closed. This needs to be done, as an always opened grasp takes up space and can unwantedly touch organs or other instruments. As the transport mechanism is actuated to transfer tissue into the lumen of the transport mechanism the grasper also needs to stay closed. The friction force of the wire ropes on the sheath makes it that the sheath is also being transported in the same direction as the tissue sample. These two situations make a voluntary closing grasper unfavourable as a lot of the time a force from the user is needed without performing a grasping operation. Another problem is that when the transport mechanism is scaled up and elongated the force to open it becomes very high.

It is favourable to use a voluntary opening configuration to counter the problems of a voluntary closing configuration. Springs keep the grasper closed when no force by the user is applied. When these springs are pretensioned in voluntary opening configuration, they counter the transportation friction force of the wire ropes on the sheath and prevent the grasp from opening. This is an upside compared to the voluntary closing configuration. A downside is that a manual force still needs to be applied to keep the grasper open.

A bi-directional grasper without a spring will stay in open or closed configuration when it is put there. Though, without a constant force from the user or a lock the grasper will open when the transport mechanism is actuated due to the transport friction force on the sheath just like the voluntary closing configuration. Without a lock this configuration is not feasible. Also, when the transport mechanism is scaled up and elongated friction of the sheath will make opening and closing require a high manual force.

4.3 Final Actuation Design

There is a possibility to take the voluntary opening configuration and lower the pretension of the springs to turn it into a bi-directional configuration that does not need a lock and still stays in the position it is put in. To achieve this the pretension of the springs is tuned beneath the static friction, but above the dynamic friction force of the wire ropes on the sheath. This way the grasper stays closed when the transport mechanism is actuated to transfer tissue into the lumen, but no constant force needs to be applied to keep the grasper open. When the transport mechanism is elongated in the future this concept can still work, though independence between the grasper and the transport mechanism is partially lost. When friction is increased due to the extra number of magnets contacting the wire ropes the springs also need to be stronger to counteract the transport mechanism. If the transport mechanism is actuated to assist in opening only a low manual force is needed. This configuration is chosen as it has the upsides of the voluntary opening configuration and bi-directional configuration without needing a manual force or lock to keep the grasper in place.

The grasper can be actuated by either a mechanism with a transmission like the trigger in Figure 34A or without a transmission with four finger holds like in Figure 34B. The stroke of the shaft needed to open and close the grasper is approximately 20mm, observed from the prototype in Figure 28. This stroke distance is suitable for human fingers. A small experiment was conducted to estimate the actuation force needed to slide the sheath back. The weight needed to start sliding three magnets with 13mm spacing was measured. Five measurements resulted in an average weight of 278g. This means that 15 magnets have a friction weight of 1390g. As springs need to overcome this weight when the transport

Table 2: Summary of up and downsides of grasper configurations.

Grasper configuration type	Configuration type upsides	Configuration type downsides
Voluntary closing	- Grasper is normally open.	- Grasper is normally open. This means that a lock or closing force needs to be applied on the sheath during insertion, extraction and when the transport mechanism is active.
Voluntary opening	- Grasper stays closed during transport mechanism actuation.	- Needs a constant force applied when grasper needs to be in open position.
Bi-directional	- Grasper stays in a fixed position. - No spring needed.	- Lock on the sheath is needed to prevent opening when transport mechanism is actuated.
Hybrid Bi-directional And Voluntary opening	- Grasper stays in a fixed position.	- Needs tunable springs to find a force level between the static and dynamic friction on the sheath.

mechanism is on it needs to be added to the opening weight. Resulting in a total opening weight of 2780g. The finger handles are mirrored around the transport mechanism sheath and the slider to not create a moment that can create extra friction forces. Because the finger configuration is comparable to a chuck pinch and the average chuck pinch for a female is 5.2kg no transmission is needed[8].

As no transmission is needed the finger holds on each side are preferred not only for their simplicity, but also because a force is applied on opposing sides of the sheath. No moment is created which means there is no extra friction in the sliding guide of the sheath.

Figure 36 displays the pretension mechanism with the finger handles implemented. In Figure 36A no pretension is applied yet. The nut is fixed in the housing. After rotating the bolt, the spring is pretensioned like displayed in Figure 36B. As the exact spring dimensions that give the correct pretension are not known, the springs are positioned on the side of the device. This makes the device relatively wide, but it also makes it easy to switch springs and adjust pretension length of the bolts. When a correct pretension is found a more compact spring can be chosen that is placed around the wire ropes of the transport mechanism. Eliminating the spring shafts on the side as shown in Figure 36C.

5 Final Design

5.1 Complete Final Design

Figure 37 shows the final design. Each main part has its own color. Figure 38 displays the main sections of the device. The grasper, the operation section followed by the sliders placed around the cam and the motor section at the end. Three outer components and the shrink tube are removed to display the inner parts of the device like the sheath magnets, sheath springs, wire rope routing and sliders positioned around the cam.

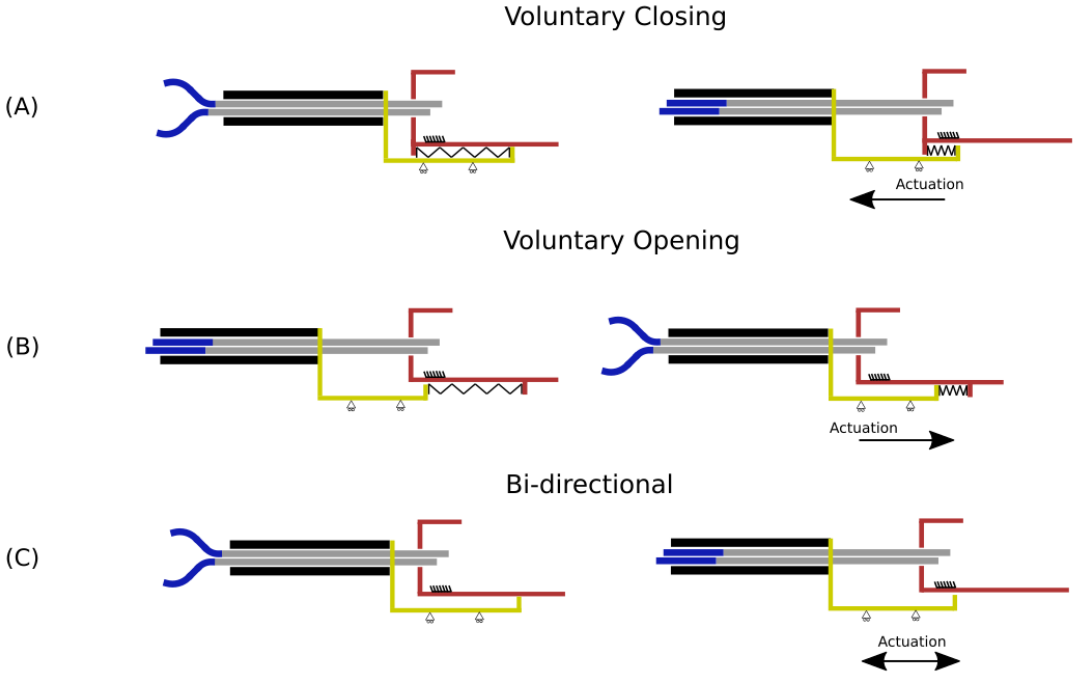

Figure 34: (A) Movement of slider (Yellow) in a voluntary closing grasp. The top shows a relaxed spring. While closing the grasp the spring is tensioned to store energy for the opening motion. (B) Movement of the slider (Yellow) in a voluntary opening grasp. The top shows a relaxed spring. While opening the grasp the spring is tensioned to store energy for the closing motion. (C) Both movements are actuated by the operator. No spring for energy storage used.

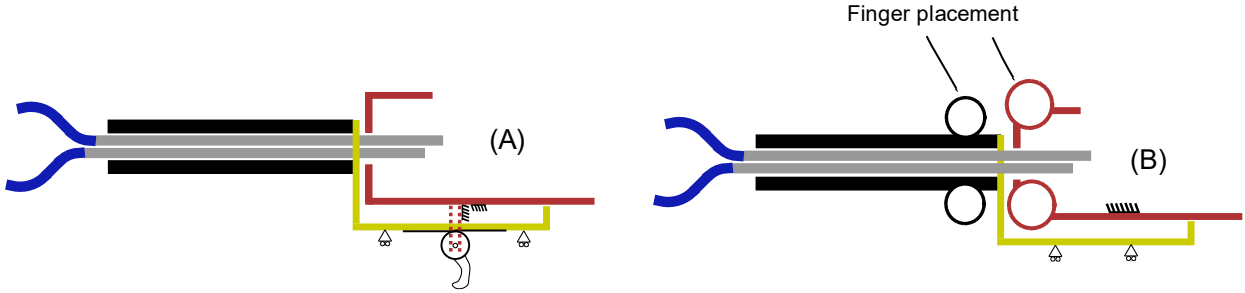

Figure 35: On the left (A) a trigger like actuation is shown connected to the slider with a flexure (black). This can actuate the slider in both directions. On the right (B) the slider and sheath are actuated by the index and middle finger on the sheath. A hold for the thumb will be on a different part of the system.

Figure 39 shows the grasper section. Eighteen 7x1 0.6mm wire ropes are divided in groups of three. Each group or three is connected in the tip by solder. A grasp shape to constrain tissue is made by bending the tips of the wire ropes and make them converge to the center. The grasp is closed by creating a bent compliant section just before the tip. In closed state three magnets straighten the wire ropes. To open the grasp the magnets are slid away from the tip, allowing the compliant section in the wire ropes to bent outwards. Previous experiments determined the bending radius of 15-degrees with a radius of 35mm combined with a straight section of 19mm does not collapse the lumen of the transport mechanism when the grasper is closed. The spacing between the magnets in the tip is 8mm. This is done with springs so the grasper tip section can be bent. Two wire rope guides are put in the grasper section. One on the tip magnet and one on the third magnet. This allows for some bending and play of the wire ropes in the section where the wire ropes are straightened by the magnet. Another reason to place the wire rope guides at the ends of the grasper section is that if the wire rope accidentally detaches from the middle magnet, it will not skip over the wire rope guides. To maintain the shape of the grasper, wire rope guides are placed every other magnet in the transport mechanism. Each time rotated one wire rope group, so support from the wire rope guides is divided over all wire rope groups.

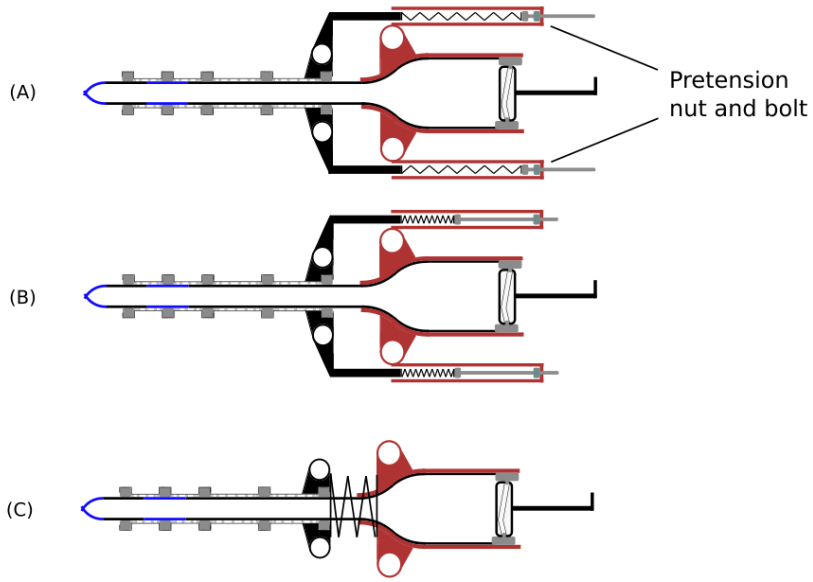

Figure 36: Pretension mechanism. A nut and bolt are used to pretension springs in A and B. In future iterations without the need of adjusting pretension or springs a more compact solution solution can be chosen as shown in C.

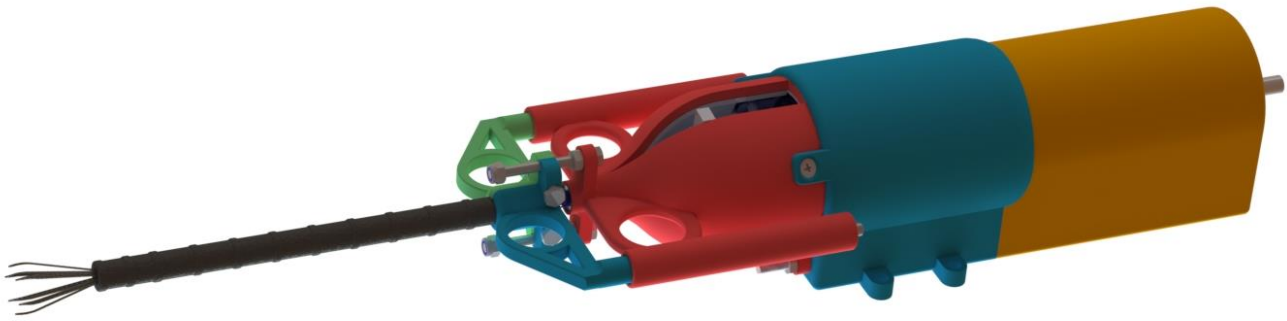

Figure 37: Final design of grasper with four finger handles for voluntary opening operation, including a cam and sliders for a functioning transport mechanism.

Four finger handles are used for operation as can be seen in Figure 40. Two of the four handles are clamped on the sheath while the other two handles are on the housing of the transport mechanism. The grasper will be operated by voluntary opening operation. Two springs keep the grasper in closed position to avoid interference of the grasper during surgery when it is not needed. When opening is desired, the sheath is slid back from the tip. During opening the springs are tensioned to support the closing motion that is done when the tissue is in the grasper. To constantly counteract the force of the transport mechanism acting on the sheath the springs are pretensioned by two bolt and nut pairs. An extra magnet with wire rope guide is placed between the two finger handle pairs to prevent buckling of the wire ropes. To keep the magnet and wire rope guide in place a spring is placed on both sides of the magnet.

A cross-section of the section with the cam and sliders that connect to the wire ropes is displayed below in Figure 41. The cam is supported by the motor shaft on the right, and a bearing on the left. The bearing transfers the load acting on the cam to the housing. The load on the cam consists of the friction force from the magnets on the wire ropes when the transport mechanism is active. A small change to the cam compared to the original design is described in Appendix III. The wire ropes are fixed in sliders, which have a pin inserted in the groove of the cam. Figure 42 is a view of the clamping mechanism to fix the wire ropes. A setscrew is perpendicularly screwed against the wire rope, fixing it in place. The design prevents any rotation of the wire rope around its axis, allowing the grasper tip to stay correctly oriented. When needed the setscrew can be loosened to replace the wire rope.

5.2 Assembly Steps

Figure 43 shows all components laid out in exploded view. A full parts list can be found in Appendix IV.

In Figure 44, the parts of the voluntary opening operation section are laid out. On the right of the figure are the finger handles that are clamped around the sheath. In the middle are the sliding guides of the handle including the nuts to mount them. On the left are the inner and outer shell that route the wire ropes to the sliders. On top and below are the springs for the voluntary opening operation with the bolts and nuts to pretension them.

The wire rope production steps of the grasper tip are displayed in Figure 45. A clamp is printed to align the wire ropes next to each other for soldering. After soldering, the compliant section is created with a bend having a radius of 35mm over a 15-degree angle. A 3D-printed cylinder with a diameter of 25mm was used as bending surface. Finally, the tip of each wire rope group was grinded into a tip and bent far enough to close half of the 3.8mm lumen.

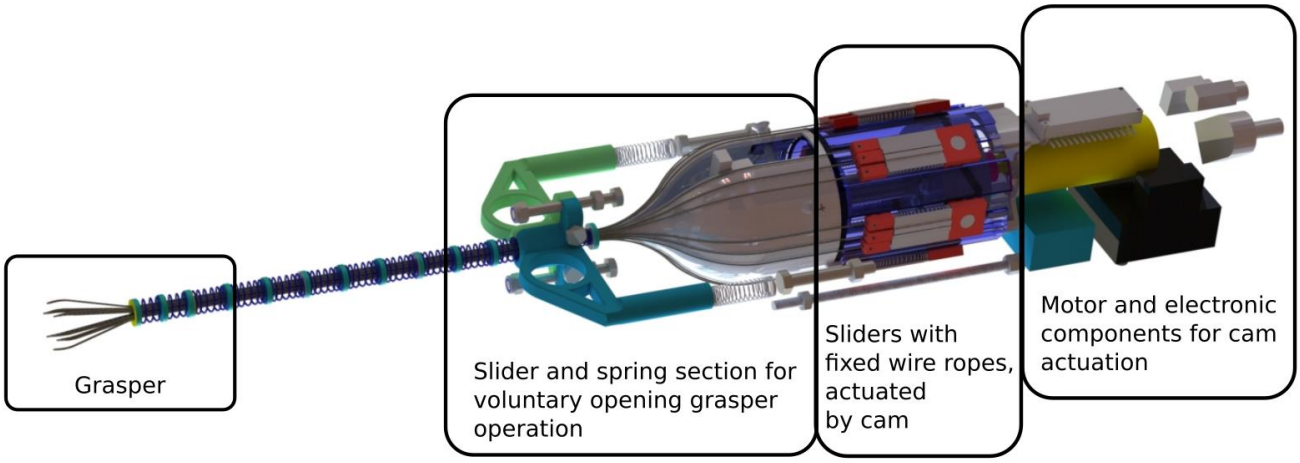

Figure 38: Final design with outer components removed and cam housing made see-through. The sections of the grasper, grasper operation, sliders with cam and motor section are highlighted.

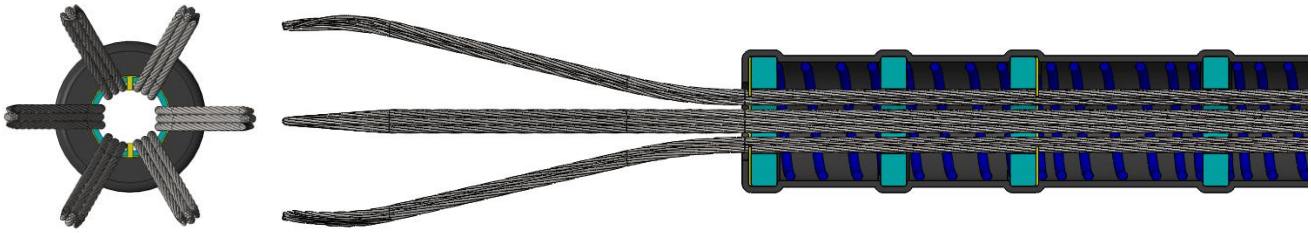

Figure 39: Final grasper design. Front and section view from the side. The grasper consists of wire ropes (grey), magnets (cyan), springs (blue), wire rope guides (yellow) and heat shrink tube (black).

After manufacturing the wire ropes the grasper, transport mechanism, operation and cam section are assembled to make sure the wire ropes are at the right length. If the dimensions are correct, it is possible to open and close the grasper with the finger handles. As shown in Figure 46, this needs to be done as it is not possible to make any changes to the system once the heat shrinking tube is put over the grasper and transport mechanism. Figure 47 displays the final system with heat shrinking tube that is used for the experiments to verify functionality of the grasper.

5.3 Working Principle

For clarification, the operational steps of the grasper are summarized below and displayed in **Error! Reference source not found.**.

1. Opening. The grasper is opened by sliding the sheath back from the grasper tip. This is done by placing the index and middle finger in the

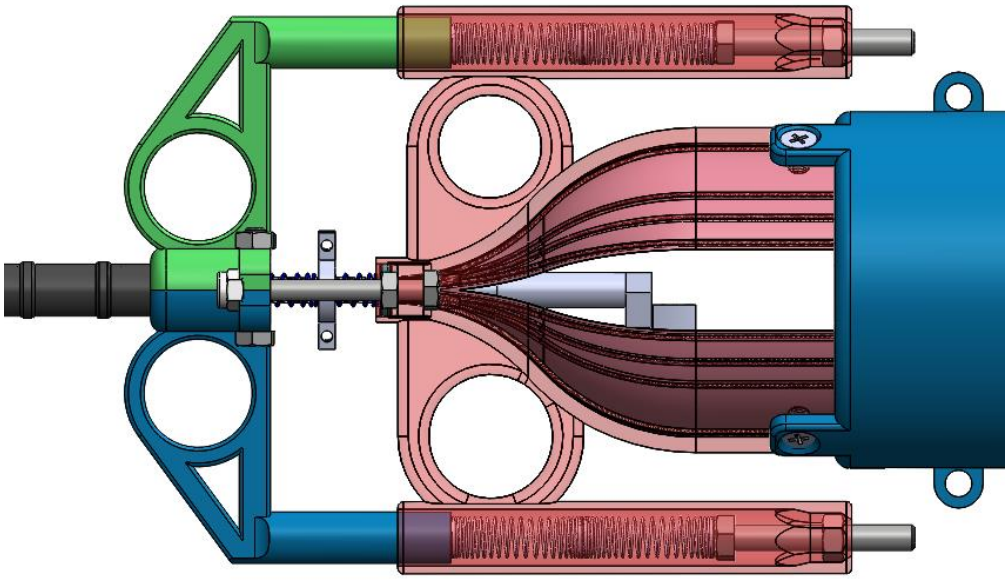

Figure 40: Four finger handle for operation of the grasper. Two parts of the handle are clamped around the sheath with two bolts. Two sliders of which only one is visible in this figure guide the handle when it pulls back the sheath to open the grasper. Springs are tensioned during the opening motion to support the closing motion. A bolt and nut are used to pretension both springs.

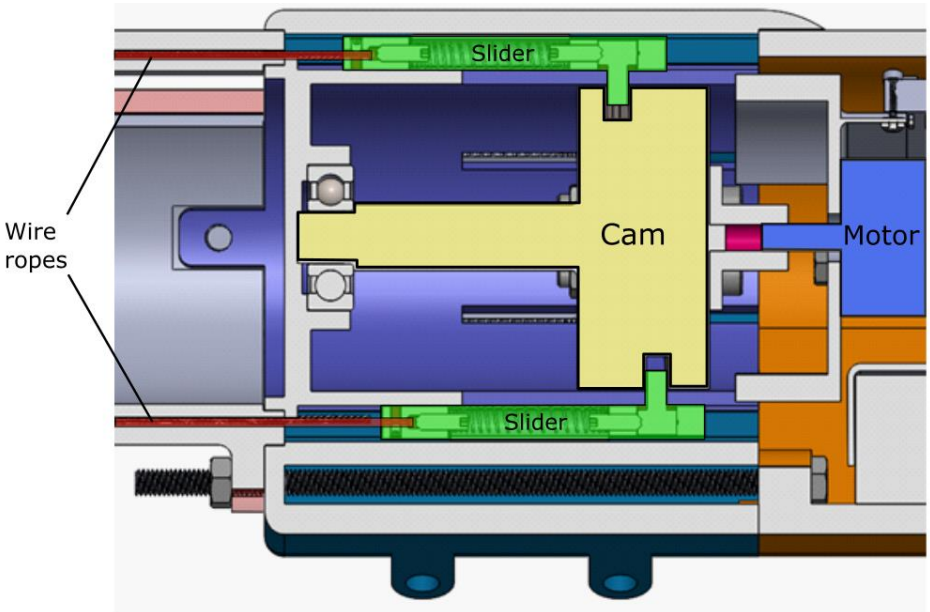

Figure 41: A cross section of the device showing two out of six sliders with their pin in the cam slot. A bearing supports the cam on the left and allows rotation while also transferring the friction foce of the transport mechanism wire ropes to the housing. On the right the motor coupling, motor mount, and motor cross section are displayed.

finger holds clamped on the sheath and the thumb and ring finger in the finger holds on the device. By pulling the finger pairs towards each other the sheath is slid back, allowing the grasper wire ropes to bend outward.

2. The open grasper is positioned around the tissue sample.

Closing. The grasper is closed by sliding the sheath back towards the tip of the grasper, straightening the compliant grasper section in with the magnets in the sheath. This is done by relaxing the fingers that keep the sheath pulled back. Springs tensioned in the opening stroke now actuate the closing stroke.

3. Tissue is transferred into the lumen by actuating the transport mechanism. When the tissue has entered the lumen a few cam rotations for transport need to be made to prevent tissue falling out when the sheath is slid back and the grasp is opened again.

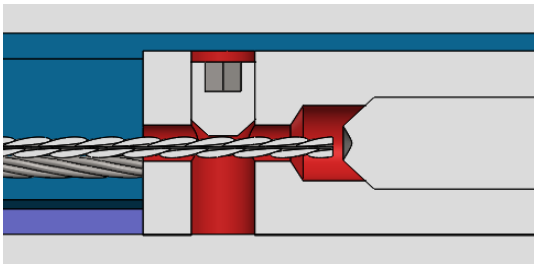

Figure 42: The wire ropes are clamped in the sliders with a setscrew. This allows quick replacement and prevents wire rope rotation around their axis.

6 Evaluation

6.1 Tests Overview

Previous research already focussed on evaluation of the transport system [4]. Different mass percentages of gelatine were tested to see if this had any influence on transport rate. Also, the difference between transport rate with and without particles in the gelatine has been examined. Therefore, evaluation will be aimed at

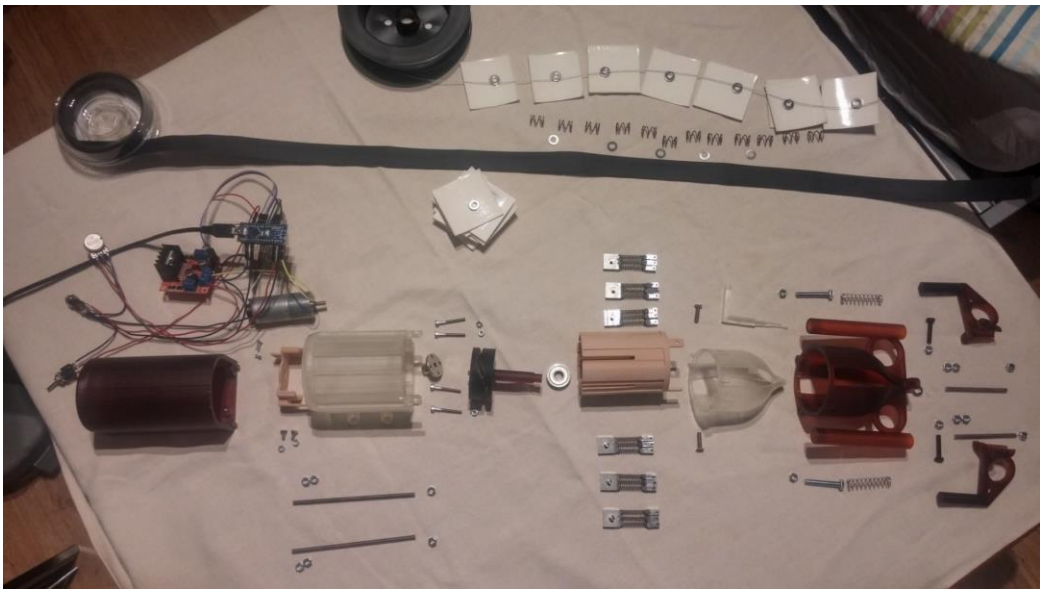

Figure 43: All components for assembly laid out in an exploded view.

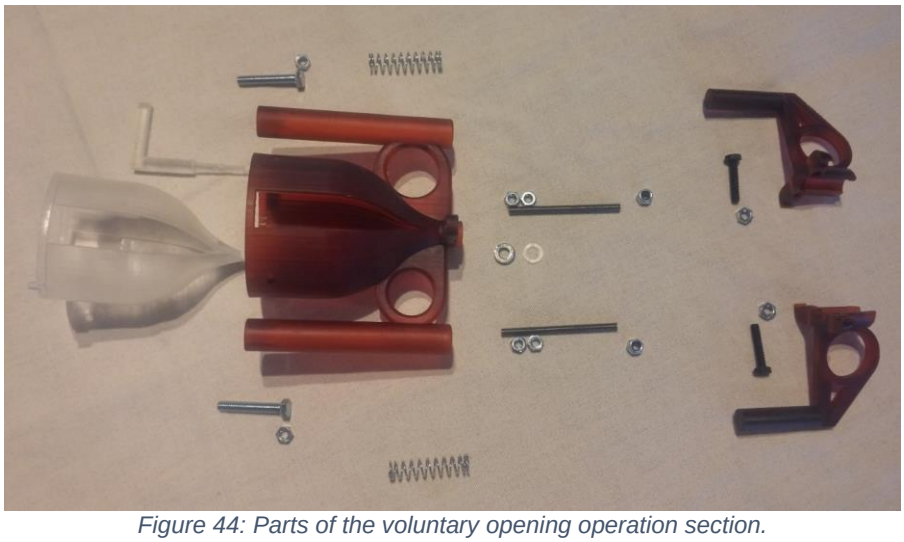

Figure 44: Parts of the voluntary opening operation section.

functionality of the grasper.

A successful grasp consists of multiple steps. First the grasp must open far enough to allow tissue to be put into the open grasper. Second when the grasp is closed it needs to constrain the tissue in three translative degrees of freedom so it cannot leave the grasper. Finally, after constraining the tissue, it needs to successfully enter the lumen to be transported by the transport system. Different phantom tissue samples and sizes will be used. After verifying the main functionality of the grasper, a phantom tissue sample is grasped from a surface in multiple orientations to simulate practical use. Also, functionality of the grasper is tested with the transport mechanism in a bend to check if the grasper does not limit the transport mechanism. All these steps need to be verified to prove a functioning grasper has been developed. First the size opening of the grasper is examined.

6.2 Grasper Opening and Closing

Goal
To check if the grasper opens far enough to let tissue in a test is executed. The circular opening will be measured for multiple instances to see if the grasper functions consistently.

A rough estimation of the needed opening force will be done with a kitchen scale to verify that the force level is not too high.

Experimental Variables
The independent variable for the grasp opening test is the state of the grasper. The grasper being open is the independent variable. The size of the opening is the dependent variable. The grasper will be opened six times and each time the size of the opening for a circular object is measured. Afterwards, the opening force is measured.

Independent variable: State of the grasper (open)
Dependent variable: Size of open circular diameter [mm]

Experimental Setup
To measure the grasp a photo of the open grasper is taken with a sheet of millimetre paper next to it. With the footage analysis tool Kinovea [15] the opening is measured. The setup is displayed in Figure 50.

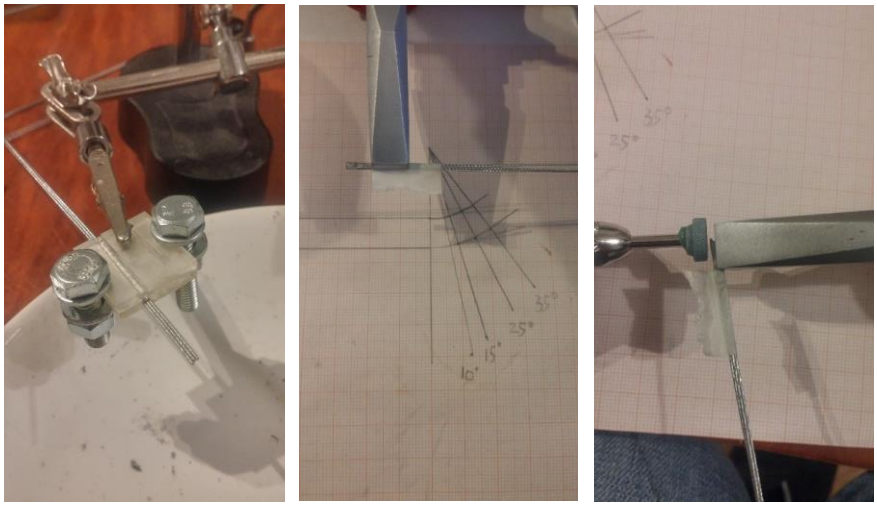

Figure 45: Grasper wire rope production steps. First, the three wire ropes are soldered together in A. Secondly the desired bend with a radius of 35mm over a 15-degrees angle is obtained shown in B. After that the tip is grinded into a point as shown in C.

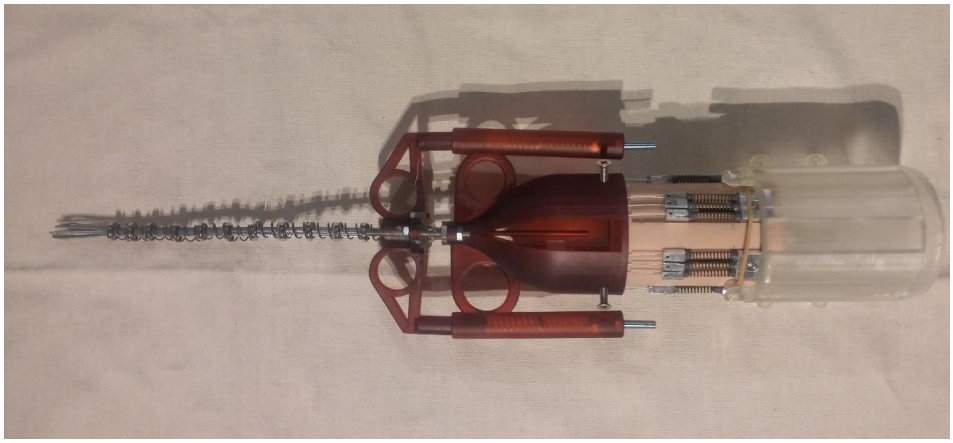

Figure 46: Test without sheath to check if the wire ropes are at the right length for opening and closing the grasp.

Figure 47: Final assembly that is used for experiments.

For measuring the needed opening force a kitchen scale is used to press on while opening the grasper.

Experimental Protocol

The grasper is opened to check if tissue can enter the opened grasp. This is done by sliding the sheath 21.5mm backwards. During opening the transport system is actuated by hand to mimic a motor driving it. A real motor is not used to make sure that any unforeseen problems will not permanently damage the prototype. While the grasper is opened, a picture is taken with millimetre paper next to it as verification that the grasp opens far enough for tissue to enter. The tissue will be 4mm in diameter. This size of tissue is chosen as it should touch all the wire ropes for transport, as the size of the lumen is 3.8mm. A photo of the open grasp is taken and analysed in the Kinovea computer program to determine the diameter of the circle that can fit in the grasp. The millimetre paper is positioned at the same depth to function as a measurement scale for the circle.

For the opening force, measurement of the scale is put on zero with the device on it. After this the grasper is opened by pushing on the handle while the whole device is resting on the scale.

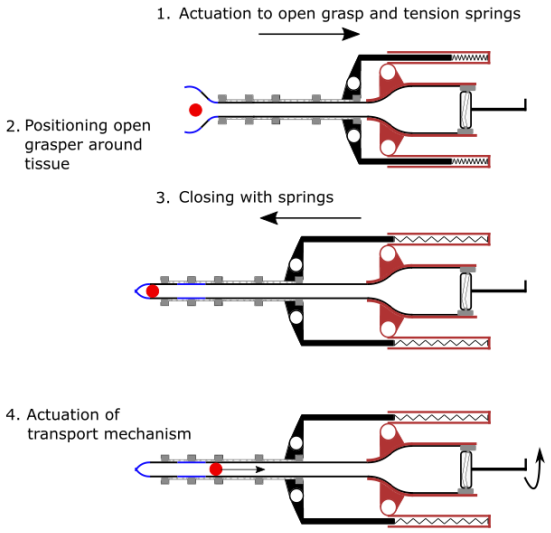

Figure 48: Working principle. Four steps that are performed to operate the grasper.

Data Analysis

Of the six circle diameters the average value and standard deviation will be calculated in MATLAB.

Results

In Figure 49 results of the opening diameter of the grasper are shown. The mean opening diameter is 9.58mm with a standard deviation of 0.58mm. All opening results were big enough for tissue of 5mm to enter the grasp. This means that the first step, the tissue entering the grasp, is possible. While the opening is consistently big enough, the wire ropes do not always open in the same way.

Opening of the grasper took approximately 3000g of force with short peaks to 3200g due to stick slip effects. It was not possible to measure exact values to constant variation of the force on the scale.

6.3 Tissue Constraining

Goal

The second step is to evaluate if the grasper can constrain multiple sizes and shapes of tissue. After closing the grasp tissue should stay in the grasper.

Experimental Variables

As independent variables the following tissue sizes and shapes are selected and tested six times. Spheres of 3mm, 4mm and 5mm. The 4mm sphere fits perfectly in the lumen but it is interesting if other sizes can also be grasped. A cylinder of 4mm by 6.5mm is also grasped in two different orientations. Parallel in length to the transport system and orthogonal to the transport system. As independent variable constraining of the tissue is determined successful or unsuccessful.

Independent variable: Tissue shape and size (Sphere 3mm, 4mm, 5mm. Cylinder 6.5mm long, 4mm diameter. In two orientations)

Figure 50: Setup to measure opening diameter of the grasper. Millimetre paper to use as scale is on the left.

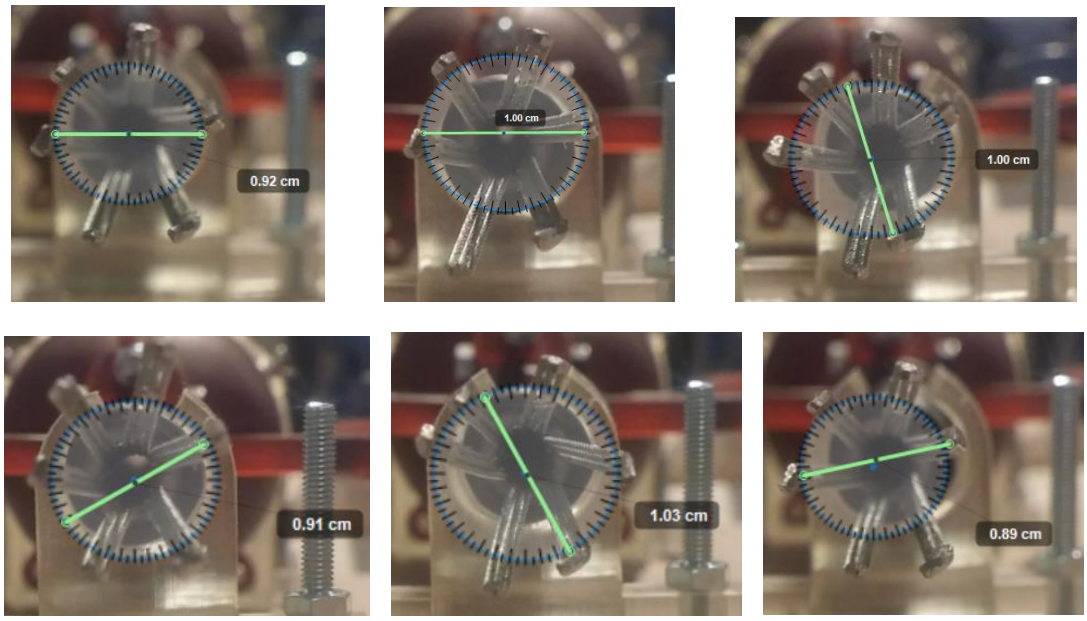

Figure 49: Circular opening diameters of grasper.

Dependent variable: Outcome of constraining of tissue sample. [Successful/Unsuccessful]

Experimental Setup
The tissue is made from 10m% gelatine in water and injected with a dose syringe into a 3D-printed mould. This mass percentage of gelatine has the same stiffness as muscle and liver tissue [16]. The tissue is put on a needle for consistent insertion of the tissue. Figure 51 displays the setup with the grasper, tissue mould and needle with a tissue sample on it. The transport mechanism is supported to prevent movement while grasping.

Experimental Protocol
To grab the tissue from a needle the grasper is opened, slid 19mm forward over the phantom tissue sample and closed. Then the grasper is then slid back and taken from the platform. To check if the grasped tissue is constrained the grasper is rotated 360 degrees around its length axis, rotated under a 45 degree angle with the tip down and held with the tip fully pointing down at a 90 degree angle. When the tissue does not fall out of the grasp it is considered constrained.

Data Analysis
The result is a total of 30 successful or unsuccessful outcomes. The number of successful attempts will be counted, and the percentage of successful constraints will be determined.

Results
All tissue samples were successfully constrained when the grasper was closed. They did not fall out when the grasper was rotated in a horizontal, 45 degree downward and fully downward orientation. It must be noted that while no tissue sample fell out. The perpendicular cylinder samples were not always constrained by shape as shown in Figure 52. Two wire rope pairs clamp the cylinder that is not centred in the grasp. In total three out of six samples that were grasped this way and did not reorient in a parallel position when the transport system was actuated.

6.4 Tissue transfer into lumen

Goal
Finally, it needs to be evaluated if the tissue samples successfully enter the lumen to be transported.

Experimental Variables
The same tissue phantoms from the constraining test will be used. The 3mm, 4mm, 5mm spheres and the two 4mm by 6.5mm cylinders with the parallel and orthogonal orientation compared to the straight transport system. The tissue samples are the independent variables while the successful or unsuccessful entrance of the lumen is the dependent variable.

Independent variable: Tissue shape and size (Sphere 3mm, 4mm, 5mm. Cylinder 6.5mm long, 4mm diameter. In two orientations)
Dependent variable: Number of cam rotations needed to transfer the tissue sample into the lumen.

Experimental Setup
The same setup and tissue phantom are used as in the constraining experiment. The tip of the sheath is supported to prevent any influence of a moving tip.

Experimental Protocol
After testing if the tissue is constrained in the grasp the system will be put on a horizontal surface and the transport system will be actuated by hand. The amount of cam rotations is counted. When the tissue enters the lumen the transition from the grasper to the transport system is marked successful.

Data Analysis
The resulting data is the amount of cam rotations needed to transfer the tissue into the lument. These will be plotted in a scatter plot to compare the results. This will be done with MATLAB.

Results
After constraining the tissue the number of cam rotations to transfer it into the lumen for transport was measured. Results for the spherical 3mm, 4mm, and 5mm are shown in Figure 53 and can be found in Appendix V. In Figure 53 it can be seen that there is a big outlier in the 3mm sphere group resulting in a standard deviation of 24.8 cam rotations with an avarage of 26.8. The 4mm sphere samples have no outliers with a standard deviation of 2.66 and a mean of 8.5 cam rotations. The 5mm samples have a standard deviation of 0.63 with a mean of 6 cam rotations for tissue transfer into the lumen of the transport mechanism. All six samples of the 3mm, 4mm and 5mm spheres were transferred into the lumen.

An analysis of variance (ANOVA) test is done to see if there is a significant difference in the mean amount of turns needed to get the tissue samples into the lumen between sample groups. For this the null hypothesis

Figure 51: Test setup for grasping tissue samples. The needle is shown with a phantom tissue sample from the mould. To grasp the tissue the grasper is opened, slid forward over the sample, and closed.

Figure 52: Cylindrical tissue being constrained by friction of two wire rope pairs.

($mean\ 3mm = mean\ 4mm = mean\ 5mm$) needs to be rejected. The analysis was done in MATLAB and had a result of p=0.0533. Not below p=0.05, commonly used as threshold to reject the null hypothesis. Thus, it cannot be concluded that the mean of one of the three is different from the others. Since only six samples were taken in each group it is possible that this changes in a larger scale experiment with more samples.

Besides looking at the influence of tissue size on the cam rotations needed to enter the lumen, different tissue shapes and orientations were also tested. Results are shown in Figure 54. A cylinder with a diameter of 4mm and a length of 6.5mm in an orientation parallel to the lumen required a mean of 4.83 cam rotations to enter it with a standard deviation of 2.13 rotations. In an orientation perpendicular to the lumen only 3 out of 6 samples succesfully entered the lumen as these sample did not align with the lumen and were cut in half by the wire ropes. One of the succesfull three took 16 cam rotations while the other two took 4 and 5 rotations. This results in a mean of 8.33 with a standard deviation of 6.66 rotations. An ANOVA test with the null hypothesis $mean\ 4mm = mean\ 4x6.5mm\ parallel = mean\ 4x6.5mm\ perpendicular$ was done. With a p=0.19 the null hypothesis could not be rejected.

General Observations

During the tests, a few observations were made. The perpendicularly oriented cylinder sample had three successful transfers into the lumen. The other three failed. One sample did not reorient to align with the lumen but was transported towards it. At the entrance it

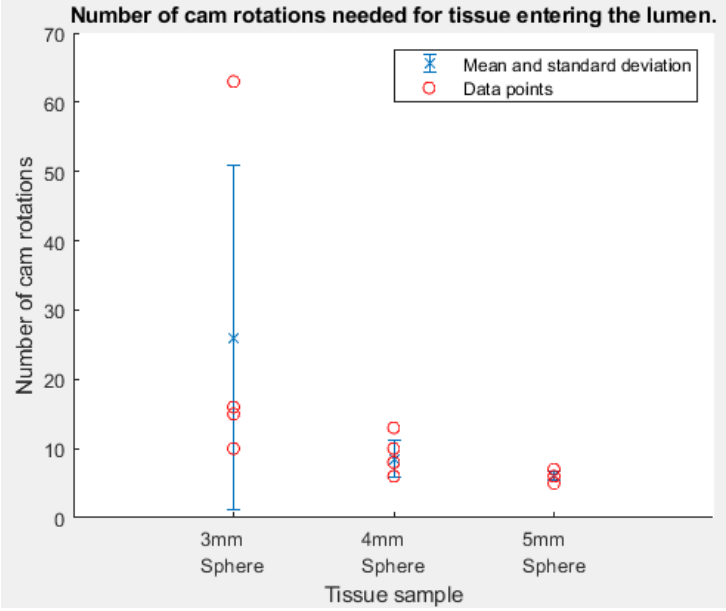

Figure 53: Plot of number of cam rotations needed for 3mm, 4mm and 5mm spherical tissue samples to enter the lumen.

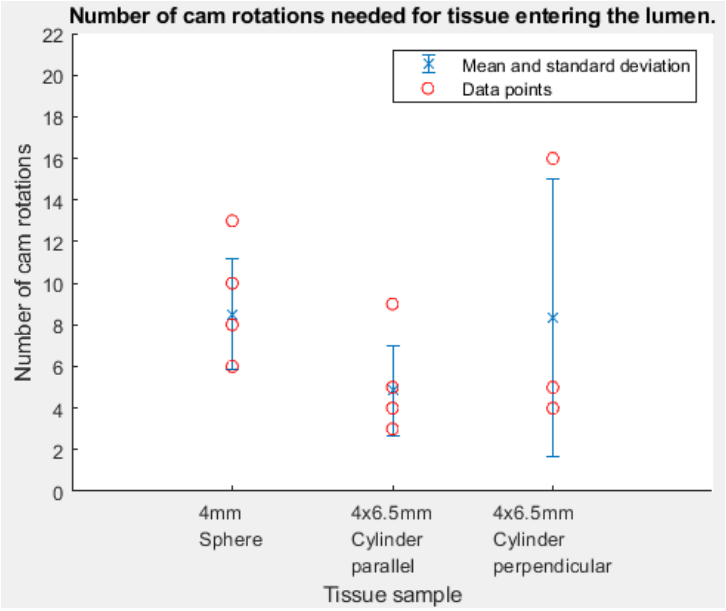

Figure 54: Plot of number of cam rotations needed for 4mm and 4x6.5mm cylindrical tissue samples in parallel and cylindrical orientation to enter the lumen.

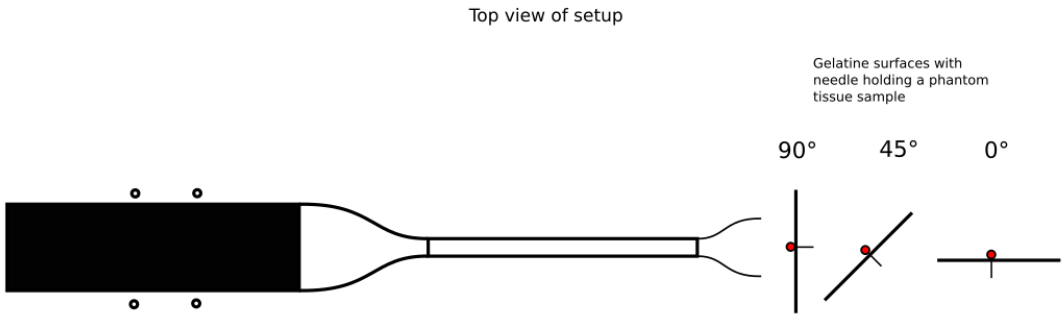

Figure 55: Orientation of gelatine surfaces to grasp a 5mm tissue sample.

was cut in half by the two wire rope groups it was clamped between. One half entered the lumen. Another sample was cut in half without any transport movement towards the lumen. The third failed sample was touching only two wire rope groups and after rolling between them for a few cam rotations it fell out.

6.5 Grasping Tissue from a Surface

Goal
It is necessary to know if the grasper can also grasp tissue directly from a surface. This may be harder as not all wire rope pairs are maximumly extended so this may be a problem. To evaluate this 4mm sphere phantom tissue is picked up from a needle. The needle is pushed through cardboard that acts like the surface it is on.

Experimental Variables
The independent variable will be the angle of the flat surface with respect to the transport system. First the tissue will be picked up fully orthogonal (90 degrees) from the grasper. The second orientation is under an angle of 45 degrees and the last parallel (0 degrees) to the surface as shown in Figure 55. The dependent variable is being successful or unsuccessful in picking up the tissue from the surface.

Independent variable: The orientation angle of the grasper with respect to the surface with tissue on it. [0 degrees, 45 degrees, 90 degrees]
Dependent variable: Outcome of constraining the tissue from the surface. [Successful/Unsuccessful]

Experimental Setup
The setup consists of cardboard that acts as a surface with a needle through it. On this needle will be 5mm spherical tissue phantom pushed far enough on it to contact the cardboard.

Experimental Protocol
To grasp the tissue the grasper is opened, slid forward in a straight line against the cardboard until it is touched. Then the grasp is closed. During these steps, the transport system is actuated by hand. When the tissue is constrained, the grasp is seen as successful.

Data Analysis
Six attempts for each orientation will be made resulting in a successful or unsuccessful try. For all three orientations this leads to 18 tries in total. Leading to a success rate for each surface orientation.

Results
Grasping tissue on a surface perpendicular to the transport system lumen was not possible without puncturing the gelatine representing a tissue surface. When an attempt was made to grasp the sample without puncturing it fell out of the grasp due to grasper tips not forming a perfect point. When puncturing was allowed all samples were successfully picked from the surface.

In a 45-degree orientation it was possible to pick tissue off the gelatine surface with barely any puncturing. For this the transport system was not actuated and the cam was put in a position to make sure puncture would occur as little as possible. Three out of six tries succeeded in in only minimally pinching the gelatine surface and successfully transferred the tissue into the lumen. Two times points of the grasper were puncturing the gelatine surface but still transferred the tissue into the lumen successfully. One time the tissue fell off the needle while attempting the grasp resulting in a failure.

Finally grasping tissue parallel to the transport lumen was conducted. Six tries were successful in grasping the tissue from the surface and transferring it into the lumen. During the grasping the transport system was turned off. Three tries of grasping with an actuated transport system failed. No surface tissue punctures were observed.

6.6 Grasping with a Bent Transport Mechanism

Goal
Besides the evaluating the grasping functionality tests need to be done to prove modifications on the original transport system did not break it and that grasping is possible with a system in a bent configuration.

Experimental Variables
To measure this the system is put in four configurations. The transport system in a straight

configuration, a 20-degree bend, 40 degree bend and 60 degree bend. These are the independent variables. The dependent variable is the successful or unsuccessful opening and closing of the grasp.

Independent variables: Bending angle over a 59mm radius. [0, 20, 40, 60 degrees]
Dependent variables: Opening and closing of grasp with system in bent configuration. [Successful/Unsuccessful]

Experimental Setup
Both the transport system and the bent corners are fixed on a plateau. The bends are 3D printed and fixed with screws to an MDF wooden plate. This is also done with the grasper. The distance between the front mounting slid in the plate and the opening of the bend is 19cm. The opening of the curved bend is on the same level as the grasper and has a diameter of 12mm. Figure 57 displays the setup with the 60-degree bend.

Experimental Protocol
The grasp is opened and closed while the transport system is in the desired angle. During opening and closing the transport system is actuated by hand.

Data Analysis
The number of successful and unsuccessful tries will be registered leading to a success rate.

Results
Finally grasping tests with a bent transport system were performed. Tissue of 5mm was successfully grasped and transferred into the lumen six times while the sheath was placed through a bend with an angle of 20-degrees and a radius of 59mm. With the transport system bent in a 40-degree angle with a radius of 59mm also all six samples were successfully grasped and transferred into the lumen. A problem appeared when the system was put in a bend with an angle of 60-degrees. Five samples were transferred into the lumen successfully but one failed. The grasp was successful, but the sample did not go into the lumen. After pulling back the transport system the sample did enter.

General Observations
In the 60-degree bend the grasper was severely deformed. Figure 56 on the left displays crossed wire rope groups in open position. In closed position a bend sideways was also observed. One wire rope of a group of three detached from the tip magnet but due to it

Table 3: Success rates of constraining and transferring phantom tissue samples in the lumen of the transport mechanism. Also displayed are the needed cam rotations and standard deviation for transferring the sample into the lumen.

Tissue sample **Test**	**3mm sphere**	**4mm sphere**	**5mm sphere**	**Cylinder 4x6.5mm axis parallel to lumen**	**Cilinder 4x6.5mm axis perpendicular to lumen**
Constraining tissue success rate	6/6	6/6	6/6	6/6	6/6
Transfer of tissue into lumen success rate	6/6	6/6	6/6	6/6	3/6
Number of cam rotations needed for transfer into lumen	26.8 $\sigma = 24.8$	8.5 $\sigma = 2.66$	6 $\sigma = 0.63$	4.83 $\sigma = 2.13$	8.33 $\sigma = 6.66$

Table 4: Lumen transfer success rate of 5mm spherical tissue grasped from surfaces under different angles.

	90-degree (perpendicular to lumen axis)	**45-degree**	**0-degree (parallel to lumen axis)**
Transfer of 5mm spherical tissue into lumen success rate	5/6	5/6	6/6

Table 5: Lumen transfer success rate per bending angle of 5mm spherical tissue grasped with the transport mechanism through a 59mm radius bend.

Bend angle with radius of 59mm	**20-degree**	**40-degree**	**60-degree**
Transfer of 5mm spherical tissue into lumen success rate	6/6	6/6	5/6

being connected to two other wire ropes it reconnected a few seconds later.

6.7 Summary of results

Six times of opening of the grasper resulted in an average opening diameter of 9.58mm with a standard deviation of 0.58mm. The needed opening force was approximately 3000g with peaks of 3200g.

The following results in the tests with grasping tissue samples were observed. Using ANOVA no significant difference in needed cam rotations to enter the transport mechanism lumen was found.

7 Discussion

Main Findings

The main goal of this study was to design a wire rope based grasper for a transport mechanism working with friction. The grasper needed to be able to grasp tissue and transfer the sample into the lumen of the transport mechanism. Opening the grasper six times resulted in an average circular opening diameter of 9.58mm with a standard deviation of 0.58mm. This is big enough for tissue suitable for the transport mechanism to enter the grasp. The six outward bent groups when in open position did not always have a constant 60 degree angle between each other.

A slight inconsistency in the angle between open wire rope groups is observed between different opening instances, though only minor. This indicates that torsion of the wire ropes is limited successfully by soldering them together in the grasper tip and clamping them in the sliders of the transport mechanism actuation. Also, the wire ropes did not angularly move over the surface of the magnet. It can be assumed that the wire rope guides placed on the magnets did function properly and kept the wire ropes in place over the full length of the transport mechanism and grasper, only allowing axial motion trough the magnets for actuation of the transport mechanism.

The enclosing performance of the grasper was tested with respect to size and shape differences of the gelatin tissue phantom. All samples were successfully constrained by the grasper, though not all samples were constrained by shape. Three samples of the perpendicularly oriented cylinder of 4mm in diameter and 6.5mm in length did not make it into the lumen due to the way they were grasped. After closing the grasper, the cyclinders were clamped by friction between two wire rope groups and did not contact any of the four others.

Because of this the cylindrical tissue sample did not reorient to align with the lumen of the transport mechanism but was rolled back and forth between the two wire rope groups. This resulted in the tissue being

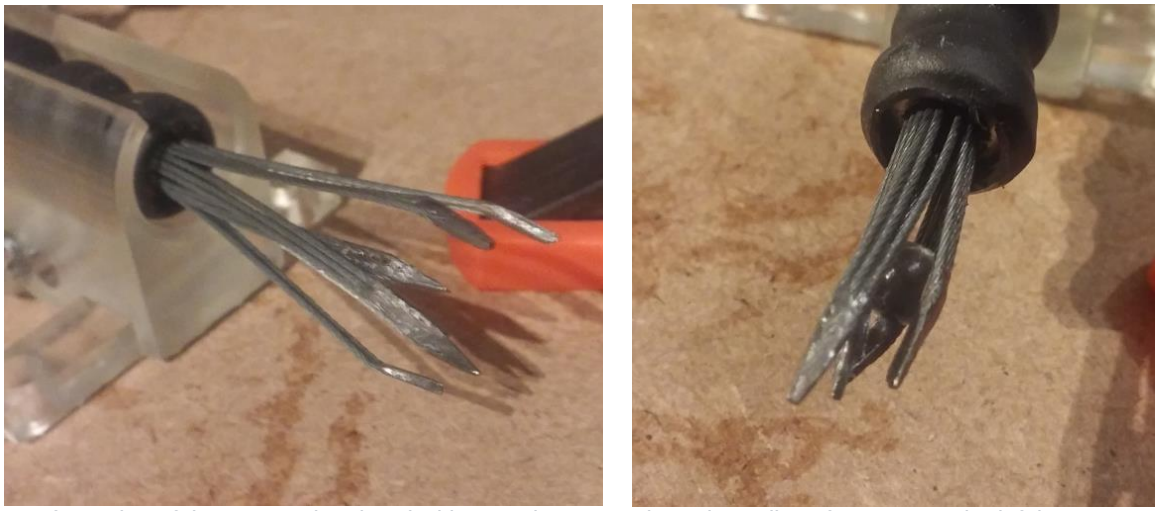

Figure 56: Deformation of the grasper in a bend with a 60-degree angle and a radius of 59mm. On the left in open configuration while on the right the grasper is closed.

Figure 57: Test setup with bent configuration. The bend displayed has a radius of 59mm and an angle of 60 degrees.

released from the grasp in one case and cutting of the tissue in the other cases. The pieces of tissue that were contacted by four wire rope groups did reorient and were transferred into the lumen quickly. This indicates that it is important to make sure non-spherical tissue samples are grasped in the centre of the lumen.

Out of the 3mm, 4mm and 5mm gelatine spheres the 5mm gelatine sphere has the fastest and most constant transfer into the lumen after six attempts. This despite the tissue being 1.2mm bigger than the lumen diameter. Further tests will need to be performed to find out what the maximum tissue size is that can be transferred into the lumen. The 4mm sphere, that has a 0.2mm bigger diameter than the lumen had a slight spread in the amount of cam rotations needed to transfer into the lumen and a higher average.

The 3mm spherical sample had a large spread in the needed cam rotations. This is not a surprise as during the tests the 3mm sample randomly stuck to wire rope groups when they were shifting back and forth making it behave unpredictably. 3mm Samples made it into the lumen while not being able to contact all six wire rope groups. This happened slowly when the sample eventually was laying on the bottom two wire rope groups that were actuated back and forth. As the grasper and transport mechanism were in horizontal orientation this was possible to happen. When the transport mechanism and grasper are pointing downward it is expected the force of gravity will prevent any transportation of the 3mm tissue sample.

The parallel grasped cylindrical tissue sample of 4mm in diameter with a 6.5mm in length was on average the fastest in entering the lumen. This is probably because of the large surface area that is in contact with the wire ropes.

Grasping tissue from a surface was possible, though the gelatine surface where the tissue phantom was placed on was punctured by the points of the grasper. This happened mainly when the orientation of the transport mechanism was perpendicular to the grasper. When the tissue was placed on a surface parallel to the grasper no puncturing could be observed. The transport mechanism could not be actuated when tissue was picked up from the 45 degree and parallel surface orientation. As the grasper movement pushed the tissue away before it entered the grasp. For precise grasping it is best to turn off actuation of the transport mechanism.

To test the effectiveness of the grasper when the flexible transport mechanism was curved, the performance of the grasper was evaluated with the flexible transport mechanism in a bend (R=59mm and angle is 20, 40 and 60 degrees). The grasper performed as expected. All tested tissue samples entered the lumen for 20 and 40 degrees. When the transport mechanism was bent over an angle of 60 degrees, one out of six samples did not enter the lumen of the transport mechanism normally. Only after moving the shaft forward in the bend the tissue sample was transferred into the lumen.

The grasper comprises of wire ropes that are per three wire ropes connected at the grasper tip. Bending the transport mechanism makes that one wire rope takes an ‘inner corner’ while the other takes an ‘outer corner’ causing a length difference between the wire ropes as shown in Figure 59. This deforms the grasper, as observed in the experiment with the transport mechanism in bent configuration. Due to the bending a wire rope shortly detached from the tip magnet. It reconnected as it was still supported by the two other wire ropes of the group. This indicates that underactuation will be necessary for reliable operation at a 60-degree bending angle or higher. The current implementation of underactuation by springs did not work because of too much hysteresis. Either the stiffness of the springs needs to be increased or a different mechanism needs to be chosen for

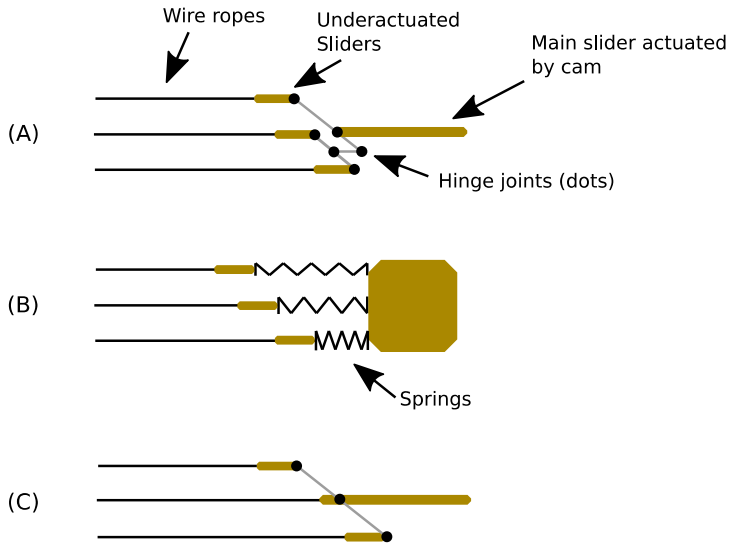

Figure 58: Underactuation options. Figure A displays a whipple tree design dividing the input force on the main slider over the subsliders. In B springs act as underactuators that compress when there is a length difference between wire ropes. The last option C is not fully underactuated as the middle wire rope is connected to the main slider. The outer wire ropes are connected to the main slider by a seesaw mechanism.

underactuation. Figure 58 displays possible underactuation options. Figure 58A shows a whipple tree and Figure 58B shows the underactuation by springs concept that was tried. Both fully underactuate the wire ropes. Figure 58C shows partial underactuation, where the middle wire rope is connected to the main slider and the outer wire ropes are connected to a seesaw mechanism. The seesaw is fixed to the main slider with a hinge, compensating the length difference of the outer wire ropes when the transport mechanism is bent. Initially the spring concept was chosen for underactuation due to its simplicity, Appendix III describes the development. Unfortunately hysteresis in the springs prevented the transport mechanism from working. As alternative to the springs the seesaw mechanism should be considered as eliminates the hysteresis problem. A challenge is implementing the hinges in the limited available space.

Limitations of the Study

A limitation to consider is that the materials used in the prototype are not suitable for medical applications. The wire ropes are made from galvanized steel, not stainless steel which is standard for medical instruments. As stainless steels have different magnetic properties tests to determine the safe bending angle and radius need to be redone. It is expected this will be successful. Magnetic properties of 1010 construction steels shown in Figure 60 are comparable to the magnetic properties of 430 stainless steel shown in Figure 61. The solder used to connect the wire ropes in the tip contains approximately 50% lead which can lead to lead poisoning and should be replaced for a medical type of solder for instance Indalloy [17]. The material in the heat shrink tube is unsuitable for medical use, a medical tube with similar characteristics should be selected. Besides this, magnets may cause problems for patients with electrical implants like pacemakers.

The test results imply that the grasper fulfils the requirements. The tests were done in a controlled environment, not in a clinical setting. Instead of using gelatine tissue phantom, the tests should be performed using real tissue to assure the grasper will also reliably transfer real tissue into the lumen. This should be done by a surgeon to get feedback on any functional or practical problems.

No statistically significant results were found. This was expected with the low number of repetitions in each test. A more extensive study needs to be performed to prove there is a correlation between the number of cam rotations and different tissue shapes entering the lumen.

Further Research

An interesting improvement to the grasper and transport mechanism is making the device steerable. This allows the grasper to be oriented such that the tissue can easily be grasped. Another possibility is adding a cutting edge to one or two wire rope groups on the straight section of the grasper tip. As the wire rope groups can already make a sawing motion, this can be used to cut tissue in the right size for the transport mechanism. It may also turn the device into a multifunctional cutting, grasping and tissue extraction instrument. This can lower the number of instruments needed in a minimally invasive surgery. Also adding an electric motor to actuate the transport mechanism would eliminate the need for the user to switch between actuating the grasper and transport mechanism.

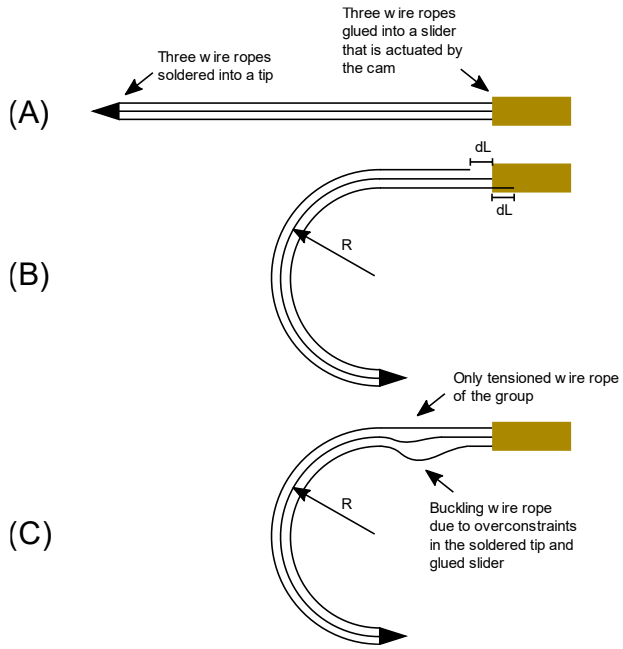

Figure 59: (A) Connection of the wire ropes in the tip and at the slider. (B) Difference in wire rope length occurs due to bending. (C) Difference in length leads to tension on one wire rope and compression on the two others of the group. This can lead to buckling.

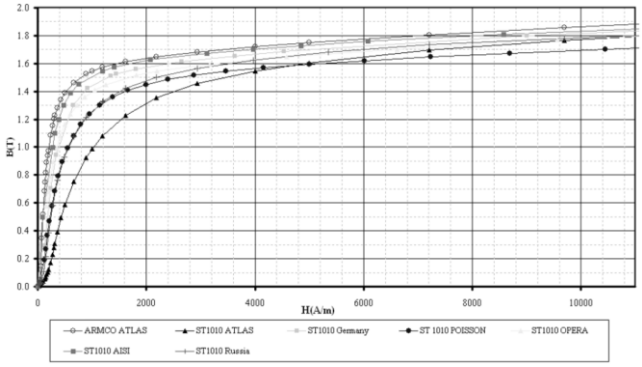

Figure 60: Magnetization curves of different heats of 1010 constructional steels used as magnetic steel in different experiments [24].

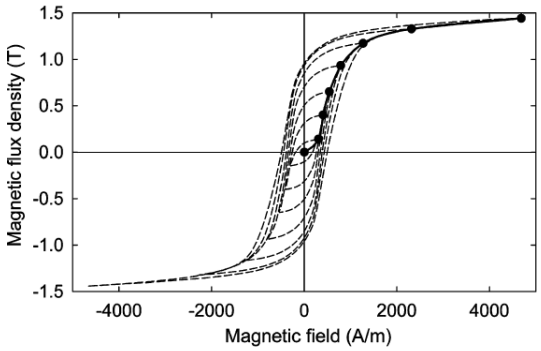

Figure 61: Room-temperature magnetization curve for 430 stainless steel. [25].

The maximum diameter of tissue that can enter the lumen with the grasper has not been determined as the biggest phantom tissue sample tested was able to be grasped and transported into the lumen of the transport mechanism. More extensive testing is needed to investigate the limits on size that can be grasped. This may be influenced by the tissue stiffness, which should thus also be investigated.

A possible improvement to the grasper is a varying straight tip section. When the cam amplitude is high, and the grasper is not positioned far enough over the tissue sample, there is a risk of a wire rope group pushing the sample out. This can happen when one of the six wire rope groups is pushed forward by cam actuation. Top prevent this the grasper tips can be given the same profile as the cam. Resulting in a single angle on the cam rotation where all wire rope group tips align as in Figure 62. There is no guarantee that this tip design will work as previously a conscious decision was made to keep a straight part between the bent compliant section and the soldered wire rope tip. This prevented lumen collapse. Increasing the grasper tip length may circumvent this problem.

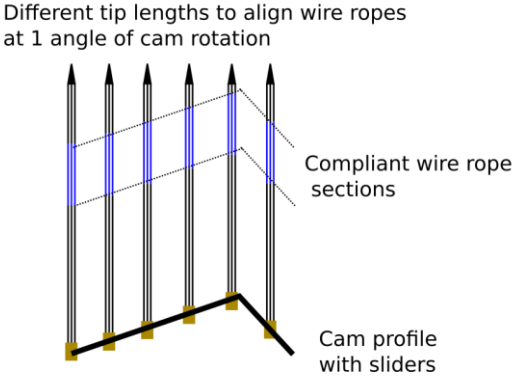

Figure 62: Aligned wire rope tips. Sliders (brown) in the camp profile actuating wire rope groups with aligned wire rope tips on one angle of a full cam rotation. The compliant wire rope sections are marked blue.

A colonoscope has a length of 133cm [18]. The current device has a length of 14cm including the 2cm wire rope straightening section. To go beyond the prototype stage a longer transport mechanism needs to be designed. This will also have implications for the current prototype design. A longer transport mechanism results in higher friction forces due to the increased number of magnets contacting the wire ropes. This will require a higher amount of torque on the transport mechanism actuation. Also, the grasper cannot be opened anymore with the four finger handle without support from the transport mechanism cam actuation. Actuating the cam helps tensioning the springs, requiring a lower manual actuation force. If cam actuation to make the transport mechanism slide back the sheath is undesired, a transmission or actuator is needed to open the grasper as the current actuation mechanism is close on the edge of an uncomfortable actuation force.

If any changes occur in the design of the transport mechanism, experiments performed during this study need to be redone to verify that the grasper design still functions. For instance, different magnet or wire rope dimensions can influence the ability of straightening the compliant section of the grasper.

8 Conclusion

A wire rope based grasper for a friction-based transport mechanism has been designed and was able to successfully grasp and transfer gelatine phantom tissue into the existing transport mechanism. Wire ropes were plastically deformed to create a compliant section for opening and closing the grasper. Closing the grasp was done by sliding the sheath with magnets over the compliant section to straighten the wire ropes. Opening was done by sliding the sheath back, away from the grasper tip allowing the wire ropes to bend outwards. To minimize deformation of the grasper three wire ropes were soldered together in the grasper's tip and the wire ropes were constrained in sliders on the other end. This prevented torsion of individual wire ropes. To prevent wire ropes from moving angularly over the magnet surface of the magnet hole, wire rope guides were made. The measures provided a consistent grasper shape but still allow actuation of the transport mechanism. Four finger handles were used in combination with springs for voluntary opening operation of the grasper. During tests this was successfully used, and operation of the device was done by one person. The opening force needed was low enough for continuous operation when opening the grasper consists of 30% of the device operation time.

The grasper opened far enough for all phantom tissue samples to enter it with an average opening diameter of 9.58mm. Fulfilling the requirement of being able to grasp tissue with a 4mm diameter, with room for bigger tissue samples of a bigger size. Tested tissue samples were 3mm, 4mm, 5mm spheres and a 4mm in diameter cylinder with a length of 6.5mm. The cylinder sample was grasped in two orientations, the tissue axis parallel and perpendicular to the lumen of the transport mechanism.

After closing, all tissue samples were constrained successfully. For spherical 3mm, 4mm and 5mm samples, transfer into the lumen of the transport mechanism was successful. No significant difference in the needed cam rotations to transfer the spherical tissue samples into the transport mechanism lumen was observed ($p= 0.053$). It must be noted that the 3mm samples did not contact all wire rope groups and had scattered results. On average the 5mm sample was transferred the quickest with a mean of six cam rotations. As this is the sample with the biggest diameter no maximum size tissue sample can be concluded. All six axial cylindrical samples were successfully transferred into the lumen but of the perpendicularly grasped samples three samples failed. The failed samples did not reorient and align with the lumen of the transport mechanism and were cut in half or fell out. This happened as the samples were not centred enough to contact more than two wire rope groups. Between the successfully transferred 4mm sphere, parallel grasped cylinder and perpendicularly grasped cylinder samples no significant difference in needed cam rotations was observed ($p=0.19$).

To verify that the grasper also functions when the transport mechanism is bent, 5mm spherical samples were successfully grasped in bends with a radius of 59mm and angles of 20 and 40 degrees. It was possible to insert and extract the grasper through the bent sections in closed configuration. When the bend was 60 degrees, one out of six samples initially did not enter the lumen. Transfer was only successful after moving the transport mechanism back and forth through the bend. It probably failed due to deformation of the grasper as the wire ropes are connected in the tip. As the deformation is probably the cause of unreliable transfer into the lumen at bends of 60 degrees or more, further research into the underactuation is desired. Despite the deformation of the tip no lumen collapse occurred.

Suggestions for future research are introducing steerability. If the grasper can orient itself the grasper can function as a standalone surgical instrument and position itself around tissue. Increasing the range of tissue sizes is also important as during surgery, tissue will not always have the same shape. For now, it can be concluded that a wire rope based grasper for the transport mechanism has successfully been developed, taking a step further towards a new surgical instrument.

Appendix I: Stiffness Measurement of Treated Wire Ropes

Besides evaluation of the way to give the wire rope a new shape the glue and solder can also give the wire rope different stiffness properties. To evaluate this a bending test is conducted. This will compare the stiffness properties between the cured wire ropes and the original wire rope.

$$\delta = \frac{FL^3}{3EI} \tag{5}$$

$$EI = \frac{FL^3}{3\delta} \tag{6}$$

	$F\ [N]$	$L\ [m]$	$\delta\ [m]$	$EI\ [N/m^2]$
Untreated wire rope	0.0147	0.06	0.01	$1.0584 * 10^{-4}$
Cyanolit treated wire rope	0.0386	0.06	0.005	$5.5584 * 10^{-4}$
Bison two component epoxy metal glue treated wire rope	0.0380	0.06	0.005	$5.472 * 10^{-4}$
Soldered wire rope	0.0201	0.06	0.004	$3.618 * 10^{-4}$

Figure 63: Bending test setup. A Futek force transducer connected to the wire rope.

Test has an unexpected outcome. The glues are stiffer and do not seem to permanently deform as soon as the soldered wire rope. This is strange as soldering was better than the glues in holding the wire rope in a bent shape. Due to plastic deformation being the easiest and most reliable method to change the wire ropes shape this will be used during production. If any extra stiffness is needed in a straight section the Cyanolit glue is most promising for its thin layer on top of the wire rope.

Appendix II: Required Magnet Force Depending on Bending Radius and Outward Angle of the Wire Rope

To get an estimation of the magnet force needed to prevent collapsing of the lumen a finite element analysis is conducted. The goal is to see the what effect bending radius and angle have on the force. The wire rope is of the type 7x1 with a total diameter of 0.6mm. This means that there are seven braided wire ropes with an individual diameter of 0.2mm. Six wire rope strands are rotated around a single core strand. A measurement was done to determine the pitch, every 11.5mm the wire rotates 360 degrees around the core. First the cross section is simplified. Each strand of the wire rope has a second moment of area of $7.8540 * 10^{-17} m^4$, calculated with Equation 7 [19]. As the wire ropes are not interconnected it is assumed that this second moment of area can be multiplied by 7 to get the total moment of area of the wire rope cross-section. It is possible that an error is introduced by this as there is friction contact between the wire ropes, though taking contact forces between wire ropes into the model greatly increases complexity and the simplified model will still give insight in the effect of altering the bending radius and bending on the needed magnet force. Thus, the total second moment of area is $5.4978 * 10^{-16} m^4$.

With the desired second moment of area the radius of the element cross-section for in the finite element analysis is calculated, also with Equation 8. The result is a radius of $1.6266 * 10^{-4} m$.
As material stiffness a young's modulus of 200GPa is used. This is for AISI301 steel. To investigate the needed magnet force to pull the wire to the edge three radii and three angle combinations are tested. Figure 64 displays the minimum angle with the minimum radius on the left and the maximum radius with the maximum angle on the right. Only the outward bending of the wire rope to open the grasp is considered. No tip shape for the grasping itself is added yet.

$$I_x = \frac{1}{4}\pi r^4 \tag{9}$$

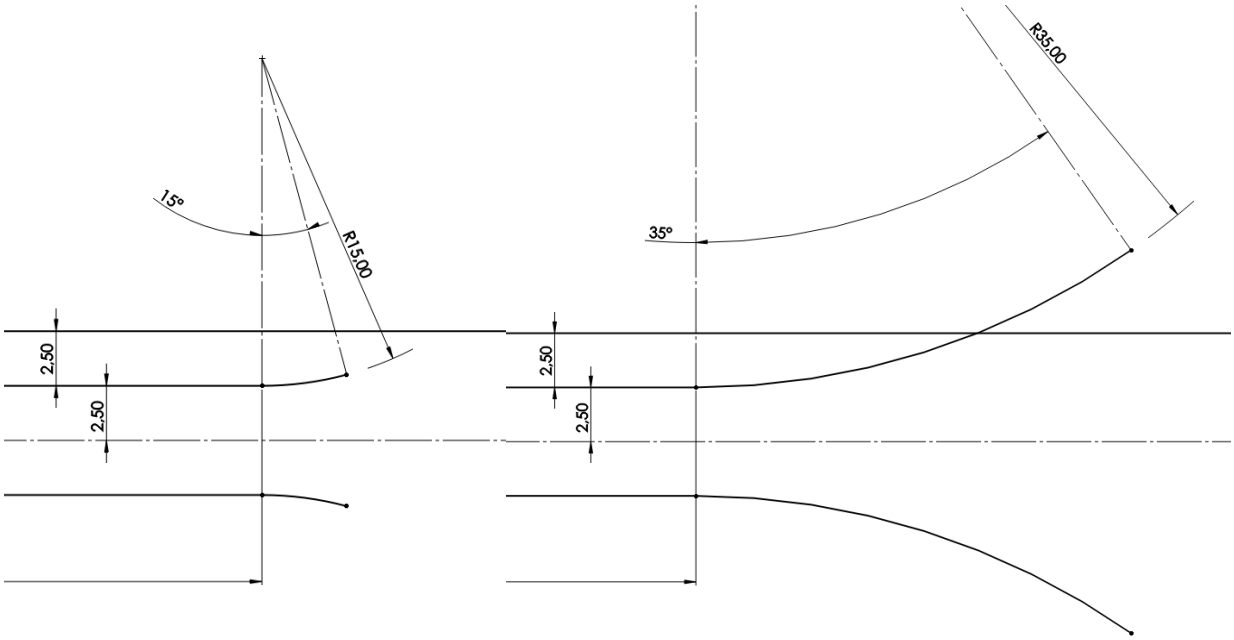

Figure 64: Picture of minimum outward shape of a radius of 15mm combined with an angle of 15 degrees and the maximum outward shape of a radius of 35mm combined with a 35 degree angle. The dotted line is the center of the lumen.

Creation of the curve and key points is displayed in Figure 65. On the left of picture (A) is the origin with key point 1 and on the right key points 2 to six are used to create the curved geometry. Key point one will be fully constrained as it is considered not to move. Key point 4 and 6 get a forced displacement to y=0. This simulates the wire rope being in the sheath. Due to the initial shape the wire rope bends downward, but this is prevented by the forced displacement. Extracting the reaction force on key point one gives the needed force to keep the wire rope pulled against the sheath and preventing a collapsed lumen. All results are shown in Table 6.

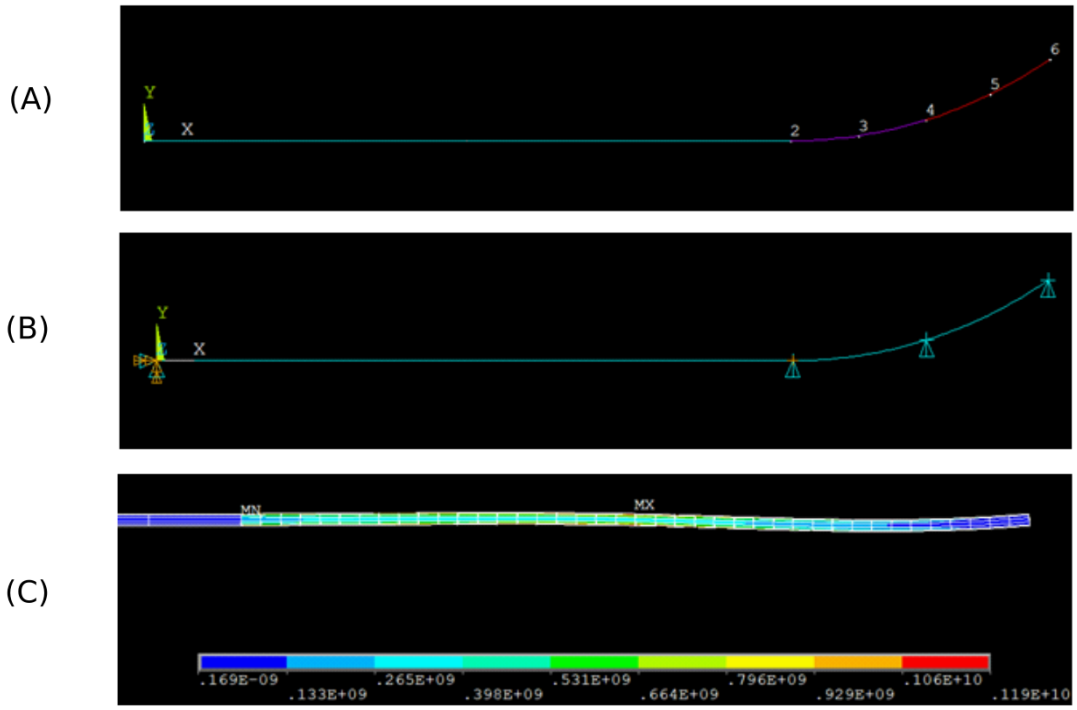

Figure 65: Ansys APDL screenshots. (A) Shows the key points used to create the curve. (B) Displays the points where constraints and forced defleflections are applied. (C) Displays the final deformed result with MX being the point where the magnet force applies.

It shows that a bigger angle results in a lower force due to the points where the reaction forces of the constraints are applied being further away from each other. This distributes the bending over a bigger length. As expected a smaller radius results in a larger force needed to keep the wire rope pulled to the wall of the sheath. A bigger bending angle results in a lower needed force to straighten the wire rope. This happens because the space between the magnets also increases. Because of the extra space the middle magnet creates a larger bending moment in the wire rope with the same force due to the longer bending arm.

Table 6: Reaction forces in key point 4 needed to prevent the collapse of the lumen.

Radius \ Angle	15 degrees	25 degrees	35 degrees
15mm	6.2161 N	3.7985 N	2.7274 N
25mm	2.2780 N	1.3765 N	0.98528 N
35mm	1.1679 N	0.70358 N	0.50316 N

Below the Ansys APDL code used to solve the problem is shown.

```
FINISH
/CLEAR,START
!set parameters

Radius_beamsection = 0.00016266
Lstraight = 0.05
Rbend = 0.035
pi = acos(-1)
Angle_bend = 15*pi/180 !degrees to rad
Angle_bend_half = Angle_bend/2
Angle_bend_quarter = Angle_bend/4
Angle_bend_threequarter = Angle_bend-Angle_bend_quarter

Xpoint1 = 0
Ypoint1 = 0

!start of curvepoints
```

```
Xpoint2 = Lstraight
Ypoint2 = 0

Xpoint3 = Lstraight + Rbend*cos(Angle_bend_quarter-pi/2)
Ypoint3 = Rbend*sin(Angle_bend_quarter-pi/2)+Rbend

Xpoint4 = Lstraight + Rbend*cos(Angle_bend_half-pi/2)
Ypoint4 = Rbend*sin(Angle_bend_half-pi/2)+Rbend

Xpoint5 = Lstraight + Rbend*cos(Angle_bend_threequarter-pi/2)
Ypoint5 = Rbend*sin(Angle_bend_threequarter-pi/2)+Rbend

Xpoint6 = Lstraight + Rbend*cos(Angle_bend-pi/2)
Ypoint6 = Rbend*sin(Angle_bend-pi/2)+Rbend

Xcenterarc = Lstraight
Ycenterarc = Rbend

/PREP7
!element selection
ET,1,BEAM189


!define cross sections flexure part
SECTYPE, 1, BEAM, CSOLID, , 0
SECOFFSET, CENT
!      Width        Height     for crossecttion
SECDATA, Radius_beamsection, 10, 3

!radius, number of divisions around circumference, divisions through radius (slightly
higher than default)


!material properties
MPTEMP,1,0          !temperature stuff
MPDATA,EX,1,,200e9  !youngs modulus
MPDATA,PRXY,1,,0.30  !posson ratio


/title, your_ title
/prep7
k,1,Xpoint1,Ypoint1                        ! sets a keypoint at (0,0)
k,2,Lstraight,0
k,3,Xpoint3,Ypoint3
k,4,Xpoint4,Ypoint4
k,5,Xpoint5,Ypoint5
k,6,Xpoint6,Ypoint6

k,7,Xcenterarc,Ycenterarc

l,1,2
LARC,2,4,7,Rbend !LARC,2,4,3
LARC,4,6,7,Rbend !LARC,4,6,5

! Meshing of lines
TYPE,1                          !element type1
SECNUM,1                   !section num1
!LSEL,S,LINE,, !select lines              LSEL,S,LINE,,Line_ID1+1 ,Line_ID2 !select
lines
LESIZE,ALL, , ,20               !mesh 20 elements per line
LMESH,ALL                  !mesh all selected elements
ALLSEL,ALL                 !reselect everything
/ESHAPE,1                         ! Display 3d version of 1d elements
```

```
/SOLU
ANTYPE, 0   !Static analisys
NLGEOM,1
!NSUBST,5,1000,1
AUTOTS,1
OUTRES,ALL,ALL    !save ALL information on ALL substeps
TIME,0.4          !hold ground&shuttle, apply imperfection

!LOADCASE 1 Folding
DK,1,ALL
DK,2,UZ,0
DK,2,UY,0
DK,2,ROTZ,0

DK,4,UZ,0
DK,4,UY,-Ypoint4

DK,6,UZ,0
DK,6,UY,-Ypoint6
!DK,6,ROTZ,-Angle_bend



!NLIST,ALL
!KLIST,ALL

ALLSEL
SOLVE
*STATUS

/post1
PRRSOL

/dscale,ALL ,1
PLDISP,0


!ANTIME,10,0.5, ,1,2,3,4

PLESOL, S,EQV, 0,1.0
```

The previous results have been used as guidance for experiments to determine the dimensions of the grasper. An attempt was made to simulate the magnet force on the wire rope to quickly create a digital design but too many parameters were unknown to create a reliable model. The model simulated is displayed in Figure 66 with the following parameters.

Dimensions:
Magnet: 10mmx2mm, hole 5mm
Wire rope: 0.529 mm diameter (surface area of 7x 0.2mm wire ropes), length 22mm (10mm in each direction out of the magnet)

Magnet properties:
Coercive force, 10.9kOe or 8,6739e+05 A/m.
Residual induction or remanence, 1.21 Tesla.

Wire rope magnetic material properties:
B-H curve of cold rolled low carbon steel from Ansys.

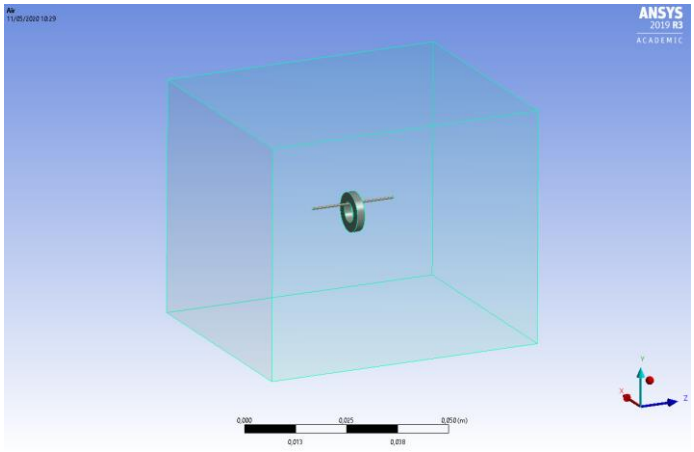

Figure 66: Dimensions of setup to simulate magnetic force on the wire rope.

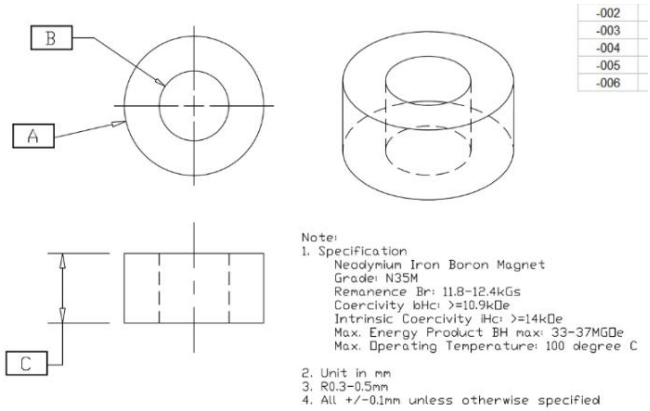

Figure 67: Magnet datasheet snippet.

Results

The calculated total force in Y-direction was 0.9N. Figure 68 displays the red and yellow area where the force on the wire rope is concentrated. In this figure the magnet is hidden.

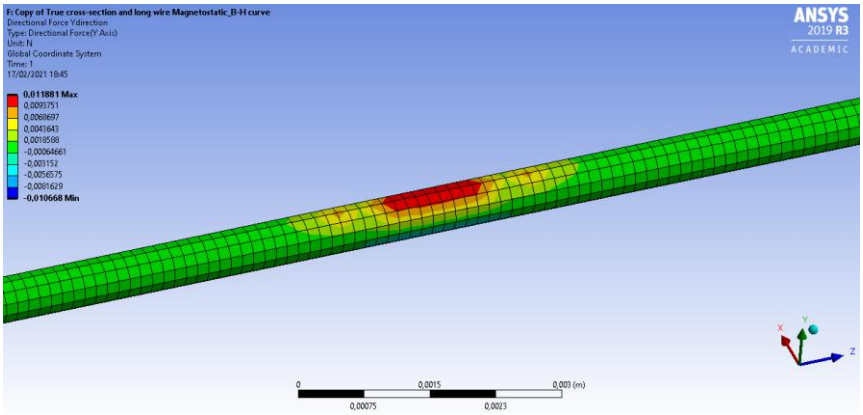

Figure 68: Concentration of magnet force on the wire rope. Red and yellow indicate a high force density.

To verify the model of the magnet force on the wire rope a test setup was 3D-printed to tension a piece of wire rope and constrain a magnet. A kitchen scale was used to measure the force needed to detach the magnet from the wire rope by pressing down on the magnet. Figure 69 displays the setup. The force at which the magnet detached was 19g plus the weight of the magnet of 2g totaling 21g. This is 0.21N, not close to the outcome of a simulation with Ansys in Appendix I that predicted 0.9N.

Figure 69: Measurement of detachment force threshold between magnet and wire rope.

As the model and experiment were not close in their results an endeavor was taken to get the magnetic properties of the wire rope. Unfortunately, the manufacturer was unable to present them as shown in the e-mail below. Because of the difficulties in obtaining the exact material properties an approach based on empirical tests was done.

Hello, Mr. Kooiman,

unfortunately, we are unable to provide any well-founded information on the subject of "magnetic properties of wire ropes".
The magnetic properties of high-tensile ropes vary significantly and it is difficult to influence them specifically.

If you know a material from which you would like to have a rope made, we would be happy to check its availability and workability.
Unfortunately, we cannot make any suggestions ourselves which alloys may be recommended without further detailed information.

If you give us details and sizes that you would like to have fulfilled, we may talk to a wire producer and check the availability.

In the field of austenitic steels the 1.4310 (AISI 302) would be strongly magnetic.
However, we cannot make precise statements about the (relative) permeability and its reproducibility in the manufacture of ropes.

--
Mit freundlichen Grüßen
With best regards

Stephan La Roche

Geschäftsführer • Managing Director

ENGELMANN
Vom Hofe Group

ENGELMANN Drahtseilfabrik GmbH • Eckenerstraße 7 • 30179 Hannover
T +49 511 63983-11 • F +49 511 63983-99
laroche@engelmann-online.de • www.engelmann-online.de
Die gesetzlichen Pflichtangaben finden Sie unter www.engelmann-online.de/pflichtangaben

Appendix III: Results Wire Rope Shaping, Modular Prototype Lumen Collapse and Wire Rope Manufacturing Steps.

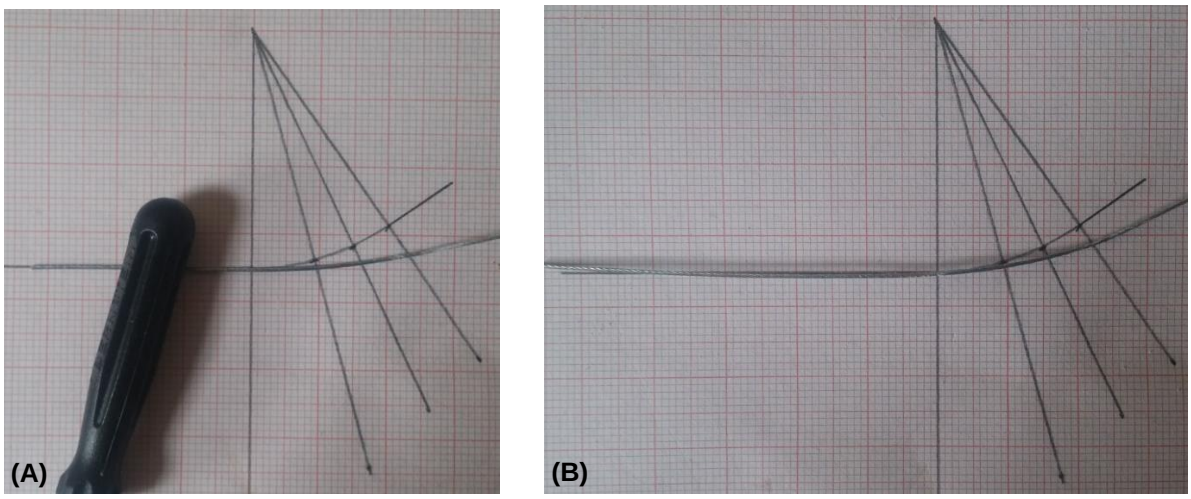

Figure 70: (A) Cyanolit treated wire rope constrained on an angle of 35°and a radius of 35mm. The wire rope barely remains curved after being released from the mould. (B) A better result is achieved when the wire rope is constrained from a radius of 35mm to a radius of 31.66mm. Instead of a straight continuing wire an angle of 8°degrees were added.

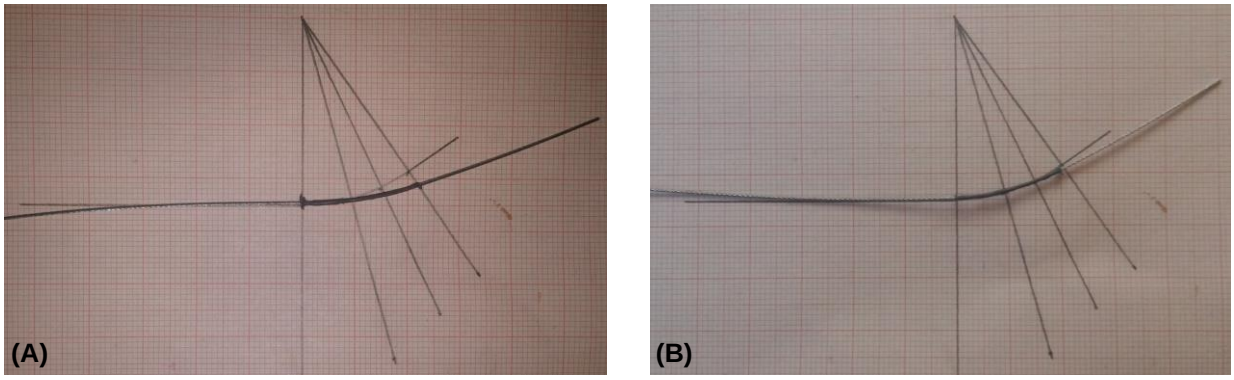

Figure 71: (B) Wire rope treated with Bison two component expoxy metal glue while being constrained in a radius of 35mm and an angle of 35°. After release from mold it straightens to its original shape. (B) Wire rope treated with Bison two component expoxy metal glue while being constrained in a radius smaller than 35mm. As can be seen the lower radius compensates partially for the deformation after releasing the wire rope from the mould. The desired shape is still not perfectly matched.

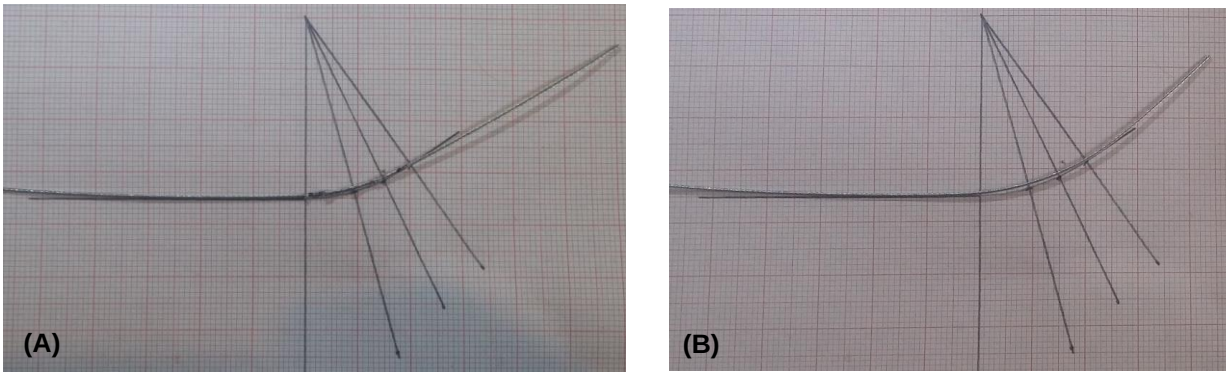

Figure 72: (A) Soldered wire rope remaining in a 35° angle and 35mm radius shape after being released from the mold. (B) Plastically deformed wire rope after bending 180°over a 10mm radius. Both follow the expected curve close.

For the experiment described in Chapter 3.4, a modular version of the transport mechanism has been developed to test different bending radii and angles and is shown in Figure 73. It can be opened from the side to see any wire ropes

detaching from the magnets. The number of magnets can be varied as well as the distances between them. A sheet of paper was used to check for plastic deformation of the wire ropes.

Figure 74 displays the group of bent wire ropes with a 35-degree angle and a 35mm radius on the left. On the right side of the figure the wire ropes are successfully straightened by the force of the magnets without collapsing into the lumen. Comparing the shape of the wire rope group before and after straightening in shows that the previously applied plastic deformation remains after straightening. Figure 75 shows that the wire ropes with a bending radius of 25mm over an angle of 35 degrees collapse. This also happens with magnets placed further apart in Figure 76. The extra distance between the outer magnets increases the bending moment in the middle with the same magnet force but it is not enough to prevent lumen collapse.

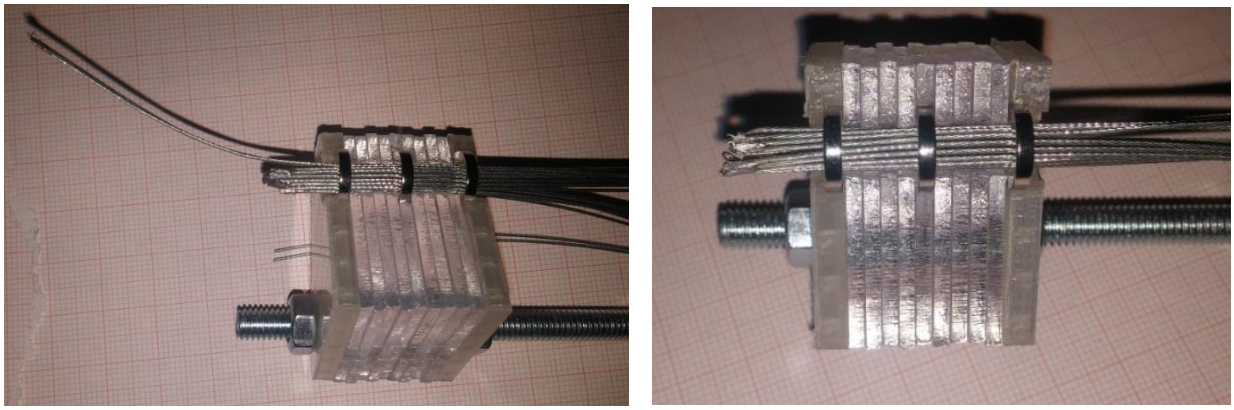

Figure 73: (Left) Bent group of three wire ropes, connected with solder at the tip. (Right) Group of wire ropes is pulled into the magnets without collapsing the lumen.

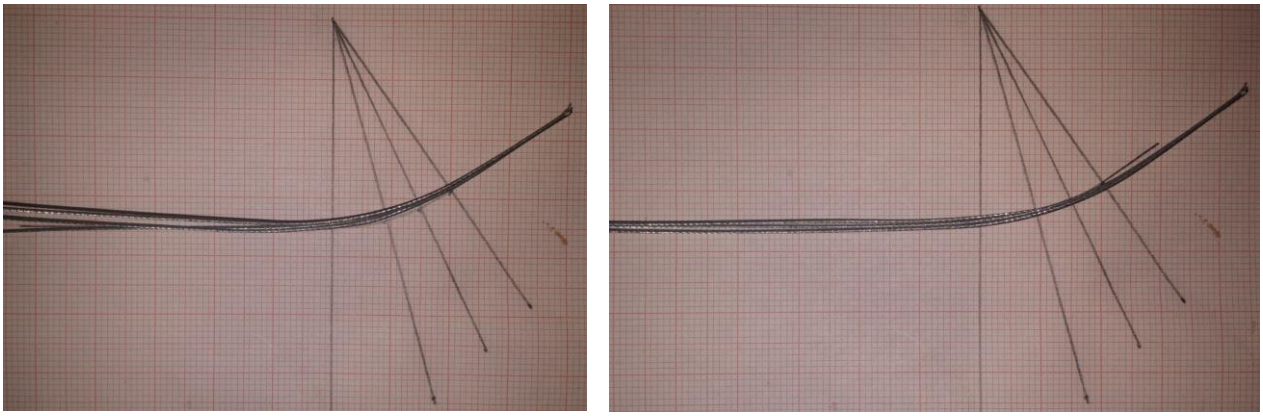

Figure 74: Shape of the wire rope before, bent in a radius of 35mm over an angle of 35° (Left) and after (Right) straightening it in the magnets multiple times. Only a minor difference is visible.

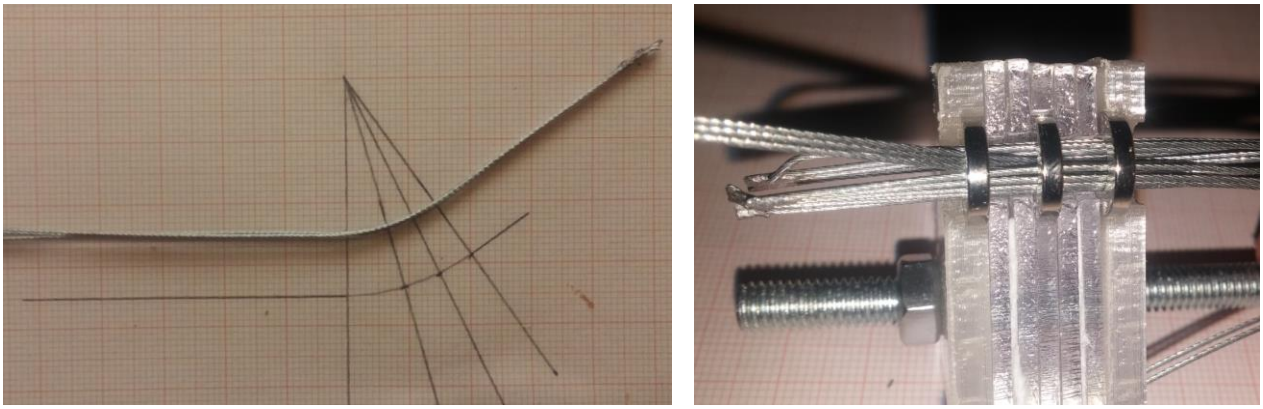

Figure 75: Wire rope bent with a radius of 25mm and an angle of 35 degrees collapses.

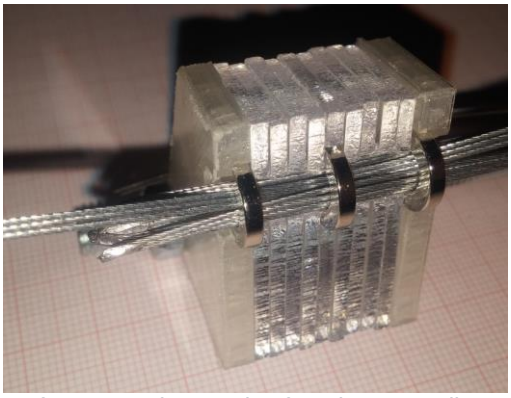

Figure 76: Wire rope bent with a radius of 25mm and an angle of 35 degrees collapses also with extra spacing between the magnets.

Wire Rope Manufacturing Steps Version 1

With the results of the previous experiment two versions of the grasper were manufactured. The first version suffered lumen collapse, improvents in the second version lead to a functioning grasper without lumen collapse. For the first version, a compliant section with a radius of 35mm over a bending angle of 25 degrees was made. After this section converging tips were added.

Production steps:

-Align 3 wire ropes.
-Bending all tips at the same time.
-Solder tips together.
-Bend de compliant curve. The tips need to be connected to not rotate individually while bending.
-Unsolder the tips.
-Cut 2 of the 3 tips shorter.
-Resolder the tips together.

The design resulted in a grasper with a consistent shape, but the lumen collapsed when the grasp was closed. As the lumen collapse did not occur with the same bending radius and larger angle on an earlier test the cause of the collapse is probably due to the soldered part being too close to the compliant section, and forcing the wire rope off the magnet in case of an imperfect orientation. In the earlier tests the soldered tip and compliant section were separated by a straight part.

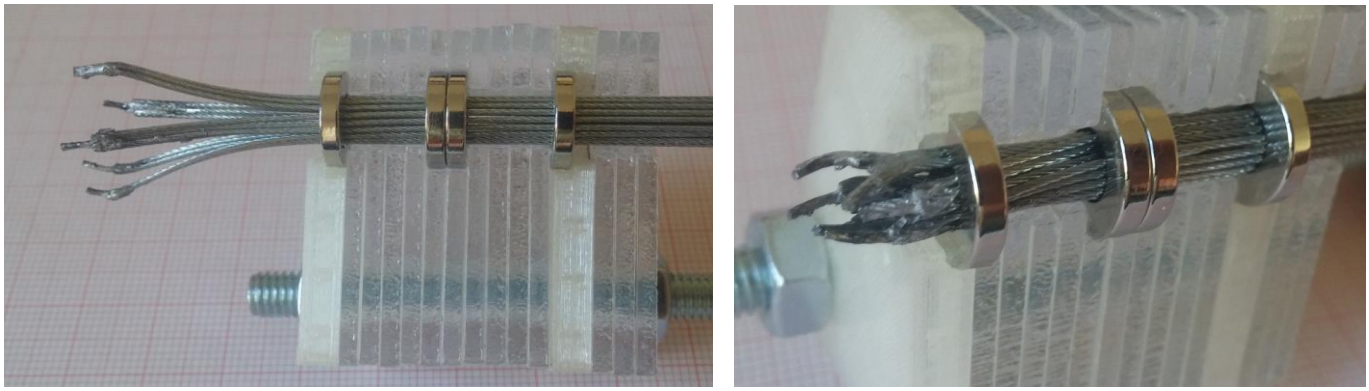

Figure 77: On the left first try of the open grasper. Each wire rope group has a consistent shape. On the right a collapsed lumen is shown. The collapse occurs due to the compliant section being directly connected to the soldered tip.

Version 2

A new design is made with a straight section between the soldered tip and compliant section. It has a bending radius of 35mm and an angle of 15 degrees. The straight section is 19mm long. The distance between the magnets was not changed as the FEM simulation showed that a bigger distance between the magnets also resulted in a lower force needed to keep the wire rope connected to the magnet in the middle.

Production steps:

For clamping the wire ropes during soldering the earlier developed glue mold was used.

-Align 3 wire ropes with the middle wire rope pointing out 7mm. This will later be bent to form the tip.
-Solder the 3 wire ropes together at the tip.
-Bend the 7mm tip.
-Apply tape to mark the straight part of the three wire ropes.
-Plastically deform the compliant section on a 15mm radius.

This design was succesful. Due to the straight section the grasper is longer than the first version but still opens far enough to grasp tissue the size of the lumen. The grasper was successfully able to pick up a piece of sponge in perpendicular orientation to the paper displayed in Figure 78. Due to the sponge being smaller than the opening distance between two wire rope groups of three, it is also possible to grasp from the side. Shifting the wire rope groups one by one manually successfully transported the sponge.

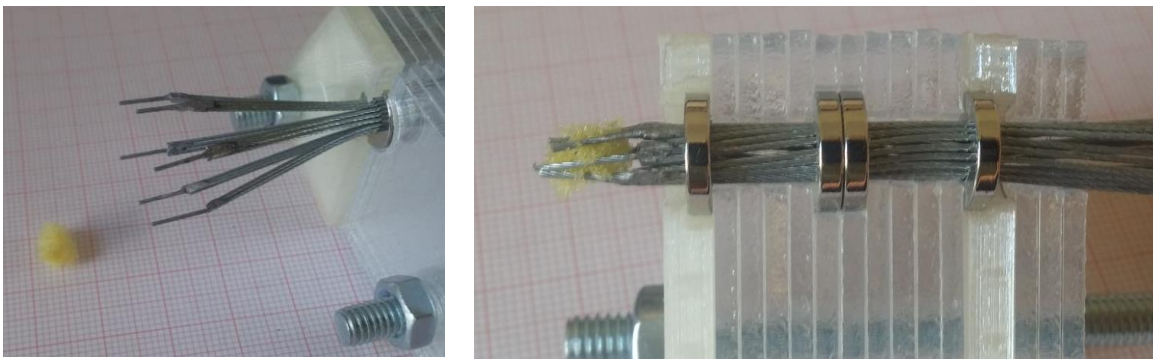

Figure 78: Multiple pictures of grasping a piece of a sponge. As can be seen on the top right torsion of the wire ropes occurs after closing and opening a few times.

Appendix III: Choosing Underactuation Springs

The wire ropes are connected in both the tip and the base where they are actuated. This creates a problem when bending the transport system. In Figure 79 the problem is shown. Bending gives the wire ropes a slightly different curvature radius as the wire ropes lie next to each other. This results in tension on one wire rope while the other two of the group are compressed with the risk of buckling. As an example an angle of $90°$ with a radius R of 59mm according to de Kater the transport system functions at this configuration [4]. The middle wire rope length for this angle is $\pi * 2R * \frac{1}{4} = \pi * 2 * 0.059 * \frac{1}{4} = 0.09268m$. The radius of the outer wire rope is 0.05906. Resulting in a length of $\pi * 2 * 0.0596 * \frac{1}{4} = 0.09361m$. The length of the inner wire rope is $\pi * 2 * 0.0584 * \frac{1}{4} =$ 0.09173m. The inner and outer wire rope have a length difference of $0.09361 - 0.09173 = 0.00188m$. Rounded this is 2mm.

On a total length of 0.25m the elongation is $\epsilon = \frac{0.00188}{0.25} = 0.00752$. With a common Youngs modulus for steel of $E = 200\ GPa$ the stress in the material can be calculated.

$$\sigma = E * \epsilon \tag{10}$$

$$\sigma = 200\,000\,000\,000 * 0.00752 = 1504MPa$$

The surface area of the cross section of the wire A rope is $\pi * 0.0001^2 * 7 = 2.199911 * 10^{-7}m^2$.

$$F = \sigma * A \tag{11}$$

Resulting in a theoretical force of $F = 1504\,000\,000 * 2.199911 * 10^{-7} = 330.87\ N$ needed to compress the inner wire rope to the same length of the outer wire rope.

This situation is theoretical, and the wire ropes will have some play sideways in the wire rope guides before the transport system. It shows that the stiffness of the wire ropes cannot be underestimated. Besides the change in length when the wire ropes are bended, fixing the wire ropes during assembly can also introduce small length differences between wire ropes. Considering that these small errors lead to unwanted high compression forces in the wire ropes of the transport system, underactuation is investigated.

Underactuation designs are shown in Figure 80. Part A displays a whipple tree mechanism that divides the input force of the main slider over the three output sliders. The design requires six joints and three bars, making it very complicated. In B a simpler design is shown using springs to compensate for wire rope length difference. Force between wire ropes is not evenly distributed and depends on the chosen spring stiffness. Because of the compliance of the springs, the wire rope that is compressed by bending the transport system does not buckle. As there are no joints needed manufacturing is relatively easy. Design C is partially underactuated. The middle wire rope is directly connected to the main slider. The outer wire ropes are connected to the main slider by a seesaw mechanism with one bar and three hinges. This divides an input force from the hinge on the main slider over the outer wire ropes but not the middle wire rope. The three hinges make the design relatively complicated to the spring underactuation. Therefore, the spring underactuation is chosen to be in the final design.

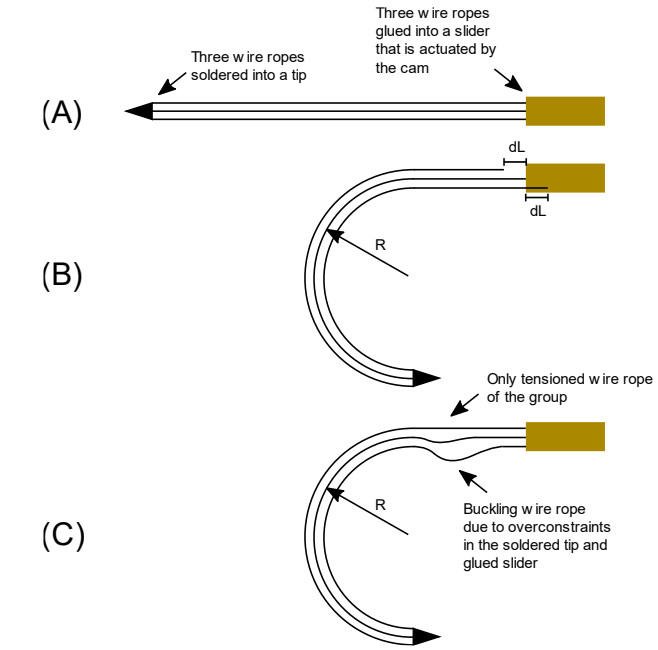

Figure 79: (A) Connection of the wire ropes in the tip and at the slider. (B) Difference in wire rope length occurs due to bending. (C) Difference in length leads to tension on one wire rope and compression on the two others of the group. This can lead to buckling.

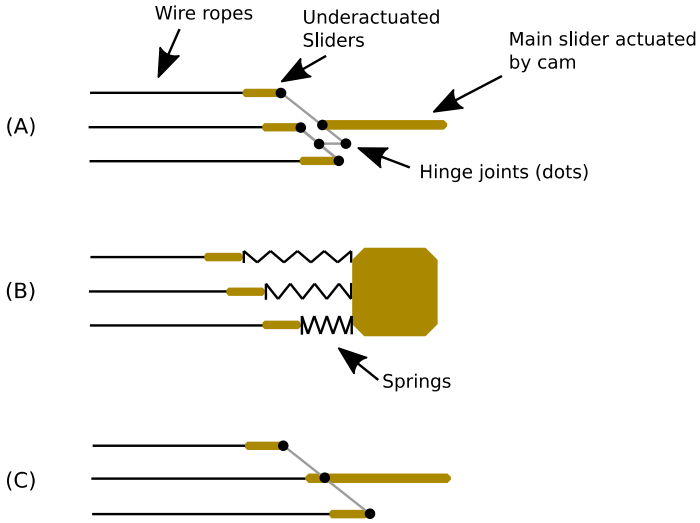

Figure 80: Underactuation options. A displays a whipple tree design dividing the input force on the main slider over the subsliders. In B springs act as underactuators that compress when there is a length difference between wire ropes. The last option C is not fully underactuated as the middle wire rope is connected to the main slider. The outer wire ropes are connected to the main slider by a seesaw mechanism.

The force on the wire ropes needs to be known in order to calculate the spring stiffness of the underactuation mechanism.

Weight total setup: 406g
Weight single magnet clamp side: 43g

Weight to be subtracted: 406-43*2=320g

Average weight before wire ropes start sliding: 960.6g with a standard deviation of 31.858g after 10 measurements.

960.6 – 320 = 640.6g

There are 18 wire ropes and 4 ring magnets in the test setup so 18*4=72 contact points.

For a straight system this would result in a friction force of 640.6/72=8.9g for each contact point.

The system will have 15 magnets, totaling in 8.9*15 = 133.5g of friction on each wire rope. Or 1.31 N. For 18 wire ropes this is 2.4kg or 23.58N.

Besides the friction from the magnets, also friction of the wire rope divertors needs to be considered as there is tension on the wire rope when it is guided towards the sliders. The factor that increases the wire rope tension T is calculated with the following formula using the wrapping angle α and friction coefficient μ between the wire rope and the guide [5].

$$\frac{T_1}{T_2} = e^{\mu\alpha} \tag{12}$$

The total wrapping angle for the two bends of the wire rope guide is $\alpha = 47.55° * 2 = 95.6°$ or $1.668\, rad$. Friction coefficient μ is unknown. 0.3 is the outcome for nitrile in this paper [20]

$$T_1 = e^{\mu\alpha} * T_2 = e^{0.3*1.668} * 1.31 = 2.16N$$

With these values the maximum spring stiffness is 1.08N/mm if 2mm of length difference is allowed.

Figure 81: Measurement setup for measuring friction force of four magnets.

Possible options from Amatec with an external diameter of 4mm.

	L0 [mm]	L1 [mm]	Pf [N/mm]	P1 [N]	d (draaddikte) [mm]	Price [Euro] Per piece, 25 total	Material
A-DF1345	22	8.33	1.19	16.24	0.5	1.07	Steel
A-DF1346	**24**	**9.51**	**1.02**	**14.84**	**0.5**	**1.07**	**Steel**
A-DF1347	31	12.44	0.76	14.14	0.5	1.07	Steel
A-RDF1345	22	8.33	1.02	13.94	0.5	1.86	RVS302
A-RDF1346	24	9.51	0.88	12.75	0.5	1.86	RVS302
A-RDF1347	31	12.44	0.65	12.14	0.5	1.86	RVS302

Cam Design Changes

The same cam design as in the design by de Kater will be used. Though because springs are added the amplitude will be increased as the springs introduce hysteresis in the system. $\frac{2.16}{1.02} = 2.12mm$ on both top and bottom of the cam groove amplitude needs to be added. Amplitude of Esther her cam is 2.5mm, 5mm in wire rope displacement. Combined with the expected hysteresis the new cam amplitude is 4.62mm, shown in Figure 82. After assembly the prototype did not transport tissue. Presumably due to too much hysteresis in the springs, creating places on the camprofile where wire rope groups do not move. This hinders the friction transport of tissue. Therefore, changes were made to concentrate the hysteresis of the springs in a narrow part of the cam. This prevents the situation where one wire rope group is slid forward by the steep part of the cam, two wire rope groups are not moving due hysteresis and only three wire rope groups contribute to transport. The updated design is shown in Figure 83. Unfortunately, the design was not able to fix the problem. Therefore, the decision was made to block the underactuation springs and use the cam profile from Figure 82.

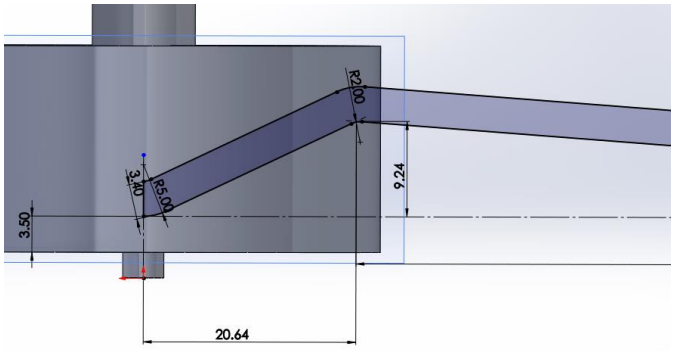

Figure 82: Cam profile with increased amplitude.

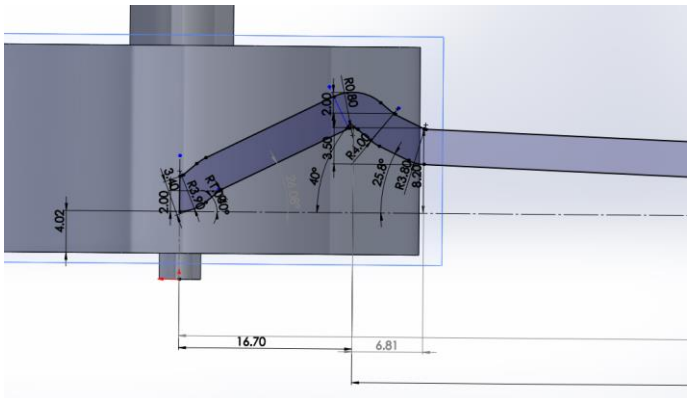

Figure 83: Cam profile to concentrate the hysteresis in the underactuation springs on a narrow part of the cam.

Appendix IV: Parts List and Design Drawings

Parts list
Below the full parts list to assemble the design is shown.

Table 7: Parts to be 3D-printed

Part description	Part number	Amount	Cost [Euro]	Where to order
Outer shell	-	1	-	DEMO
Inner shell	-	1	-	Formlabs printer 3mE
Cam	-	1	-	DEMO
Motor and battery housing	-	1	-	DEMO
Slider and bearing holder	-	1	-	DEMO
Slider outer shell	-	1	-	Formlabs printer 3mE
Sheath slider	-	2	-	DEMO
Spring blocker	-	18	-	Formlabs printer 3mE

Table 8: Parts to be milled or turned

Part description	Part number	Amount	Cost [Euro]	Where to order
Main Slider	-	6	-	Workshop
Subslider	-	18	-	Workshop
Pin main slider	-	6	-	Workshop
Tap staff 4mm for nuts for sheath slide guide		2	-	Workshop

Table 9: Wire rope, sheath componens and springs for voluntary opening operation.

Part description	Part number	Amount	Cost [Euro]	Where to order
Wire rope 7x1 0.6mm	-	6m	-	Engelmann
Underactuation springs	A-DF1346	25 (18 needed)	26.75 (for 25 pieces)	Amatec
Springs in sheath to space magnets	C0360-029-0500M	16 (12 needed)	40.16	Amatec
Spring in sheath. As try out	C0360-026-0500M	1	2.93	Amatec
Conrad components permanent magnet ring N35M 1.24T	506018	15	26.70	Conrad
Shrink tube 12mm (2 meter)	1570958	1	3.57	Conrad
Shrink tube 14.7 (1 meter)	1572512	1	0.64	Conrad
Sheet metal 0.1mm, for lasering wire rope guides	-	1	-	TU Delft workshop
Spring voluntary opening	-	4	-	Het Tanthof B.V.

Table 10: Standard components used.

Part description	Part number	Amount	Cost [Euro]	Where to order
M1.6x8 DIN 912 Inbus screw		2		Microschroeven.nl
M1.6 DIN 934 nut	888715	2	0.56	Conrad
M2x2 DIN 916 setscrew	1062669	18 (50)	7.03	Conrad
M2.5x8 DIN 916 setscrew		18 (25)	4.75	Microschroeven.nl
M2.5x6 DIN 916 setscrew		18 (25)	4.75	Microschroeven.nl
M3x6 DIN 933 Hexagon head screw		4 (10)	1.50	Microschroeven.nl
M3 DIN 934 nut		8		Already owned

M3x10 sunken philipshead screw		2		Already owned
M3x25 DIN 912 Inbus screw		4 (10)	1.40	Microschroeven.nl
M4x20 DIN 933 Hexagon head screw	128169	2	3.12	Conrad
M4 thread 2 times 105mm (500mm ordered)	237108	1	1.44	Conrad
M4 DIN 934 nut	888719	10	0.70	Conrad
M4 DIN 985 nyloc nut	223409	2 (10)	1.72	Conrad
M5x35 DIN 933 Hexagon head screw		2		Bouwmarkt
M5 DIN 934 nut		2		Already owned
M5x10 DIN 916 Setscrew	222523	6 (20)	2.37	Conrad
Staff 4mm length 50mm		2		Workshop

Table 11: Electrical components for actuating the transport mechanism.

Part description	**Part number**	**Amount**	**Cost [Euro]**	**Where to order**
Tumble switch	701343	1	0.99	Conrad
DC 12v power connector	1582319	1	1.27	Conrad
9V battery	-	1	-	Already owned
9V battery connector	-	1	-	Already owned
H-bridge motor driver L298N	-	1	-	Already owned
Potentiometer 10k kiwi-electronics	KW-1520	1	1.15	Kiwi-electronics
Arduino Nano V3.0 Compatible	000206	1	6.00	Tinytronics
40 pins header male – 90 degrees for Arduino Nano	000248	2	0.50	Tinytronics
Sheet metal 1.0mm for motor mount	-	1	-	Workshop
Sheet metal 1.0mm for battery mount	-	1	-	Workshop
6V Motor with gearbox 300rpm	JGA25-370	1	7.50	Already owned
Motor coupling	-	1	3	Already owned
Oxelo abec 5 skate bearing for cam	2961269	1	1.4	Decathlon
9V powersupply	-	1	-	Already owned

Drawings

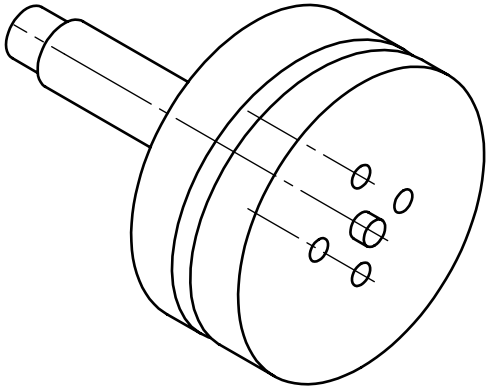

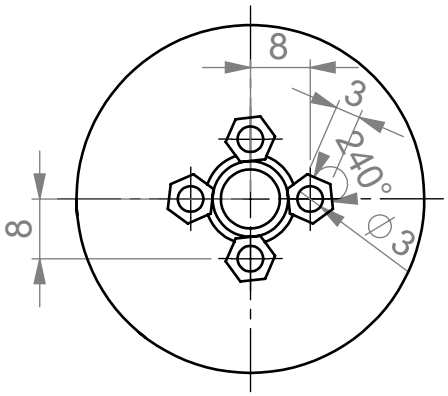

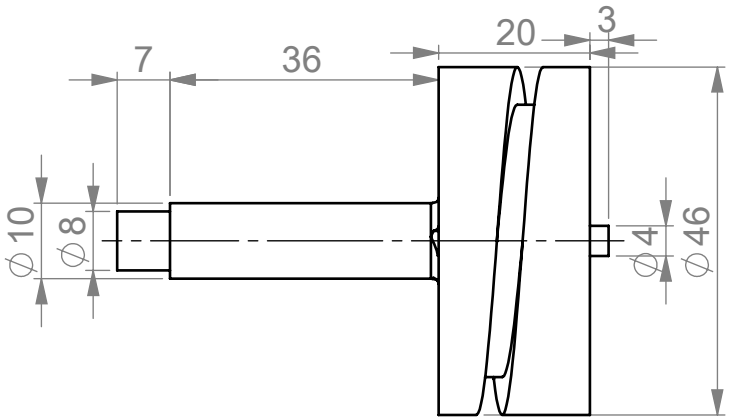

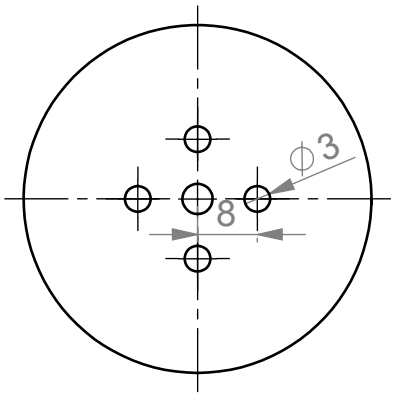

TU Delft Delft University of Technology	name Cam	units mm	scale 1:1	quantity <<nr>>	date 12/05/2021
		material		mass gr	remark <<remarks>>
	author <<names & student numbers>>	group <<group>>	format A4	drawing no. <<drawing no.>>	

C:\Users\Hugo\OneDrive\01 - Afstuderen TU\01 First prototype\Bigger_diameter\TU_Templates\TU_Templates\

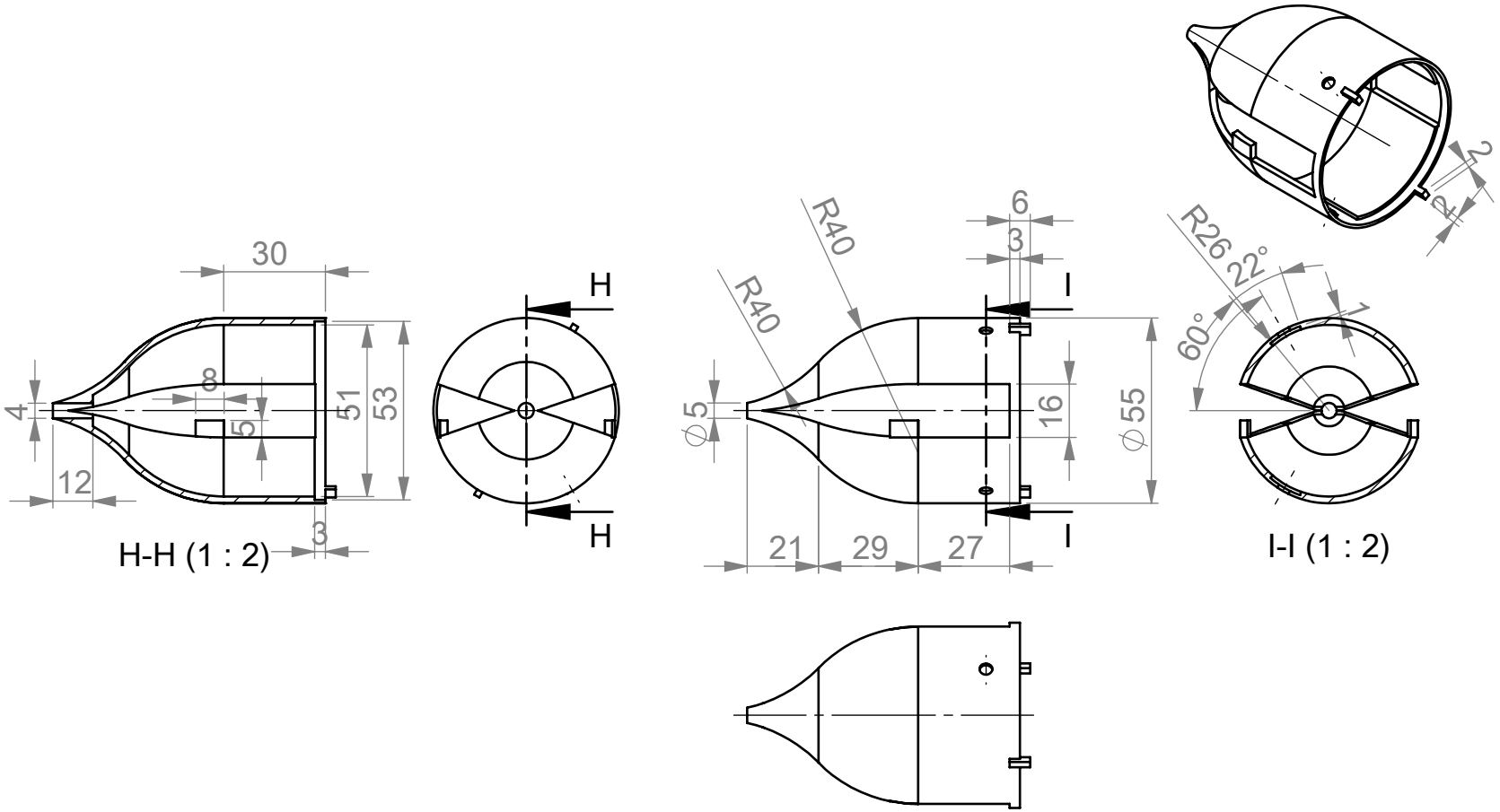

TU Delft Delft University of Technology	name Inner_shell	units mm	scale 5:1	quantity <<nr>>	date 12/05/2021	remark <<remarks>>
		material			mass gr	
	C:\Users\Hugo\OneDrive\01 - Afstuderen TU\01 First prototype\Bigger_diameter\TU_Templates\TU_Templates\	author <<names & student numbers>>		group <<group>>	format A4	drawing no. <<drawing no.>>

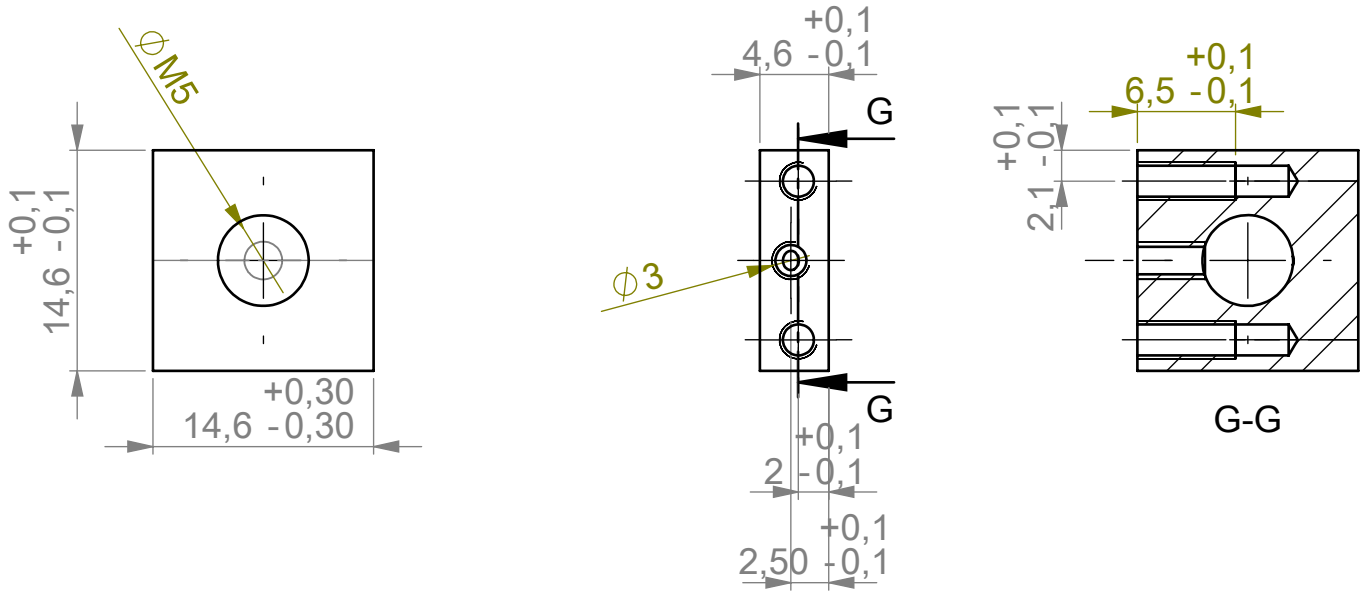

Delft University of Technology

Main_slider_drawing3.1

name	units mm	scale 2:1	quantity <<nr>>	date 12/05/2021	remark <<remarks>>
material Aluminium				mass gr	
author <<names & student numbers>>		group <<group>>	format A4		drawing no. <<drawing no.>>

C:\Users\Hugo\OneDrive\01 - Afstuderen TU\01 First prototype\Bigger_diameter\TU_Templates\TU_Templates\

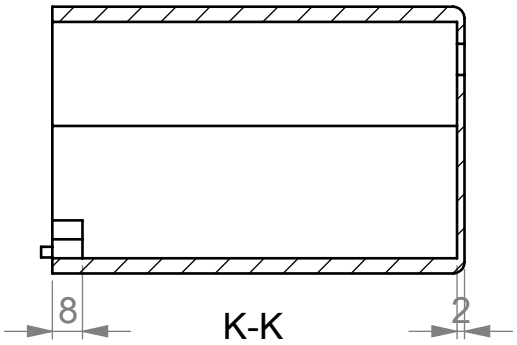

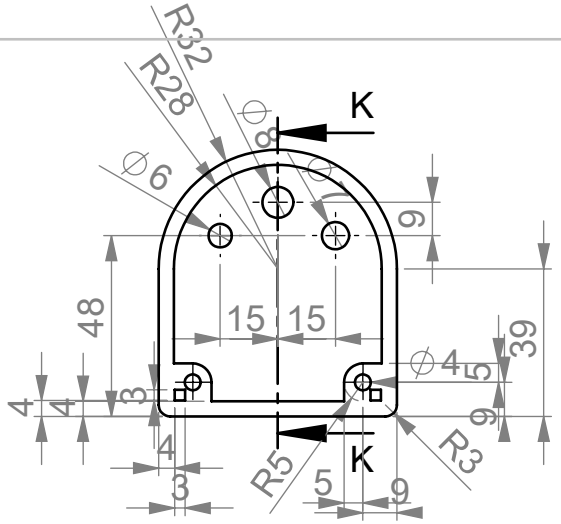

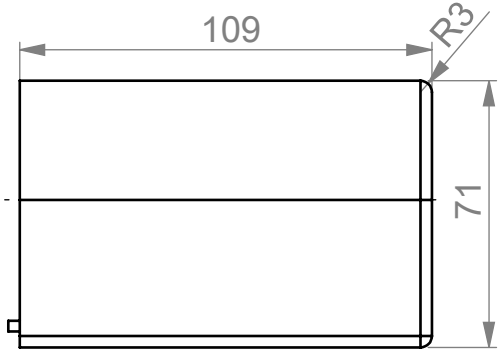

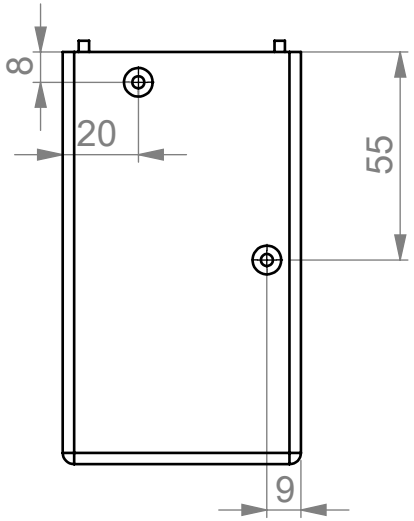

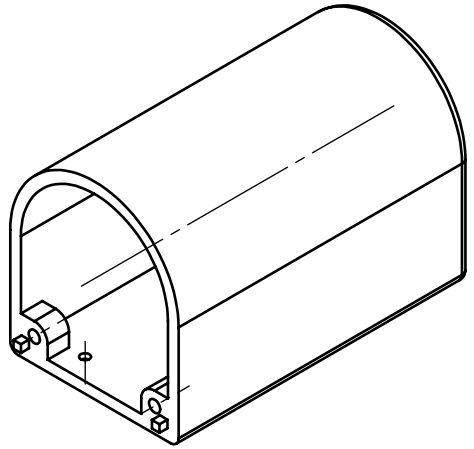

TU Delft Delft University of Technology	name Motor_battery_housing C:\Users\Hugo\OneDrive\01 - Afstuderen TU\01 First prototype\Bigger_diameter\TU_Templates\TU_Templates\	units mm	scale 1:2	quantity <<nr>>	date 12/05/2021
		material		mass gr	remark <<remarks>>
		author <<names & student numbers>>	group <<group>>	format A4	drawing no. <<drawing no.>>

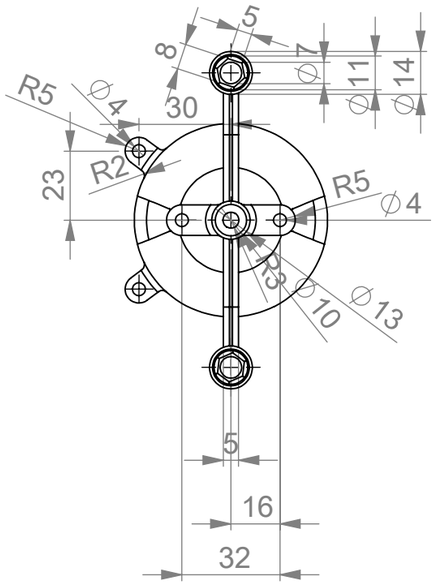

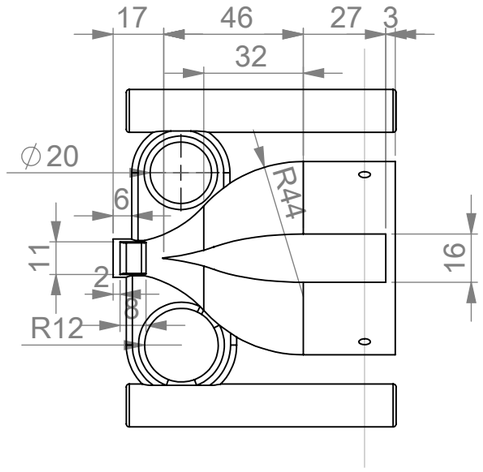

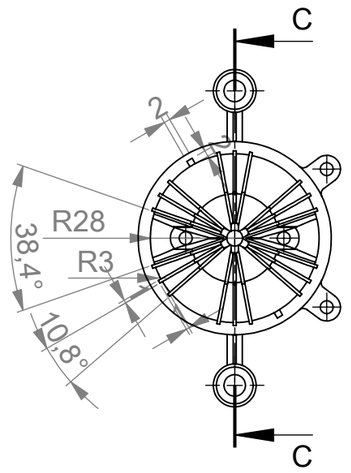

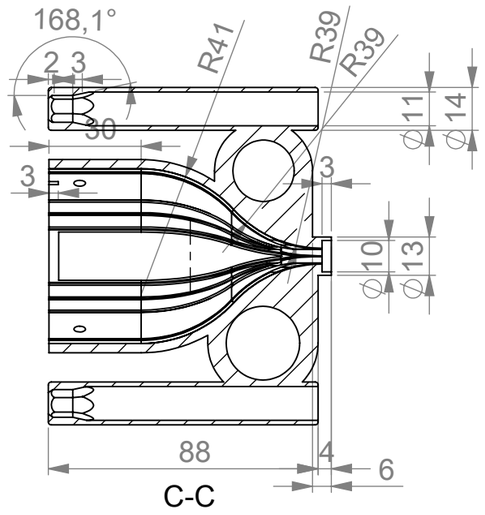

C-C

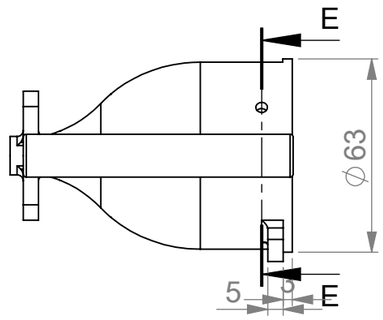

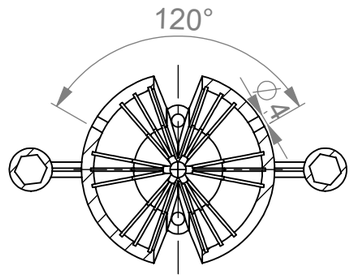

E-E

	units mm	scale 1:2	quantity <<nr>>	date 12/05/2021
material				mass gr
author <<names & student numbers>>			group <<group>>	

remark <<remarks>>

name

Outer_shell_drawing

C:\Users\Hugo\OneDrive\01 - Afstuderen TU\01 First prototype\Bigger_diameter\TU_Templates\TU_Templates\

TU Delft Delft University of Technology

format A3

drawing no. <<drawing no.>>

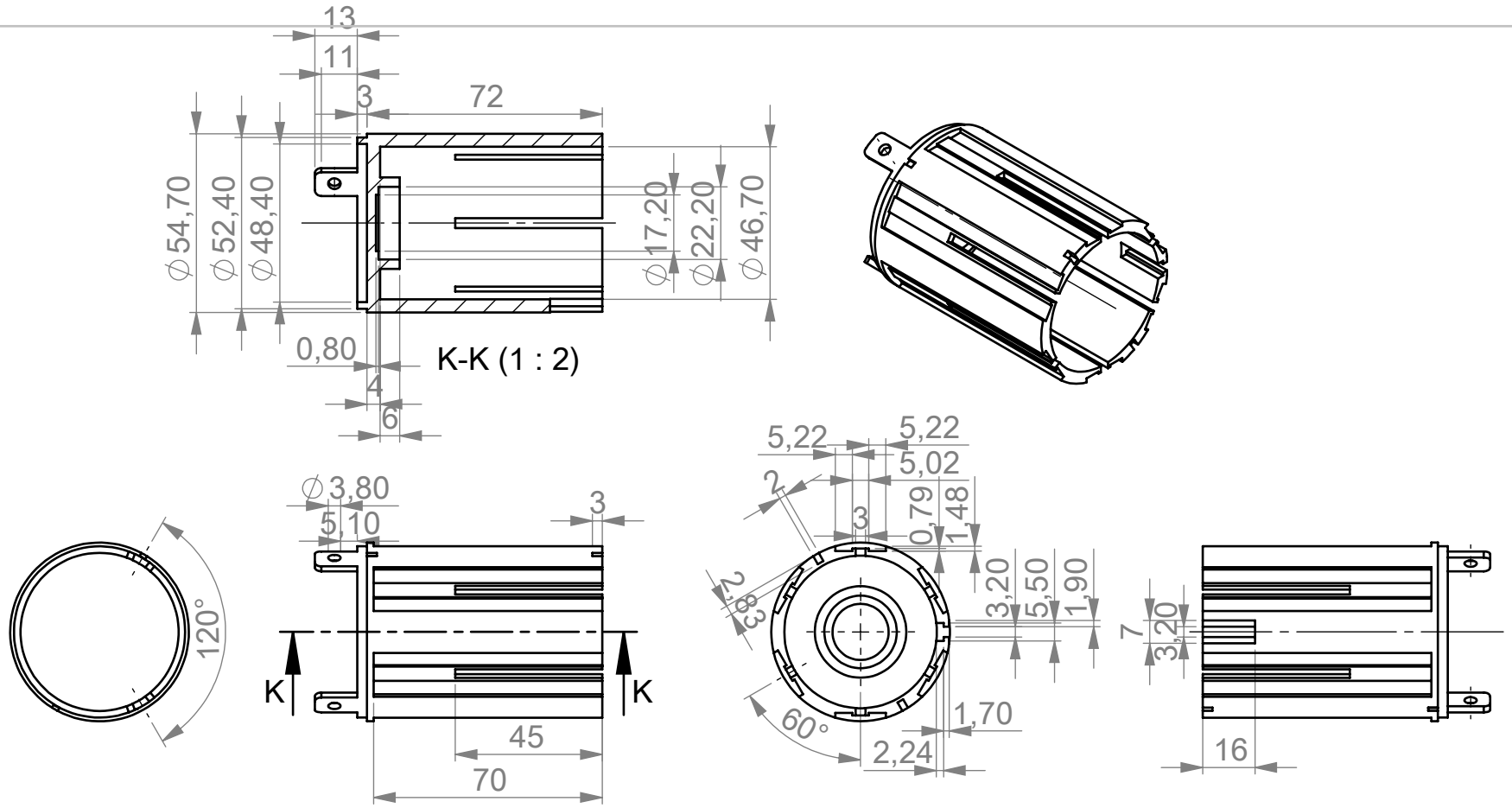

Slider_and_bearing_holder

Delft University of Technology	name	units mm	scale 1:1	quantity <<nr>>	date 12/05/2021
		material		mass gr	remark <<remarks>>
	author Hugo Kooiman 4108132		group <<group>>	format A4	drawing no. <<drawing no.>>

C:\Users\Hugo\OneDrive\01 - Afstuderen TU\01 First prototype\Bigger_diameter\TU_Templates\TU_Templates\

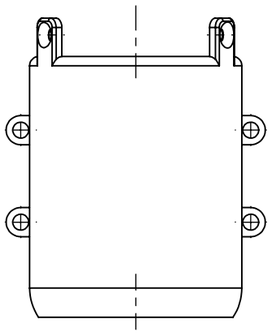

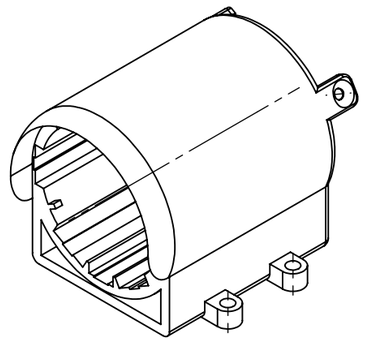

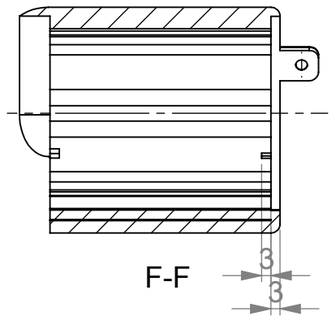

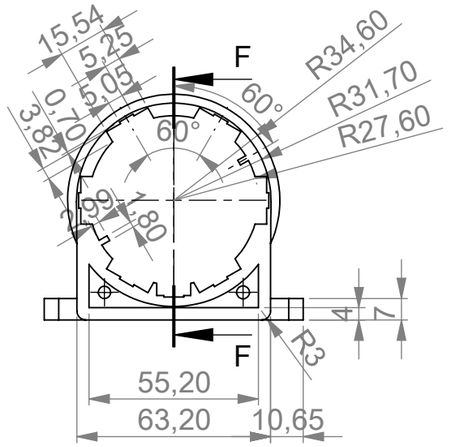

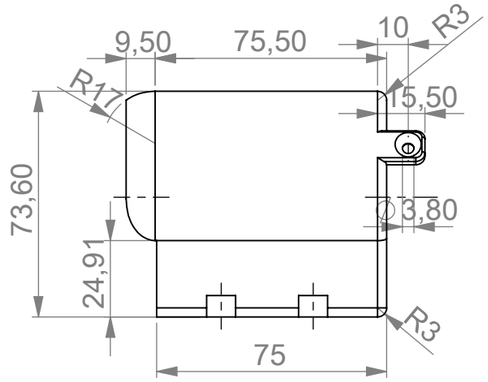

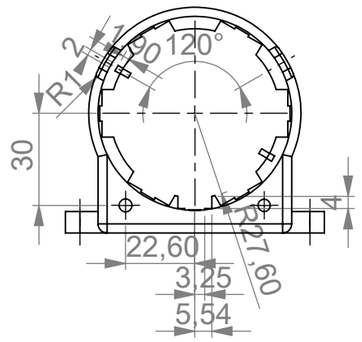

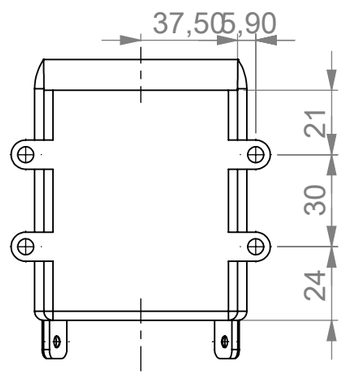

	units mm	scale 1:2	quantity <<nr>>	date 12/05/2021
material				mass gr
author Hugo Kooiman 4108132			group <<group>>	

remark
<<remarks>>

name
Slider_Outer_shell_drawing2

C:\Users\Hugo\OneDrive\01 - Afstuderen TU\01 First prototype\Bigger_diameter\TU_Templates\TU_Templates\

TU Delft Delft University of Technology

format
A3

drawing no.
<<drawing no.>>

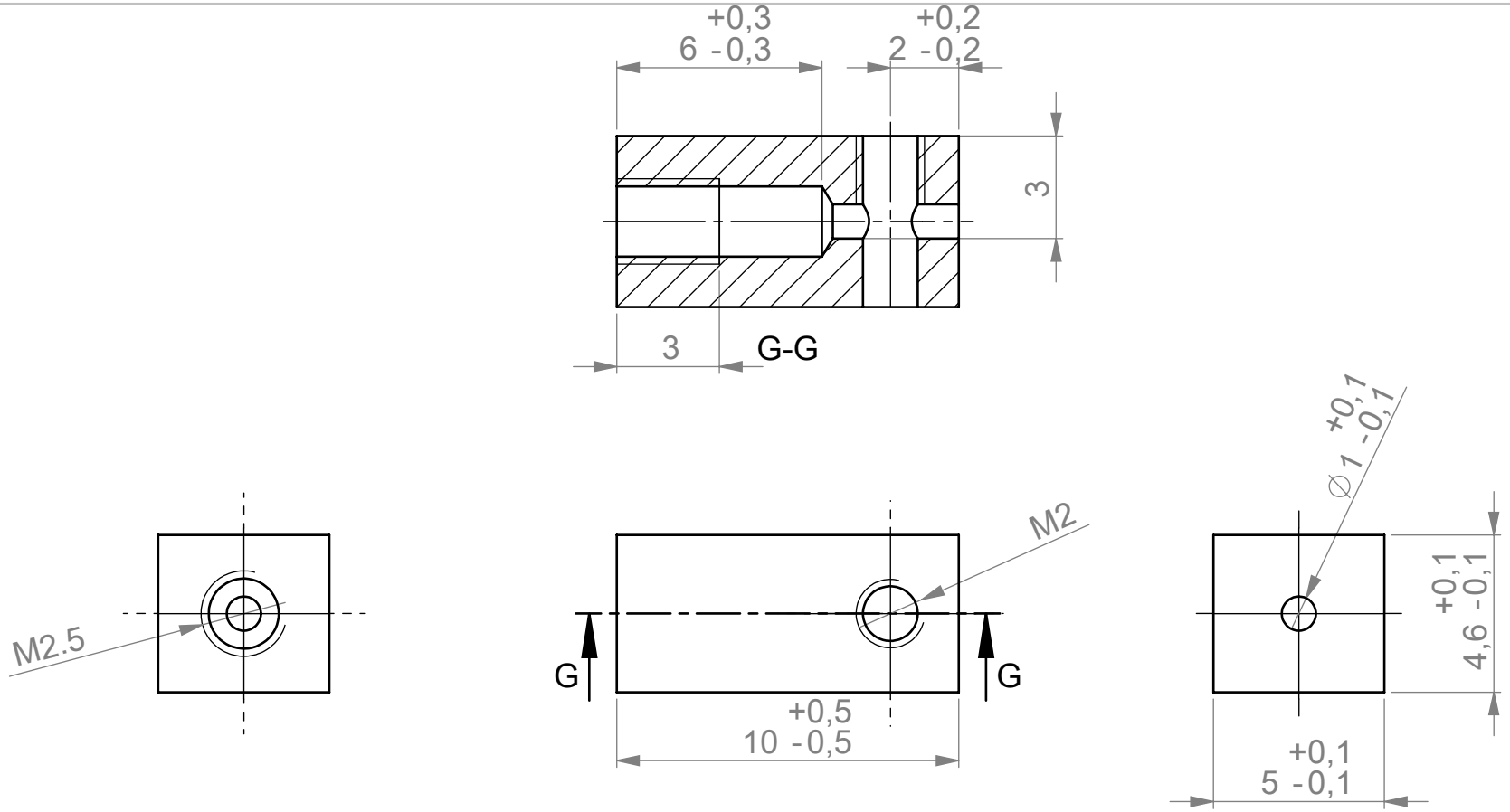

TU Delft Delft University of Technology	name Subslider_drawing2.1 C:\Users\Hugo\OneDrive\01 - Afstuderen TU\01 First prototype\Bigger_diameter\TU_Templates\TU_Templates\	units mm	scale 5:1	quantity <<nr>>	date 12/05/2021	remark <<remarks>>
		material Aluminium			mass gr	
		author <<names & student numbers>>		group <<group>>	format A4	drawing no. <<drawing no.>>

Appendix V: Experiment Results

Grasper opening test

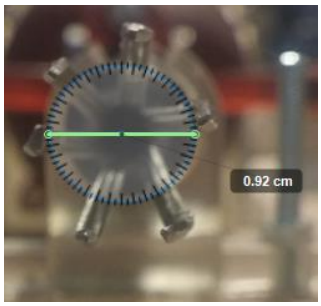

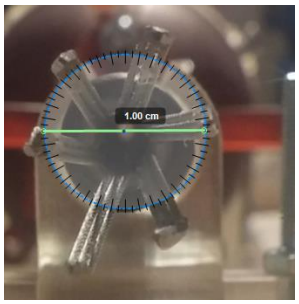

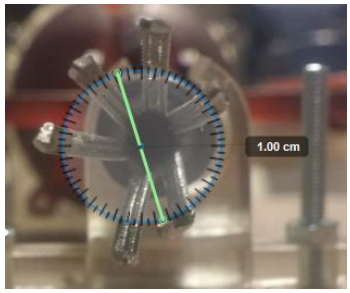

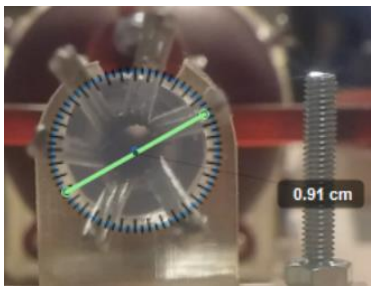

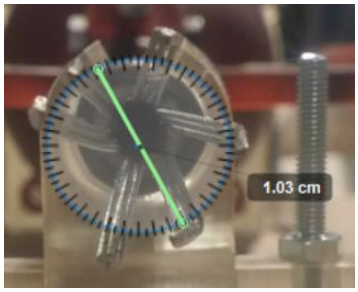

Tissue constraining test, Tissue transfer into lumen test

Official results after lubrication of cam and wire ropes:

Sphere diameter [mm]	Number of cam rotations before entering lumen	Transfer to lumen successful [Yes/No]	Constraining successful? [Yes/No]	Comments
3	63	Yes	Yes	Tissue was waving back and forth and appeared to go into the lumen by luck.
3	16	Yes	Yes	Tissue was waving back and forth and seemed to only contact 2 wire rope pairs.
3	15	Yes	Yes	Tissue was waving back and forth but somehow made it in.
3	10	Yes	Yes	
3	10	Yes	Yes	
3	10	Yes	Yes	Tissue doesn't seem to stick anymore like in the first three tries without lubrication of the cam and wire rope guides. Maybe surface is influenced by previous tests?

Sphere diameter [mm]	Number of cam rotations before entering lumen	Transfer to lumen successful [Yes/No]	Constraining successful? [Yes/No]	Comments
4	6	Yes	Yes	Slight back and forth motion of tissue.
4	10	Yes	Yes	Slight back and forth motion of tissue.
4	6	Yes	Yes	
4	13	Yes	Yes	Slight back and forth motion of tissue on the edge of lumen.
4	8	Yes	Yes	

4	8	Yes	Yes	

Sphere diameter [mm]	Number of cam rotations before entering lumen	Transfer to lumen successful [Yes/No]	Constraining successful? [Yes/No]	Comments
5	7	Yes	Yes	
5	5	Yes	Yes	
5	6	Yes	Yes	
5	6	Yes	Yes	
5	6	Yes	Yes	
5	6	Yes	Yes	

Tissue shape and orientation	Number of cam rotations before entering lumen	Transfer to lumen successful [Yes/No]	Constraining successful? [Yes/No]	Comments
Cylinder 6.5x4mm Parallel	5	Yes	Yes	Moved in quickly, last part was a bit slow
Cylinder 6.5x4mm Parallel	3	Yes	Yes	Moved in quickly
Cylinder 6.5x4mm Parallel	4	Yes	Yes	Moved in quickly
Cylinder 6.5x4mm Parallel	4	Yes	Yes	Moved in quickly
Cylinder 6.5x4mm Parallel	4	Yes	Yes	
Cylinder 6.5x4mm Parallel	9	Yes	Yes	Stopped for a bit at the lumen edge, maybe because of wire guide.

Tissue shape and orientation	Number of cam rotations before entering lumen	Transfer to lumen successful [Yes/No]	Constraining successful? [Yes/No]	Comments
Cylinder 6.5x4mm Perpendicular	(cut at 2) 6	No	Yes	Tissue was cut in half after 2 cycles. The half was successfully transferred into the lumen after 6 cycles
Cylinder 6.5x4mm Perpendicular	4	Yes	Yes	Tissue reoriented and was quickly transferred into the lumen.
Cylinder 6.5x4mm Perpendicular	15	No	Yes	Tissue did not reorient and was rolling between 2 wire rope groups. After 15 cycles ejected.
Cylinder 6.5x4mm Perpendicular	5	Yes	Yes	Tissue was touching both sides and reoriented quickly
Cylinder 6.5x4mm Perpendicular	7	No	Yes	Tissue did not rotate and reorient. It was transported towards the lumen and a part was 'decapitated' as a part entered the lumen.
Cylinder 6.5x4mm Perpendicular	16	Yes	Yes	Entered lumen slowly. Small chip came off the tissue

Grasping tissue from a surface

For all results a 5mm sphere has been used.

Surface with tissue orientation to grasper.	Transfer to lumen successful [Yes/No].		
90 degrees	No	Moving	When points were not pinching into tissue surface the tissue fell out
90 degrees	Yes	Moving	Points of grasper were going into surface tissue
90 degrees	Yes	Moving	Points of grasper were going into surface tissue
90 degrees	Yes	Moving	Points of grasper were going into surface tissue
90 degrees	Yes	Moving	Points of grasper were going into surface tissue
90 degrees	Yes	Moving	Points of grasper were going into surface tissue
90 degrees	Yes	Stil	Points of grasper were going into surface tissue
90 degrees	Yes	Stil	Points of grasper were going into surface tissue
45 degrees	Yes	Stil	Points of grasper were going into the tissue
45 degrees	Yes	Stil	Only minimal puncture
45 degrees	No	Stil	Try with near zero puncture
45 degrees	Yes	Stil	Try with near zero puncture
45 degrees	Yes	Still	Try with near zero puncture
45 degrees	Yes	Still	Try with near zero puncture
45 degrees	Yes	Moving	Tissue punctured a lot
0 degrees	Yes	Still	No surface puncture
0 degrees	Yes	Still	No surface puncture
0 degrees	Yes	Still	No surface puncture
0 degrees	Yes	Still	No surface puncture
0 degrees	Yes	Still	No surface puncture
0 degrees	Yes	Still	No surface puncture
0 degrees	No	Moving wire ropes	
0 degrees	No	Moving wire ropes	
0 degrees	No	Moving wire ropes	
0 degrees	Yes	Still	No surface puncture

Grasping with a bent transport system

A 5mm sphere of gelatin phantom tissue was used for each try. The bend of the transport system had a radius of 59mm.

Corner 20 deg	Yes	No function problems
	Yes	No function problems
	Yes	No function problems
	Yes	No function problems
	Yes	No function problems
	Yes	No function problems
Corner 40 deg	Yes	No function problems
	Yes	No function problems
	Yes	No function problems
	Yes	No function problems
	Yes	No function problems
	Yes	No function problems
		Bending of wire ropes observed due to curve. Also, one half of the grasper doesn't fully open.
Corner 60 deg	Yes	No function problems
	Yes	No function problems
	Yes	No function problems
	Yes	No function problems
	No	Grasp was successful but lumen transfer Happened after sliding the device 12mm back.
	Yes	Worked ok again

Appendix VI: Matlab Code

```
clear all
close all
clc
%% Opening grasper circular

opening_data = [9.2 10 10 9.1 10.3 8.9]';
grasper_state = {'Open grasper'};
%opening_data_categorical = categorical(opening_data_categorical,{'Open
grasper'},'Ordinal',true)

opening_std = std(opening_data); %standard deviation
opening_avg = mean(opening_data); %average

figure
hold on
ylim([0 11])
errorbar(opening_avg,opening_std,'x')
scatter([1 1 1 1 1 1], opening_data)
set(gca,'xtick',[1],'xticklabel',grasper_state)
ylabel('Grasp circular opening diameter [mm]')
%boxplot(opening_data)

%% Transfer into lumen data

data_3mm_trans_lumen = [63 16 15 10]';
data_3mm_trans_lumen_avg = mean(data_3mm_trans_lumen);
data_3mm_trans_lumen_std = std(data_3mm_trans_lumen);

data_4mm_trans_lumen = [6 10 6 13 8 8]';
data_4mm_trans_lumen_avg = mean(data_4mm_trans_lumen);
data_4mm_trans_lumen_std = std(data_4mm_trans_lumen);

data_5mm_trans_lumen = [7 5 6 6 6 6]';
data_5mm_trans_lumen_avg = mean(data_5mm_trans_lumen);
data_5mm_trans_lumen_std = std(data_5mm_trans_lumen);

data_cil_parallel_trans_lumen = [5 3 4 4 4 9]';
data_cil_parallel_trans_lumen_avg = mean(data_cil_parallel_trans_lumen);
data_cil_parallel_trans_lumen_std = std(data_cil_parallel_trans_lumen);

data_cil_perp_trans_lumen = [4 5 16]';
data_cil_perp_trans_lumen_avg = mean(data_cil_perp_trans_lumen);
data_cil_perp_trans_lumen_std = std(data_cil_perp_trans_lumen);


%% Transfer into lumen Creating plots
avgs = [data_3mm_trans_lumen_avg data_4mm_trans_lumen_avg data_5mm_trans_lumen_avg];
stds = [data_3mm_trans_lumen_std data_4mm_trans_lumen_std data_5mm_trans_lumen_std];
tissue_shapes = {'3mm','4mm','5mm'};
row2 = {'Sphere','Sphere','Sphere'};
row3 = {'','',''};
labelArray = [tissue_shapes;row2;row3];
tickLabels = strtrim(sprintf('%s\\newline%s\\newline%s\n', labelArray{:}));

%Plot 3,4,5mm spheres
figure
hold on
```

```
xlim([0 6])
avg_std_plot = errorbar([1 2 3],avgs,stds,'x');
data_points = scatter([1 1 1 1], data_3mm_trans_lumen,'r');
scatter([2 2 2 2 2 2], data_4mm_trans_lumen,'r')
scatter([3 3 3 3 3 3], data_5mm_trans_lumen,'r')
%scatter([1 1 1 1 1 1], opening_data)
          %old  %set(gca,'xtick',[1:5],'xticklabel',tissue_shapes)

ax = gca();
ax.XTick = 1:3;
ax.XLim = [0,4];
ax.XTickLabel = tickLabels;

title('Number of cam rotations needed for tissue entering the lumen.')
xlabel('Tissue sample')
ylabel('Number of cam rotations')
legend([avg_std_plot data_points],'Mean and standard deviation', 'Data points')

%% Plot 4mm, Cil parallel, Cil perpendicular
avgsCils = [data_4mm_trans_lumen_avg data_cil_parallel_trans_lumen_avg
data_cil_perp_trans_lumen_avg];
stdsCils = [data_4mm_trans_lumen_std data_cil_parallel_trans_lumen_std
data_cil_perp_trans_lumen_std];
tissue_shapes = {'4mm','4x6.5mm','4x6.5mm'};
row2 = {'Sphere','Cylinder','Cylinder'};
row3 = {'','parallel','perpendicular'};
labelArray = [tissue_shapes;row2;row3];
tickLabels = strtrim(sprintf('%s\\newline%s\\newline%s\n', labelArray{:}));

figure
hold on
xlim([0 6])
ylim([0 22])
avg_std_plotCil = errorbar([1 2 3],avgsCils,stdsCils,'x');
data_pointsCil = scatter([1 1 1 1 1 1], data_4mm_trans_lumen,'r');
scatter([2 2 2 2 2 2], data_cil_parallel_trans_lumen,'r')
scatter([3 3 3], data_cil_perp_trans_lumen,'r')

ax = gca();
ax.XTick = 1:3;
ax.XLim = [0,4];
ax.XTickLabel = tickLabels;

title('Number of cam rotations needed for tissue entering the lumen.')
xlabel('Tissue sample')
ylabel('Number of cam rotations')
legend([avg_std_plotCil data_pointsCil],'Mean and standard deviation', 'Data points')


%% One way ANOVA

Ysph = [data_3mm_trans_lumen' data_4mm_trans_lumen' data_5mm_trans_lumen'];
groupsph = {'3mm Sphere','3mm Sphere','3mm Sphere','3mm Sphere','4mm Sphere','4mm
Sphere','4mm Sphere','4mm Sphere','4mm Sphere','4mm Sphere','5mm Sphere','5mm
Sphere','5mm Sphere','5mm Sphere','5mm Sphere','5mm Sphere'};
[p,tbl,stats] = anova1(Ysph,groupsph);

%ANOVA1 4mm sphere and 4x6.5mm cylinder parallel
Ysphcilperppar = [data_4mm_trans_lumen' data_cil_parallel_trans_lumen'
data_cil_perp_trans_lumen'];
groupsphcilperppar = {'4mm Sphere','4mm Sphere','4mm Sphere','4mm Sphere','4mm
Sphere','4mm Sphere','Cylinder 6.5x4mm parallel','Cylinder 6.5x4mm parallel','Cylinder
```

```
6.5x4mm parallel','Cylinder 6.5x4mm parallel','Cylinder 6.5x4mm parallel','Cylinder
6.5x4mm parallel','Cylinder 6.5x4mm perpendicular','Cylinder 6.5x4mm
perpendicular','Cylinder 6.5x4mm perpendicular'};
[psphcilperppar,tblsphcilperppar,statssphcilperppar] =
anova1(Ysphcilperppar,groupsphcilperppar);
```

Bibliography

[1] E. E. Starck, J. C. McDermott, A. B. Crummy, W. D. Turnipseed, C. W. Acher, and J. H. Burgess, “Percutaneous aspiration thromboembolectomy.,” *Radiology*, vol. 156, no. 1, pp. 61–66, 1985.

[2] A. V. Gregory P. Schmitz, Juan Diego Perea, Ming-ting WU, Richard T. Chen, “Minimally invasive micro tissue debriders having targeted rotor positions,” WO2014/066542A1, 2014.

[3] C. E. Miller, “Methods of tissue extraction in advanced laparoscopy,” *Curr. Opin. Obstet. Gynecol.*, vol. 13, no. 4, pp. 399–405, 2001.

[4] E. P. De Kater, “The Design of a Flexible Friction-Based Transport Mechanism,” 2022.

[5] A. Van Beek, *Advanced Engineering Design Lifetime Performance and Reliability*. 2012.

[6] I. Steeg van der, “Design of The Endo-Tubular Friction Carrier The Design of The Endo-Tubular Friction Carrier,” no. I, 2018.

[7] M. E. Aguirre and M. Frecker, “Design and optimization of hybrid compliant narrow-gauge surgical forceps,” in *ASME 2010 Conference on smart materials, adaptive structures and intelligent systems*, 2010, pp. 779–788.

[8] P. K. Ng, M. C. Bee, A. Saptari, and N. A. Mohamad, “A review of different pinch techniques,” *Theor. Issues Ergon. Sci.*, vol. 15, no. 5, pp. 517–533, 2014.

[9] H. MONOD, “Contractility of muscle during prolonged static and repetitive dynamic activity,” *Ergonomics*, vol. 28, no. 1, pp. 81–89, 1985.

[10] J. D. Brown, J. Rosen, L. Chang, M. Sinanan, and B. Hannaford, “Quantifying surgeon grasping mechanics in laparoscopy using the blue DRAGON system,” *Stud. Heal. Technol. Informatics-Medicine Meets Virtual Real. 13*, pp. 34–36, 2004.

[11] D. Hellier, F. Albermani, B. Evans, H. De Visser, C. Adam, and J. Passenger, “Flexural and torsional rigidity of colonoscopes at room and body temperatures,” *Proc. Inst. Mech. Eng. Part H J. Eng. Med.*, vol. 225, no. 4, pp. 389–399, 2011.

[12] Y. Han, Y. Uno, and A. Munakata, “Does flexible small-diameter colonoscope reduce insertion pain during colonoscopy?,” *World J. Gastroenterol.*, vol. 6, no. 5, p. 659, 2000.

[13] Panacol, “Cyanolit®: Superglue for Superfast Bonding,” 2021. [Online]. Available: https://www.panacol.com/products/adhesive/cyanolit. [Accessed: 11-Jan-2021].

[14] Bison, “EPOXY METAL DOUBLE SYRINGE 24 ML (BLISTER),” *bison.net*, 2021. [Online]. Available: https://www.bison.net/en/product.2267. [Accessed: 11-Jan-2021].

[15] J. Charmant, “Kinovea.” Kinovea.org, 2021.

[16] M. Scali, P. A. H. Veldhoven, P. W. J. Henselmans, D. Dodou, and P. Breedveld, “Design of an ultra-thin steerable probe for percutaneous interventions and preliminary evaluation in a gelatine phantom,” *PLoS One*, vol. 14, no. 9, p. e0221165, 2019.

[17] I. Corporation, “Solder Alloys.” [Online]. Available: https://www.indium.com/products/solders/solder-alloys/. [Accessed: 20-Jan-2021].

[18] W. Dickey and D. Garrett, “Colonoscope length and procedure efficiency,” *Am. J. Gastroenterol.*, vol. 97, no. 1, pp. 79–82, 2002.

[19] R. C. Hibbeler, “Mechanics of Materials, 2008.” Prentice Hall.

[20] A. J. Loeve, T. Krijger, W. Mugge, P. Breedveld, D. Dodou, and J. Dankelman, “Static friction of stainless steel wire rope--rubber contacts,” *Wear*, vol. 319, no. 1–2, pp. 27–37, 2014.

[21] U. Cerkvenik, *Biomechanics of a parasitic wasp ovipositor: Probing for answers*. Wageningen: Wageningen University, 2019.

[22] J. A. Cronin, M. I. Frecker, and A. Mathew, “Design of a compliant endoscopic suturing instrument,” *J. Med. Device.*, vol. 2, no. 2, 2008.

[23] J. Arata *et al.*, “Articulated minimally invasive surgical instrument based on compliant mechanism,” *Int. J. Comput. Assist. Radiol. Surg.*, vol. 10, no. 11, pp. 1837–1843, 2015.

[24] S. Sgobba, “Physics and measurements of magnetic materials,” *arXiv Prepr. arXiv1103.1069*, 2011.

[25] J. C. Kappatou, G. D. Zalokostas, D. A. Spyratos, and others, “Design optimization of axial flux permanent magnet (AFPM) synchronous machine using 3D FEM analysis,” *J. Electromagn. Anal. Appl.*, vol. 8, no. 11, p. 247, 2016.